Les Cahiers du GERAD ISSN: 0711–2440

Extracting latent states with high frequency option prices

D. Amaya, J.-F. Bégin, G. Gauthier

G–2016–66

August 2016

GERAD HEC Montréal
3000, chemin de la Côte-Sainte-Catherine
Montréal (Québec) Canada H3T 2A7

Tél. : 514 340-6053
Téléc. : 514 340-5665
info@gerad.ca
www.gerad.ca

Extracting latent states with high frequency option prices

Diego Amaya [a]

Jean-François Bégin [b]

Geneviève Gauthier [b c]

[a] *Wilfrid Laurier University, Waterloo (Ontario) Canada N2L 3C5*

[b] *Department of Decision Sciences, HEC Montréal, Montréal (Québec) Canada, H3T 2A7*

[c] *GERAD & Department of Decision Sciences, HEC Montréal, Montréal (Québec) Canada, H3T 2A7*

damaya@wlu.ca
jean-francois.begin@hec.ca
genevieve.gauthier@hec.ca

August 2016

Les Cahiers du GERAD

G–2016–66

Abstract: We propose the option realized variance as a new observable covariate that integrates high frequency option prices in the inference of option pricing models. Using several simulation and empirical studies, this paper documents the incremental information offered by this variable. Our empirical results show that the information contained in this new covariate improves the inference of model variables such as the instantaneous variance, return jumps, and variance jumps of the S&P 500 index. Parameter estimates indicate that the risk premium breakdown between jump and diffusive risks is affected by the omission of this information.

Keywords: High frequency data, option realized variance, options, jump-diffusions, particle filter

1 Introduction

The existing literature on option pricing has almost exclusively focused on model specification[1] and estimation,[2] but has not given much regard to the incremental information offered by observable variables. This paper addresses this issue by enlarging the set of observable covariates with the option realized variance (ORV). This novel source of information parsimoniously integrates high frequency option prices into the list of observable covariates.

Identification of model components relies on time series of observable variables. The first set of observable covariates corresponds to the time series of underlying asset prices, which contain information about physical measure dynamics. Traditional discrete-time models such as those studied in Engle (1982) and Bollerslev (1986) employ these prices directly to infer volatility process dynamics. In continuous-time models, these prices have been used to analyze the role of jumps on returns and their volatility (Eraker et al., 2003). Advances in econometrics have allowed researchers to estimate different characteristics of the return variation using measures such as the realized variance and bipower variation (Andersen et al., 2001; Barndorff-Nielsen and Shephard, 2004, among others). In the context of option pricing, Christoffersen et al. (2012a) and Christoffersen et al. (2015) show that these realized measures reduce option pricing errors significantly, providing evidence of the economic value of high frequency asset prices.

A second important source of information comes from the rich cross section of option prices. These prices not only provide information about the dynamics under the risk-neutral measure, but also about the parameters that govern the conditional return distribution. For instance, Bates (2000) uses option contracts on the S&P 500 index to extract implicit distributions of competing jump-diffusion models. Combining both underlying asset returns and option prices, Eraker (2004) conducts an empirical analysis of jump-diffusion models by looking at their ability to simultaneously fit option and return data. Johannes et al. (2009) propose a filtering methodology based on return and option datasets to disentangle jumps and diffusive components. More recently, the emergence of derivative contracts on these options has allowed studies such as Cont and Kokholm (2013) and Bardgett et al. (2015) to extract information about the expected future realized variance.

To understand the information content of option realized variances, we employ a model of stock returns that exhibits stochastic volatility, jumps in returns with stochastic intensity, and independent jumps in variance using the general framework of Duffie et al. (2000). These characteristics are similar to those studied in Pan (2002), Eraker et al. (2003), Broadie et al. (2007) and Johannes et al. (2009), among others. We favour this specification over more sophisticated ones because it is flexible enough to capture dynamic properties of stock returns while providing analytical tractability to conduct empirical analysis with time series of option panels.

Jumps in the variance process are generally difficult to infer as the contributions to diffusive and jump components of the variance process are hard to disentangle. The inclusion of option realized variances in the inference process circumvents this issue because it brings in non-redundant information. Contrary to Andersen et al. (2015b), we use a parametric approach to characterize model components from high frequency option prices. A distinctive characteristic of ORV is that, depending on its moneyness, specific features of the underlying processes can be isolated. For instance, deep out-of-the-money options have very low deltas and vegas, so most of the variability in option prices comes from discontinuous sample paths generated by jumps in returns and volatility.

The paper conducts simulated and empirical studies on the incremental information content of several information sources. In addition to returns and a panel of daily option implied volatilities (IV), we add measures of the index return variance such as realized variance and bipower variation. We complement this sample with the newly proposed option realized variance, which is available every day for each option in the

[1]In the recent literature, few model features have been considered: jumps in volatility (Eraker et al., 2003; Pan, 2002; Todorov and Tauchen, 2011), co-jumps (Chernov et al., 2003; Eraker, 2004; Broadie et al., 2007), jump arrival intensities (Bates, 2000), and multifactor stochastic volatility with jumps (Bardgett et al., 2015), among others.

[2]A non-exhaustive list of methods for the estimation of these models includes Markov chain Monte Carlo methods (Jones, 1998; Eraker, 2001), nonparametric approaches (Aït-Sahalia and Lo, 1998) the simulated method of moments (Duffie and Singleton, 1993; Gallant and Tauchen, 2010), the generalized method of moments (Pan, 2002), and approximate maximum likelihood (Bates, 2006), among others.

panel. An extensive Monte Carlo study that relies on an extension of Johannes, Polson, and Stroud's (2009) filter shows that option realized variances contribute significantly to the identification of variance jumps.

In our empirical study, we employ intraday data from options on the S&P 500 index and from futures prices on the E-mini S&P 500 to document several properties of the option realized variance.[3] Using a sample of daily observations that extends from July 2004 to December 2012, we analyze the large cross section of option data by constructing ORV surfaces across moneynesses and maturities. We find that there is an important level of commonality between ORVs and the realized variance of index returns, especially when large, sporadic shocks happen.[4] This degree of commonality is expected as a result of intense trading activity in both markets (Stephan and Whaley, 1990). We also assess the economic relationship between ORVs and index return variations with predictive regressions: lagged values of selected ORVs predict the one-day ahead realized variance and jump variation activity.[5]

The paper then investigates several empirical implications of adding ORVs as additional observable covariates in the estimation of option pricing models. We first observe that the addition of ORV produces less frequent larger jumps in the variance process and more frequent smaller negative jumps in the price process. Next, we find that the addition of this new covariate increases the compensation for bearing price jump risk (i.e. 0.1% without ORV vs 1.6% with ORV, on average) and decreases the compensation for diffusive risk premium (i.e. 4.4% when ORV is excluded and 1.8% when ORV is used). Thus, in total, the average risk premium that results from using both information sets is similar, but the risk premium breakdown between diffusive and jump risks is different. Third, regarding the uncertainty around the estimation of latent quantities, posterior standard deviations show that adding ORV to the information set decreases this uncertainty. The most staggering decrease is observed for variance jumps, which experience approximately a fivefold decrease. Finally, in- and out-of-sample analyses show that the inclusion of all information sources produces smaller forecasting errors of implied volatilities.

Several studies in the literature of asset pricing employ non-parametrical methods to infer the underlying structure of stock returns and their volatilities from high frequency prices.[6] We focus on a parametrical approach to study the incremental information offered by intraday prices. Our results suggest that not all sources give the same information and that there is unique information about specific features of the model in each source. Our paper also contributes to the literature with a parsimonious measure that summarizes intraday information from option prices. In line with Andersen et al. (2015a), we document that the cross section of option high frequency prices, summarized by the option realized variance in this study, contains relevant information about the discontinuous part of the variance process.

This paper is also related to studies that deal with the filtering of continuous-time jump-diffusion models.[7] Our paper differs from this literature in several ways. First, we propose a filter based on the sequential importance resampling (SIR) algorithm (Gordon et al., 1993) that, in addition to index returns and option prices, employs realized variance, bipower variation, and option realized variances as observable sources. Second, contrary to Johannes et al. (2009), we estimate the proposed model using the filter, which requires

[3] Recently, we have been made aware that Audrino and Fengler (2015) have developed, independently, a competing measure of the option realized variance similar to ours. Whereas they use option log-prices to compute their measure, we employ option prices. We privilege the use of option prices because the variance measure resulting from these prices does not depend on the price of the option itself, which is important for large-scale optimizations in empirical option pricing studies.

[4] Events such as the financial crisis of 2008, the flash crash episode of 2010, or the downgrade of the U.S. debt in 2011 have common spikes in all time series.

[5] The jump variation activity is measured as the positive difference between realized variance and bipower variation.

[6] Todorov and Tauchen (2011) find evidence of discontinuous co-movements between the instantaneous volatilities and returns using high frequency data of VIX and the S&P 500 index. Andersen et al. (2015a) employ a nonparametric framework to infer latent instantaneous volatilities and jump intensities with intraday Black-Scholes implied volatilities. Using the rich information embedded in option prices, the authors find that the dynamics for IV of deep OTM puts behave as a pure jump process, whereas those of near-the-money are better characterized by a diffusive process. Bandi and Reno (2016) use high frequency data for the S&P 500 index to estimate its realized variance over intraday intervals. Using a novel moment-based procedure, the authors find support for the existence of independent jumps in the instantaneous volatilities and co-jumps between the price process and that of the volatility.

[7] Johannes et al. (2009) and Bardgett et al. (2015) use an optimal filtering methodology that combines time-discretization schemes with Monte Carlo methods to obtain latent states. Eraker (2004) employs Markov chain Monte Carlo simulation to estimate the posterior distribution of parameters, as well as volatility and jump processes.

special attention to the way the likelihood function is approximated and provides a less computationally intensive procedure than the one employed in Eraker (2004).

The rest of this paper is organized as follows. Section 2 describes the model and provides insights about the information content of observable variables. Section 3 presents the estimation methodology of the model. Simulated-based results are given in Section 4. Section 5 conducts a nonparametric study of option realized variances. Section 6 presents the option pricing implications of adding ORVs in the estimation set. Finally, Section 7 concludes.

2 Framework

The goal of this section is to present a model that captures different properties of asset prices. The building block is the square root stochastic volatility specification of Heston (1993). To adequately model fat tails of return distributions, a compound Poisson process with Gaussian jumps is added to the price process.[8] Although both stochastic volatility and jumps in the price process can generate rich dynamics, Bakshi et al. (1997), Bates (2000) and Pan (2002) find that volatility dynamics resulting from this specification tend to be misspecified. As explained by Andersen et al. (2001) and Alizadeh et al. (2002), two factors generate volatility: a rapidly changing factor and a highly persistent slowly moving one. The latter could be modelled by jumps in variance process. Therefore, exponentially distributed jumps are also added to the variance process.[9]

We deliberately focus our attention on a model with the following latent factors: diffusive stochastic volatility, log-equity jumps, and instantaneous variance jumps. These three risk factors induce different behaviour in the asset price and hence can be identified from an econometric perspective, given the right amount of data (Eraker et al., 2003). This insight is explored in the second part of this section, in which we discuss the list of available data sources and link these quantities to different features of the data generating process.

2.1 Model

The model is part of the family of stochastic volatility models with jumps (SVJ). This affine jump-diffusion model yields semi-closed form solutions for option pricing as shown in Duffie et al. (2000). Under the objective measure $\mathbb{P}$, the process governing the dynamics of the log-equity price, Y, and its instantaneous stochastic variance, V, are

$$\begin{aligned} dY_t &= \alpha^{\mathbb{P}}_{t^-} dt + \sqrt{V_{t^-}} dW_{Y,t} + dJ_{Y,t}, && (1)\\ dV_t &= \kappa\left(\theta - V_{t^-}\right) dt + \sigma\sqrt{V_{t^-}} dW_{V,t} + dJ_{V,t}, && (2)\\ W_{Y,t} &= \rho W_{V,t} + \sqrt{1-\rho^2} W_{\perp,t},\\ J_{Y,t} &= \sum_{n=1}^{N_{Y,t}} Z_{Y,n}, \quad Z_{Y,n} \sim \mathcal{N}(\mu_Y; \sigma_Y^2)\\ J_{V,t} &= \sum_{n=1}^{N_{V,t}} Z_{V,n}, \quad Z_{V,n} \sim \mathrm{Exp}(\mu_V) \end{aligned}$$

where $\{W_{V,t}\}_{t\geq 0}$ and $\{W_{\perp,t}\}_{t\geq 0}$ are two independent standard $\mathbb{P}$-Brownian motions and $\left\{\alpha^{\mathbb{P}}_{t^-}\right\}_{t\geq 0}$ is a predictable process such that

$$\alpha^{\mathbb{P}}_{t^-} = r - q + \left(\eta_Y - \frac{1}{2}\right) V_{t^-} + \left(\gamma_Y - \left(\varphi^{\mathbb{P}}_{Z_Y}(1) - 1\right)\right)\lambda_{Y,t^-}. \tag{3}$$

[8]This kind of jump process is used by Bates (1996), Bakshi et al. (1997), Duffie et al. (2000), Pan (2002), Eraker et al. (2003), Johannes et al. (2009) to name a few.

[9]Among others, Duffie et al. (2000), Eraker et al. (2003), Johannes et al. (2009) and Andersen et al. (2015b) use exponentially distributed variance jumps. Note that Bates (2000), Duffie et al. (2000), Pan (2002), Eraker et al. (2003) and Todorov and Tauchen (2011) provide evidence for the presence of positive jumps in volatility.

The risk-free interest rate is given by r and the instantaneous dividend yield by q. The parameters η_Y and γ_Y capture the diffusive and jump risk premiums, respectively.[10] The function $\varphi^{\mathbb{P}}_{Z_Y}(1)$ is the cumulant generating function of Z_Y evaluated at 1. The drift process $\alpha^{\mathbb{P}}_{t^-}$ is a by-product of the Radon-Nikodym derivative used in this study. We refer the interested reader to Section B.1 of the Appendix for more details.

Log-equity jumps are generated by a Poisson process $\{N_{Y,t}\}_{t\geq 0}$ with stochastic intensity that depends on the instantaneous variance: $\lambda_{Y,t^-} = \lambda_{Y,0} + \lambda_{Y,1}V_{t^-}$. The size of these jumps are given by Gaussian random variables with mean μ_Y and standard deviation σ_Y.[11] Regarding jumps in volatility, these are governed by a Poisson process $\{N_{V,t}\}_{t\geq 0}$ that has a constant intensity $\lambda_{V,t^-} = \lambda_{V,0}$. Variance jump sizes $\{Z_{V,n}\}_{n=1}^{\infty}$ are given by independent exponentially distributed random variables with mean μ_V.

2.2 Links between theoretical and empirical quantities

We now analyze variables commonly used to conduct inference of models displaying latent characteristics, such as those embedded in Equations (1) and (2).

The first group of observables corresponds to time series of index prices, which contain information under the physical measure. In principle, high frequency prices are sufficient to extract all the information required for inferring latent components. In practice, however, parametric estimation from these prices would require the use of a very large sample set. The realized variance and bipower variation help reduce this dimensionality problem by keeping important information about the price and variance processes.

The second group is composed of options written on the S&P500 index.[12] Option implied volatilities capture the wedge between the physical and the risk-neutral measure, which should provide more precise estimates of model parameters. In addition to this variable, we consider the variance of the option price as a complementary information source.

2.2.1 Index prices as a first source of information

Log-prices constitute the fundamental source of information available under the physical measure:

$$\text{Observable \#1:} \quad Y_t. \tag{4}$$

One of the interesting properties of these prices, as pointed out in Merton (1980), is that information about volatility can be obtained by arbitrarily increasing the sample frequency. Moreover, as discussed in nonparametric studies (see Barndorff-Nielsen and Shephard, 2004), this source not only provides information about the volatility process, but also about jumps in asset prices.

The fundamental variable that links intraday log-prices with price volatility is the quadratic variation (QV). This variable employs intraday log-prices over the interval $[0, t]$ in the following way:

$$QV_t = [Y, Y]_t = \lim_{N\to\infty} \sum_{j=1}^{N} \left(Y_{tj/N} - Y_{t(j-1)/N}\right)^2$$

where N is the number of elements in an equidistant grid dividing the interval $[0, t]$. Under the proposed jump-diffusion model, the quadratic variation is composed of the integrated variance and the log-price jump induced variation:

$$QV_t = \int_0^t V_{s^-}\, ds + \sum_{n=1}^{N_{Y,t}} (Z_{Y,n})^2.$$

[10] Our Radon-Nikodym derivative explained in Appendix A.1 includes four equivalent martingale measure coefficients: Λ_{Y,u^-}, Λ_{V,u^-}, Γ_Y and Γ_V. The process Λ_{Y,u^-} is $\eta_Y\sqrt{V_{u^-}}$, as in Heston (1993) among others. Λ_{V,u^-} is defined analogously. Moreover, γ_Y is a nontrivial function of Γ_Y. Even though η_V and Γ_V are not involved directly in our $\mathbb{P}$-measure modelling, these two parameters deal with the change of measure of the variance diffusive and jump components.

[11] For this model, the jump convexity correction is given by $\varphi^{\mathbb{P}}_{Z_Y}(1) - 1 = \exp\left(\mu_Y + \frac{\sigma_Y^2}{2}\right) - 1$.

[12] An interesting extension would be to consider the VIX index and its derivatives within a joint framework as the one proposed in Bardgett et al. (2015). We leave for future research the question of identifying the value added by these derivatives and choose to explore in detail what options written on the S&P 500 contribute in terms of information.

In the model considered in Equation (1), the quadratic variation depends explicitly on log-equity price jumps sizes $Z_{Y,n}$, the number of price jumps $N_{Y,t}$, and the path followed by the volatility process through $\int_0^t V_{s^-} ds$. The impact of jumps on the instantaneous variance is implicitly captured in the integrated variance over time. Over a time interval of length Δ (e.g. one day), the increments of the quadratic variation are given by:

$$\Delta QV_{t-\Delta,t} = QV_t - QV_{t-\Delta} = \int_{t-\Delta}^{t} V_{s^-}\, ds + \sum_{n=N_{Y,t-\Delta}+1}^{N_{Y,t}} (Z_{Y,n})^2. \tag{5}$$

As argued by Andersen et al. (2001), estimates of these increments can be obtained with the realized variance (RV), which is computed from intraday log-prices in the following way:

$$\text{Observable \#2:} \quad RV_{t-\Delta,t} = \sum_{j=1}^{N} \left(Y_{t-\Delta+j\Delta/N} - Y_{t-\Delta+(j-1)\Delta/N}\right)^2. \tag{6}$$

In general, if N is large enough, $\Delta QV_{t-\Delta,t}$ and $RV_{t-\Delta,t}$ should be similar.[13]

Whereas the quadratic variation provides an overall measure of price volatility, the integrated variance, defined by

$$I_t = \int_0^t V_{s^-}\, ds$$

depends only on the diffusive component of the variance process and its jumps. Increments of the integrated variance over a time period of length Δ are given by:

$$\Delta I_{t-\Delta,t} = I_t - I_{t-\Delta} = \int_{t-\Delta}^{t} V_{s^-}\, ds, \tag{7}$$

which can be estimated using the realized bipower variation:

$$\text{Observable \#3:} \quad BV_{t-\Delta,t} = \frac{\pi}{2} \sum_{j=2}^{N} \left|Y_{t-\Delta+j\Delta/N} - Y_{t-\Delta+(j-1)\Delta/N}\right| \left|Y_{t-\Delta+(j-1)\Delta/N} - Y_{t-\Delta+(j-2)\Delta/N}\right|. \tag{8}$$

In general, if N is large enough, $\Delta I_{t-\Delta,t}$ and $BV_{t-\Delta,t}$ should be similar.[14] Thus, in order to identify log-price jump activity, it is necessary to combine the information contained in RV and BV.

2.2.2 Option-based information

Option prices provide an additional source of information because they are sensitive to changes in price and volatility. Under usual conditions, the price of an option is given by

$$O_t = \mathbb{E}_t^{\mathbb{Q}} \left[e^{-r(T-t)} F(Y_T, K) \middle| Y_t, V_t \right],$$

where $F(Y_T, K)$ is the payoff at time T, K the strike price of the option, and $\mathbb{Q}$ a risk-neutral probability measure. Several authors highlight different advantages of adding these prices to the information set. First, these prices are conditional functions of stock returns, which allows researchers to estimate parameters governing the shape of these distributions (Jackwerth and Rubinstein, 1996; Dumas et al., 1998). Second, option prices help capture the wedge between the measures $\mathbb{P}$ and $\mathbb{Q}$, thus providing information about volatility and jump risk premiums (Chernov and Ghysels, 2000; Pan, 2002; Eraker, 2004; Santa-Clara and Yan, 2010; Christoffersen et al., 2012b). Third, option prices are highly informative about the instantaneous variance level (Broadie et al., 2007).[15]

[13] Protter (2004) shows that $RV_{t-\Delta,t}$ converges uniformly in probability to $\Delta QV_{t-\Delta,t}$ as the number of intraday observations increases.

[14] In a similar class of models, Barndorff-Nielsen and Shephard (2004) prove that $BV_{t-\Delta,t}$ converges to $\Delta I_{t-\Delta,t}$ as the number of intraday observations increases.

[15] Within the proposed framework, semi closed-forms for option prices exist and are provided in Appendix A.3.

Rather than using option prices directly, we employ the implied volatility (IV) resulting from the Black-Scholes formula:[16]

$$\text{Observable \#4:} \quad \sigma_{t,i}^{BS},\ t \in \{1, 2, ..., n_t\}. \tag{9}$$

This change of variable does not only provide measures that are invariant to price levels, but also ones that can be characterized with OTM call and put options of different maturities (the so-called IV surface). We digress from the pure common calibration approach and use a time series of cross sections of options to capture the links between physical and risk-neutral parameters.

The literature in option pricing has relied almost exclusively on end-of-day option prices. With the availability of high frequency option prices, we now explore how to construct variables that capture information from fine grids. To this end, we extend the well-established concept of realized variance of log-prices to option prices and compute what we call the option realized variance (ORV).

To understand ORV, we need to first look at the quadratic variation of the option price, as the former quantity corresponds to an approximation of the latter. In the proposed framework, we can characterize this variation for a European option as[17]

$$\begin{aligned}[O, O]_t = & \int_0^t \left(\left(\frac{\partial O_u}{\partial y} (Y_{u^-}, V_{u^-}) \right)^2 + 2\sigma\rho \frac{\partial O_u}{\partial y} (Y_{u^-}, V_{u^-}) \frac{\partial O_u}{\partial v} (Y_{u^-}, V_{u^-}) + \sigma^2 \left(\frac{\partial O_u}{\partial v} (Y_{u^-}, V_{u^-}) \right)^2 \right) V_{u^-} du \\ & + \sum_{0<u\le t} \left\{ O_u (Y_u, V_u) - O_u (Y_{u^-}, V_{u^-}) \right\}^2 . \end{aligned} \tag{10}$$

The last term of Equation (10) is associated with the jump variation contribution and can be rewritten as:

$$\begin{aligned} & \sum_{0<u\le t} \left\{ O_u (Y_u, V_u) - O_u (Y_{u^-}, V_{u^-}) \right\}^2 \\ = & \sum_{0<u\le t} \left\{ O_u (Y_u, V_u) - O_u (Y_{u^-}, V_u) \right\}^2 + \sum_{0<u\le t} \left\{ O_u (Y_u, V_u) - O_u (Y_u, V_{u^-}) \right\}^2 , \end{aligned}$$

where the first term relates to log-equity jumps and the second one to variance jumps.

The realized equivalent of the change in option quadratic variation

$$\Delta OQV_{t-\Delta,t} = [O, O]_t - [O, O]_{t-\Delta}$$

is the option realized variance. This variable is computed from intraday option prices according to the following expression:

$$\text{Observable \#5:} \quad ORV_{t-\Delta,t,i} = \sum_{j=1}^{N} \left(O_{t-\Delta+j\Delta/N} - O_{t-\Delta+(j-1)\Delta/N} \right)^2 ,\ t \in \{1, ..., n_t\}. \tag{11}$$

Several properties of option realized variances can be characterized from Equation (10). Notice first that the option realized variance depends on the delta of the option through

$$\frac{\partial O_t}{\partial y} = \frac{\partial O_t}{\partial S} S$$

and the variance vega $\frac{\partial O_t}{\partial v}$. Accordingly, the moneyness of the option will determine which aspects of the data generating process drive the option realized variance. If we consider a deep in-the-money (ITM) call

[16] There is indeed a bijection between option prices and implied volatilities. See Renault (1997) for the benefits of using implied volatilities over option prices.

[17] Since the option price is a smooth function of Y and V, Itō's lemma can be applied to determine its quadratic variation. Details are available in the Internet appendix B.2. Internet appendix B.2.1 provides a description on how to compute the derivatives used in Equation (10).

option, its delta is close to one and the sensitivity to the instantaneous variance close to zero, so the option quadratic variation for this option will be approximately equal to:

$$[O,O]_t^{\mathrm{ITM}} \cong \int_0^t \exp(2Y_{u^-})V_{u^-}\,du + \sum_{0<u\le t}(\Delta O_u)^2.$$

In this case, we would expect the quadratic variance of this option to be "perfectly elastic" to the integrated variance and jump induced variation (in a day without jumps we should expect the option quadratic variance for such a derivative to be proportional to the integrated variance of the underlying).[18] Therefore, information obtained using ITM option quadratic variance is somewhat redundant when one has already included realized variance as a source of information. If we consider an ATM option, the variance vega is at its highest value and delta should be close to $\frac{1}{2}$, so Equation (10) is approximated to:

$$[O,O]_t^{\mathrm{ATM}} \cong \int_0^t \left(\frac{\exp(2Y_{u^-})}{4} + \rho\sigma\frac{\partial O_u}{\partial v} + \sigma^2\left(\frac{\partial O_u}{\partial v}\right)^2\right)V_{u^-}\,du + \sum_{0<u\le t}(\Delta O_u)^2.$$

For this level of moneyness, we would expect that the option quadratic variation responds more than proportionally to changes in the integrated variance. Finally, for deep OTM options, delta and variance vega should be close to zero, so most of the option quadratic variation comes from jump-induced variation. In this case we have:

$$[O,O]_t^{\mathrm{OTM}} \cong \sum_{0<u\le t}(\Delta O_u)^2.$$

The behaviour of this type of option is not new to the finance literature; Andersen et al. (2015a) show nonparametrically that OTM put options behave like a pure-jump process. In this paper we show that the quadratic variation of OTM and deep OTM options captures this information, which help to identify jump activity in variance and log-price processes by bringing an alternative variable to the existing list of observable covariates.

We end this section by summarizing how realized moments and other observed quantities can be combined to identify different risk sources. First, the difference between the realized variance and the bipower variation,

$$RV_{t-\Delta,t} - BV_{t-\Delta,t} \cong \sum_{n=N_{Y,t-\Delta}+1}^{N_{Y,t}} (Z_{Y,n})^2,$$

provides information about the presence and importance of log-equity price jumps; however, this difference does not give enough information to identify the sign of the jump. To this end, deep out-of-the-money (OTM) call (put) options are contracts that capture, to some extent, the sign of price jumps since their prices change quite drastically as soon as there is a substantial increase (decrease) in the underlying price.

Second, OTM option realized variations, combined with realized measures of log-equity prices, help to identify jumps in the volatility process. As discussed before, the OTM option realized variance can be approximated by

$$ORV_{t-\Delta,t}^{\mathrm{OTM}} \cong \sum_{t-\Delta<u\le t}\left(O_u\left(Y_u,V_u\right) - O_u\left(Y_{u^-},V_u\right)\right)^2 + \sum_{t-\Delta<u\le t}\left(O_u\left(Y_u,V_u\right) - O_u\left(Y_u,V_{u^-}\right)\right)^2.$$

In the absence of log-equity price jumps, $RV_{t-\Delta,t} - BV_{t-\Delta,t}$ is close to zero, so $ORV_{t-\Delta,t}^{\mathrm{OTM}}$ becomes

$$ORV_{t-\Delta,t}^{\mathrm{OTM}} \cong \sum_{t-\Delta<u\le t}\left(O_u\left(Y_u,V_u\right) - O_u\left(Y_u,V_{u^-}\right)\right)^2.$$

The previous equation shows that $ORV_{t-\Delta,t}^{\mathrm{OTM}}$ encompasses information about the presence of variance jumps.

[18] Empirically, we could look at this by running log-regressions of ORV over RV for different moneyness (controlling with a variable related to jumps, or excluding days with detected jumps). We should observe that coefficients for ATM are higher than those of ITM, and that the latter should be higher than those of OTM. Subsection 4.2 shows examples of these regressions using simulated data.

3 Filtering and estimation

This section provides details about the implementation of a SIR-type filter following Gordon et al. (1993). Our approach differs from the current literature in two ways. First, we propose a filter based on the SIR that employs realized variance, bipower variation and option realized variances as observable sources. Second, we show how to estimate the model using the filter, which requires special attention to the way the likelihood function is computed.

3.1 Filtering algorithm

The filter is constructed over samples of daily observations[19], so we define the elapsed time between two consecutive time steps by $\Delta = 1/252$ and denote the observed sample by $\{z_{k\Delta}\}_{k=1}^{T}$, where

$$z_{k\Delta} = \left[Y_{k\Delta}, RV_{(k-1)\Delta,k\Delta}, BV_{(k-1)\Delta,k\Delta}, \boldsymbol{\sigma}_{k\Delta}^{BS}, \mathbf{ORV}_{(k-1)\Delta,k\Delta}\right],$$

$\boldsymbol{\sigma}_{k\Delta}^{BS} = \left[\sigma_{k\Delta,1}^{BS}, ..., \sigma_{k\Delta,n_{k\Delta}}^{BS}\right]$ being the implied volatility vector of the $n_{k\Delta}$ options considered that day and $\mathbf{ORV}_{(k-1)\Delta,k\Delta} = \left[ORV_{(k-1)\Delta,k\Delta,1}, ..., ORV_{(k-1)\Delta,k\Delta,n_{k\Delta}}\right]$ the corresponding vector of option realized variances.

As it is the case for any particle filter, the first step is to simulate particles for the latent variables. The interconnection between instantaneous variance and log-price processes requires the generation of the complete model. More precisely, assuming that the log-price $Y_{(k-1)\Delta}$ and its instantaneous variance $V_{(k-1)\Delta}$ are known at the end of day $k-1$, the variables are simulated based on a time discretization of Equations (1) and (2). Intraday steps are required to capture the possibility of having multiple jumps in a single day and to ensure that the Euler discretization scheme is not too far away from the original model. Appendix B.2.1 provides a detailed description of the simulation step.

The calculation of option realized variances requires the generation of intraday latent quantities. In this regard, an aggregation step is proposed. Specifically, we use the simulation method of Appendix B.2.1 to generate paths on a fine grid (i.e. M intraday values per day). To obtain end-of-day quantities, we aggregate the M simulated values as explained in Appendix B.2.2.

The aggregation produces daily simulated particles:

$$x_{k\Delta} = \left[Y_{k\Delta}, V_{k\Delta}, \Delta I_{(k-1)\Delta,k\Delta}, \Delta QV_{(k-1)\Delta,k\Delta}, \mathbf{IV}_{k\Delta}\left(Y_{k\Delta}, V_{k\Delta}\right), \mathbf{\Delta OQV}_{(k-1)\Delta,k\Delta}\right]$$

where $\Delta I_{(k-1)\Delta,k\Delta}$ is the integrated variance generated as a by-product of the simulation stage, $\Delta QV_{(k-1)\Delta,k\Delta}$ is the simulated quadratic variation derived from the integrated variance and the simulated jumps, $\mathbf{IV}_{k\Delta}\left(Y_{k\Delta}, V_{k\Delta}\right)$ represents the vector of the $n_{k\Delta}$ model implied volatilities based on the simulated log-price and variance values, and $\mathbf{\Delta OQV}_{(k-1)\Delta,k\Delta}$ is the vector of the corresponding option quadratic variation calculated from Equation (10).

Further distributional assumptions about the measurement errors are required to connect the observed variables to the state variables. Since the realized variance is based on a finite sample of returns, it has not converged to its limit. Hence, the relative error in the realized variance follows[20]

$$\frac{\Delta QV_{(k-1)\Delta,k\Delta} - RV_{(k-1)\Delta,k\Delta}}{RV_{(k-1)\Delta,k\Delta}} \sim \mathcal{N}\left(0, \eta_1^2\right). \tag{A.1}$$

Similarly, the relative error between bipower variation and integrated variance is assumed to be normally distributed:

$$\frac{\Delta I_{(k-1)\Delta,k\Delta} - BV_{(k-1)\Delta,k\Delta}}{BV_{(k-1)\Delta,k\Delta}} \sim \mathcal{N}\left(0, \eta_2^2\right). \tag{A.2}$$

[19] There is a vast literature on how many intraday data points should be used to avoid the microstructure noise effect and what procedures can be implemented to get rid of it. This will be discussed in the empirical study section. For now, we assume that realized variance, bipower variation and option realized variance have been measured adequately.

[20] We are aware of Barndorff-Nielsen and Shephard (2002)'s asymptotic results as the number M of intraday observations tends to infinity. However, the time discretization of our empirical implementation is too coarse to pretend that the asymptotic distribution has been reached. In fact, the goal here is to get an estimation procedure as efficient as possible and a large M makes the simulation step very time consuming. The Monte Carlo study shows that good precision is attained with quite small M.

The relative implied volatility error of the i^{th} option of the sample is assumed to have a Gaussian distribution:

$$\frac{IV_{k\Delta,i}\left(Y_{k\Delta},V_{k\Delta}\right)-\sigma_{k\Delta,i}^{BS}}{\sigma_{k\Delta,i}^{BS}}\sim\mathcal{N}\left(0,\eta_3^2\right) \tag{A.3}$$

where $IV_{k\Delta,i}\left(Y_{k\Delta},V_{k\Delta}\right)$ is the model IV and $\sigma_{k\Delta,i}^{BS}$ is the market implied volatility.

Finally, as shown in Protter (2004), $ORV_{(k-1)\Delta,k\Delta,i}$ converges to $\Delta OQV_{(k-1)\Delta,k\Delta,i}$. Again the relative error is presumed to be Gaussian:

$$\frac{\Delta OQV_{(k-1)\Delta,k\Delta,i}-ORV_{(k-1)\Delta,k\Delta,i}}{ORV_{(k-1)\Delta,k\Delta,i}}\sim\mathcal{N}\left(0,\eta_4^2\right). \tag{A.4}$$

All these relative errors are assumed to be independent.

3.2 Estimation

In the SIR method, the proposal distribution depends on the most recent values of state variables. To ensure that the joint estimation is not dominated by one particular source, the likelihood associated with each observation receives a weight inversely proportional to the number of sources of a given type. That is, log-equity price, RV, and BV receive a weight of 1, and σ^{BS} and ORV a weight of one over $n_{k\Delta}$.[21] Based on Assumptions (A.1), (A.2), (A.3) and (A.4), the weighted contribution to the likelihood function at time $k\Delta$ for particle $x_{k\Delta}$ is

$$\begin{aligned}
f\left(z_{k\Delta}\middle|\,x_{k\Delta}\right)=\;&\phi\left(Y_{k\Delta};\mu_{k\Delta},\sigma_{k\Delta}^2\right)\,\phi\left(\frac{\Delta QV_{(k-1)\Delta,k\Delta}-RV_{(k-1)\Delta,k\Delta}}{RV_{(k-1)\Delta,k\Delta}};0,\eta_1^2\right)\\
&\times\phi\left(\frac{\Delta I_{(k-1)\Delta,k\Delta}-BV_{(k-1)\Delta,k\Delta}}{BV_{(k-1)\Delta,k\Delta}};0,\eta_2^2\right)\left(\prod_{i=1}^{n_{k\Delta}}\phi\left(\frac{IV_{k\Delta,i}(Y_{k\Delta},V_{k\Delta})-\sigma_{k\Delta,i}^{BS}}{\sigma_{k\Delta,i}^{BS}};0,\eta_3^2\right)\right)^{1/n_{k\Delta}}\\
&\times\left(\prod_{i=1}^{n_{k\Delta}}\phi\left(\frac{\Delta OQV_{(k-1)\Delta,k\Delta,i}-ORV_{(k-1)\Delta,k\Delta,i}}{ORV_{(k-1)\Delta,k\Delta,i}};0,\eta_4^2\right)\right)^{1/n_{k\Delta}},
\end{aligned}$$

where $\phi(\cdot\,;m,s^2)$ is the density function of a Gaussian variable with mean m and variance s^2. The conditional expectation $\mu_{k\Delta}$ and standard deviation $\sigma_{k\Delta}$ are defined in Appendix B.1. Let

$$f\left(z_{k\Delta}\right)=\frac{1}{N_x}\sum_{x_{k\Delta}}f\left(z_{k\Delta}\middle|\,x_{k\Delta}\right)$$

be the average likelihood at time $k\Delta$ across particles and the log-likelihood function up to time $k\Delta$ to be defined recursively:

$$\mathcal{L}\left(z_{\Delta:k\Delta}\right)\propto\mathcal{L}\left(z_{\Delta:(k-1)\Delta}\right)+\log f\left(z_{k\Delta}\right).$$

As usual in the SIR filter, particles are resampled according to their weights before handling the information of the following day. More precisely, the path $x_{\Delta:(k+1)\Delta}$ is resampled proportionally to its likelihood, that is,[22]

$$\omega\left(x_{\Delta:k\Delta}\right)\propto\omega\left(x_{\Delta:(k-1)\Delta}\right)f\left(z_{k\Delta}\middle|\,x_{k\Delta}\right).$$

Although the particle filter approximation of the likelihood function at any point is asymptotically consistent in the number of particles, the log-likelihood function is not a continuous function of the parameters. Indeed, particle filters are known for being ill-suited for maximum likelihood estimation when using naive resampling methodologies. The likelihood function is not a continuous function of the model parameters and this could cause problems for gradient-based optimizers (e.g. Hürzeler and Künsch, 2001). To circumvent the issue, we use the continuous resampling of Malik and Pitt (2011) which allows for continuous likelihood as a function of the unknown parameters under rather general conditions.

[21] This idea is similar to the weighted likelihood estimator. Hu and Zidek (2002) study the properties of the weighted likelihood estimator and show that the key asymptotic results continue to hold.

[22] Because of our particular resampling strategy, $\omega\left(x_{\Delta:(k-1)\Delta}\right)=1/N_x$, N_x being the number of particles, and the weight reduces to $\omega(x_{k\Delta})\propto f\left(z_{k\Delta}\middle|\,x_{k\Delta}\right)$.

4 Simulation-based results

This section provides simulated-based results using the model proposed in Section 2. Section 4.1 studies the performance of the filter introduced in Section 3 with respect to the information provided by different sources. Section 4.2 analyzes the information conveyed in ORV. Finally, Section 4.3 conducts a robustness test on the approximation employed by the filter in order to compute ORV from intraday option prices.

Table 1 shows the parameters employed in the tests of this section. These parameters are qualitatively consistent with the ones estimated in the current literature, e.g. Eraker et al. (2003) and Eraker (2004), among others.[23,24]

Table 1: Model parameters used in the simulation study.

Log-price process		Variance process		Standard deviations of error terms	
η_Y	0.500	η_V	-0.500	η_1	0.050
γ_Y	0.005	Γ_V	1.000	η_2	0.050
r	0.010	κ	4.000	η_3	0.050
q	0.010	θ	0.020	η_4	0.050
ρ	0.000	σ	0.500		
$\lambda_{Y,0}$	15.000	$\lambda_{V,0}$	15.000		
$\lambda_{Y,1}$	40.000	μ_V	0.030		
μ_Y	–0.020	V_0	0.020		
σ_Y	0.020				
Y_0	log(1000)				

The long-term expected variance $\theta = 0.02$ corresponds to about $\sqrt{0.02} = 14\%$ annualized volatility. The parameter ρ is constrained to zero to reduce the signal to noise ratio, making it more difficult to estimate the volatility. The average log-price jump intensity is 15.8%, meaning that about 16 jumps per year are expected. The log-equity price jumps are on average negative, with an average magnitude of -2% and standard deviation of 2%. The average variance jump is about 3%. The theoretical average diffusive risk premium is given by $\eta_Y\theta = 1\%$. The jump risk premium is about $\gamma_Y\,(\lambda_{Y,0} + \lambda_{Y,1}\theta) = 7.9\%$. Our results are robust to other choices of η_Y and γ_Y. Consistent with most econometric studies, η_V is negative: the $\mathbb{Q}$-measure variance persistence is thus lower than its $\mathbb{P}$ counterpart (3.75 vs. 4, respectively) and the long-term expected variance is higher under the risk-neutral measure (0.0213 vs. 0.02, respectively). Finally, since Γ_V is higher than zero, the average variance jump size under the $\mathbb{Q}$-measure is slightly higher (0.0309) than the one under the physical measure (0.03). Throughout the simulation experiments, we use 50,000 particles in the filter.

4.1 Filter's performance as a function of information

We simulate 100 sample paths of the data generating process (DGP) using the Broadie and Kaya (2006) drift-interpolation scheme of van Haastrecht and Pelsser (2010). The sampling frequency is set at $1/1,560$ of a day (one sample every 15 seconds during a 6.5 hour trading day) and the length of a path is set to one year. Based on a path of the DGP, quantities such as integrated variance and realized variance are computed over a daily frequency. Additional to a path of the DGP, we also compute samples of intraday option prices. Our sample is composed of short-term options (30 days to maturity) with call-equivalent deltas of 0.20, 0.35, 0.50, 0.65, and 0.80, and a sample of long-term options (90 days to maturity) with same call-equivalent deltas. Intraday option prices are used to compute option realized variances for each day, while implied volatilities are deduced from end-of-the-day option prices. To take into account measurement errors, all end-of-day quantities include error terms as defined in Assumptions (A.1) to (A.4). These observations constitute our set of observables, from which the filter is run for different data aggregation periods of $M = 1, 2, 3, 5$, and 10. We regard $M = 15$ as the *true* filter that avoids discretization errors.

We start with a graphical illustration of how different sources of information impact estimates from the filter. Figure 1 compares the true instantaneous variance with five different densities for a randomly selected

[23]They are also consistent with the ones estimated in Subsection 6.1.
[24]A few other specifications have been tested and results were qualitatively robust to these other parameters.

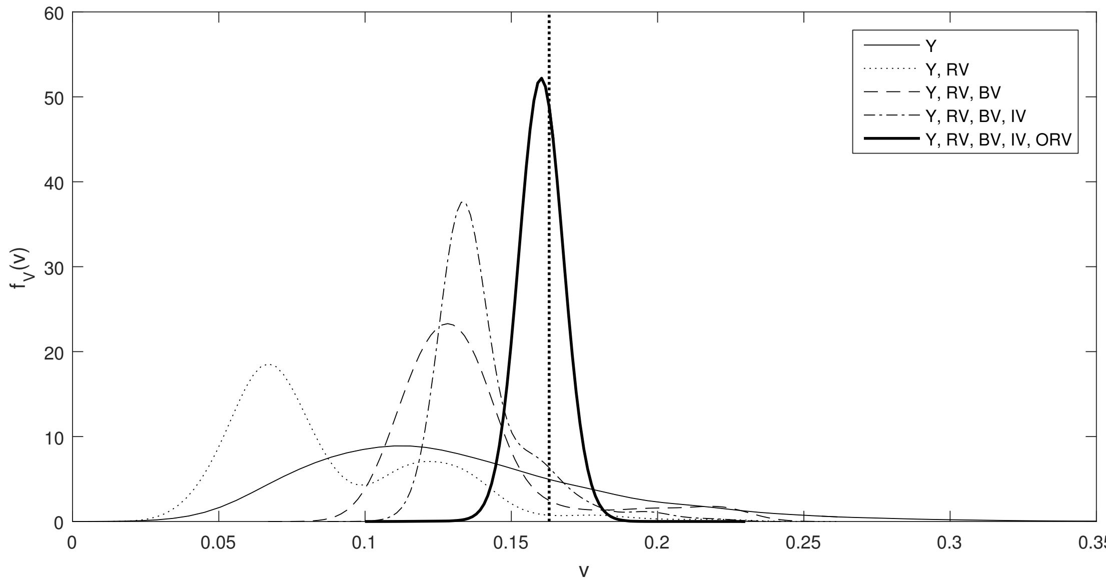

Figure 1: Example of instantaneous variance densities using different data sources. Y means daily log-equity value, RV means realized variance, BV means bipower variation, IV means implied volatility here, and ORV means option realized variance. The parameters of Table 1 are used. The vertical line represents the true instantaneous variance value. The density are constructed by using Gaussian kernels along with simulated particles obtained using the SIR-based methodology.

day during which a variance jump occurred. Each density corresponds to the posterior instantaneous variance density function obtained from running the filter with a specific set of variables (i.e. the information set). When only returns are employed in the filter, we observe that the filter lacks precision as values are highly dispersed on the left of the true value. When BV is included, the distribution exhibits a mode closer to the true value with a heavy tail on the right. However, the main mode still exhibits a downward bias. This shift in the distribution is evidence of the valuable information that BV adds about the presence of return jumps in the total variation. An interesting impact in the distribution is observed when option prices are included in the data set, since the data points cluster closer to the true variance value producing a distribution that is noticeably more peaked, that is, the variability of the estimator is reduced, but the downward bias is still present. Finally, the inclusion of option realized variances centers the distribution around the true value.

We now turn to a more detailed analysis of the filter performance with different information sources. This time we employ the root mean square error (RMSE) to compare the approximate filtered mean with the true filtered one. We also look at the performance of the filter by comparing the approximate filtered mean with the true simulated variable.

Table 2 summarizes the performance of the information source and the filter for different quantities of interest. Consider first the case of the instantaneous variance in Panel A. Notice that no matter which information set is employed, increasing M has little effect on the performance of the filter for this variable. This effect comes as no surprise due to the low discretization bias present at daily frequencies. On the other hand, we do observe large differences depending on the source of information. The most important case corresponds to a fourfold decrease when RV is combined with log-returns. We still observe improvements of about 10% each time other observable variables are included in the information set, which goes in line with the patterns observed in Figure 1. This result complements the findings of Johannes et al. (2009), in which the authors report similar gains when daily option prices are included in addition to asset returns. The large improvement offered by RV is also observed when filtering other measures of variance such as the quadratic variation (Panel B) and the integrated variance (Panel C).

Concerning the performance of jump estimation, Panel D shows results regarding log-equity jump sizes and Panel E does so for volatility jumps. The results indicate that data augmentation benefits the identification of log-equity jump sizes when RV is added to the information set, but it has little effect when other sources are employed. Most of the gains in RMSE come from the inclusion of RV and to some extent from BV.

There is little or no benefit when option prices and ORVs are added. These results contrast with those of volatility jumps, where there is little benefit from including RV in the filter and the largest RMSE gains are observed when ORV is included, yielding an almost threefold decrease in RMSE for $M = 10$. Notice also how data augmentation helps reduce RMSE for volatility jump size estimation, which shows how difficult it is to estimate jumps in volatility at the daily level even if parameters are known. If we look at the sum of the RMSE for both types of jumps, we observe that the information content of ORV is very useful for volatility jump estimation, even with no data aggregation ($M = 1$).

Previous results about jump size estimation are complemented with jump detection results from Table 3. The focus of this set of results is on the ability of a given source to identify the occurrence of jumps. A jump is detected when the filtered jump probability is greater than 50%. This statistic, when compared with a true simulated jump, provides an idea of the general performance of the filter. On the other hand, when the statistic is compared with the filtered jump (a jump detected with the filter using $M = 15$), it quantifies the ability of a given source to identify the occurrence of a jump despite the discretization bias. According to Panel A, the log-equity price jump times are filtered adequately when log-equity values and

Table 2: RMSE for instantaneous variance, integrated variance, quadratic variance, log-equity jump, and instantaneous variance jump across 100 simulated paths.

Panel A: Instantaneous variance

	RMSE (true)					RMSE (filtered)				
M	1	2	3	5	10	1	2	3	5	10
Y	45.3727	45.3084	45.2952	45.4023	45.2129	44.5724	44.4998	44.4871	44.5901	44.4032
Y and RV	13.0213	12.7496	12.6884	12.8059	12.7801	10.7389	10.3756	10.3173	10.4251	10.4052
Y, RV and BV	9.4220	9.2457	9.2334	9.1858	9.1822	6.0334	5.7427	5.6798	5.5678	5.5961
Y, RV, BV and IV	8.5055	7.8533	7.5305	7.5164	7.4777	5.3885	4.6257	4.0116	4.0009	3.9404
Y, RV, BV, IV and ORV	7.4964	6.2555	6.1310	6.0846	6.0782	4.8187	2.1469	1.8278	1.7732	1.7131

Panel B: Quadratic variation increment

	RMSE (true)					RMSE (filtered)				
M	1	2	3	5	10	1	2	3	5	10
Y	0.3121	0.3116	0.3120	0.3125	0.3118	0.3082	0.3074	0.3079	0.3085	0.3077
Y and RV	0.0304	0.0304	0.0311	0.0313	0.0310	0.0249	0.0245	0.0254	0.0255	0.0256
Y, RV and BV	0.0278	0.0282	0.0283	0.0291	0.0286	0.0210	0.0203	0.0209	0.0218	0.0212
Y, RV, BV and IV	0.0287	0.0278	0.0278	0.0287	0.0279	0.0214	0.0202	0.0202	0.0216	0.0212
Y, RV, BV, IV and ORV	0.0292	0.0203	0.0202	0.0216	0.0208	0.0259	0.0147	0.0157	0.0164	0.0148

Panel C: Integrated variance increment

	RMSE (true)					RMSE (filtered)				
M	1	2	3	5	10	1	2	3	5	10
Y	0.1753	0.1752	0.1752	0.1758	0.1750	0.1738	0.1737	0.1737	0.1742	0.1734
Y and RV	0.0363	0.0351	0.0350	0.0353	0.0351	0.0325	0.0311	0.0310	0.0314	0.0311
Y, RV and BV	0.0173	0.0169	0.0170	0.0170	0.0169	0.0096	0.0091	0.0090	0.0090	0.0090
Y, RV, BV and IV	0.0209	0.0162	0.0159	0.0159	0.0158	0.0142	0.0085	0.0079	0.0079	0.0078
Y, RV, BV, IV and ORV	0.0271	0.0129	0.0119	0.0116	0.0114	0.0234	0.0060	0.0044	0.0042	0.0040

Panel D: Log-equity jump

	RMSE (true)					RMSE (filtered)				
M	1	2	3	5	10	1	2	3	5	10
Y	6.2694	6.2618	6.2613	6.2577	6.2576	5.9798	5.9723	5.9721	5.9718	5.9724
Y and RV	2.2770	2.2232	2.2296	2.2608	2.2431	1.5404	1.4689	1.4931	1.5001	1.5047
Y, RV and BV	1.8560	1.8554	1.8715	1.9002	1.8427	0.9038	0.8786	0.9379	0.9998	0.9654
Y, RV, BV and IV	1.9777	1.8463	1.8800	1.8820	1.8203	1.0732	0.8666	0.9402	0.9799	0.9765
Y, RV, BV, IV and ORV	3.9788	1.9680	1.8765	1.9214	1.8785	3.5345	1.0410	1.0325	0.9730	0.9531

Panel E: Instantaneous variance jump

	RMSE (true)					RMSE (filtered)				
M	1	2	3	5	10	1	2	3	5	10
Y	9.8003	9.7880	9.7880	9.7862	9.7837	9.3859	9.3742	9.3746	9.3737	9.3705
Y and RV	9.8022	9.1877	9.1002	9.0421	9.0619	9.3878	8.7586	8.6670	8.6477	8.6606
Y, RV and BV	9.8147	8.6952	8.4181	7.9956	7.9411	9.4020	8.2883	7.9502	7.5375	7.4418
Y, RV, BV and IV	9.0258	6.2434	5.8524	5.7860	5.7234	8.5814	5.7711	5.3274	5.2712	5.2238
Y, RV, BV, IV and ORV	4.5677	2.0562	1.9963	1.9173	1.9068	4.2681	0.9991	0.9616	0.9880	0.9240

[1] Y means daily log-equity, RV means realized variance, BV means bipower variation, IV means implied volatility, and ORV means option realized variance.
[2] Quantities were multiplied by 1,000.
[3] Filtered values are computed as the mean of resampled particles obtained via a SIR particle filter with $M = 15$ and using Y, RV, BV, IV and ORV.

Table 3: Average jump times in percentages.

Panel A: Average log-equity jump times	Hit (true)					Hit (filtered)				
M	1	2	3	5	10	1	2	3	5	10
Y	93.61	93.63	93.64	93.65	93.65	95.30	95.33	95.34	95.35	95.35
Y and RV	96.85	96.97	96.97	96.97	96.96	98.65	98.77	98.78	98.76	98.76
Y, RV and BV	97.90	97.90	97.90	97.89	97.86	99.77	99.76	99.77	99.76	99.74
Y, RV, BV and IV	97.94	97.92	97.92	97.92	97.89	99.78	99.78	99.77	99.78	99.77
Y, RV, BV, IV and ORV	98.29	98.00	97.95	97.95	97.91	99.87	99.85	99.81	99.82	99.82

Panel B: Average log-equity jump times	Hit (true)					Hit (filtered)				
M	1	2	3	5	10	1	2	3	5	10
Y	94.08	94.08	94.08	94.08	94.08	96.53	96.53	96.53	96.53	96.53
Y and RV	94.08	94.15	94.29	94.41	94.48	96.53	96.60	96.73	96.88	96.94
Y, RV and BV	94.08	94.47	94.79	95.03	95.12	96.53	96.91	97.24	97.48	97.58
Y, RV, BV and IV	94.31	95.21	95.33	95.37	95.38	96.76	97.67	97.79	97.83	97.85
Y, RV, BV, IV and ORV	97.60	97.33	97.29	97.31	97.33	99.74	99.80	99.78	99.80	99.79

[1] In this table, we show the average number of times a jump has been adequately filtered (i.e. whether the probability of having a jump on a given day is higher than 0.5). Hit reveals the proportion of time that jumps are adequately filtered.
[2] Y means daily log-equity, RV means realized variance, BV means bipower variation, IV means implied volatility, and ORV means option realized variance.
[3] Filtered values are computed as the mean of resampled particles obtained via a SIR particle filter with $M = 15$ and using Y, RV, BV, IV and ORV.

realized variance are included, with a level of concordance of about 96.9% (98.7% with the discretization bias). This level is slightly improved when more sources are employed. As observed with jump sizes, the detection of volatility jumps is improved when ORV are employed, with concordance levels of 97.3% (99.7% with the discretization bias).

4.2 Information embedded in ORV

The previous tests highlight the benefit of using ORV as a source for disentangling jumps and volatility in the filtering process. The tests conducted in this section study the link between ORV and information contained in RV and jumps.

The first experiment consists of simulating 1,000 paths of one day for which there are no jumps in the DGP. Each path is generated at a frequency of $1/1,560$ of a day using the Broadie and Kaya (2006) drift-interpolation scheme of van Haastrecht and Pelsser (2010). Each time a path is simulated, the parameters of a 30-day European call option are simulated so that ORV can be computed along the path. The option's delta is uniformly simulated between 0.1 and 0.9 and the initial spot variance between 0.01 and 0.10.

The simulated data produces daily values of RV and ORV for a random sample of options, which allows us to measure the degree of redundancy between these two variables with the following regression:

$$ORV_i = \gamma_1 \left(\frac{\partial O_i}{\partial y}\right)^2 RV_i + \gamma_2 \left(2\frac{\partial O_i}{\partial y}\frac{\partial O_i}{\partial v}\right) RV_i + \gamma_3 \left(\frac{\partial O_i}{\partial v}\right)^2 RV_i + \varepsilon_i. \tag{12}$$

This regression model comes from fixing the option derivatives in Equation (10) to their beginning-of-the-day values, so that the impacts of changes in RV are only modulated by option parameters from sample to sample.

Table 4 reports estimate results of the regression. The R-squared close to one reveals that, in the absence of jumps, ORV is redundant with respect to the information embedded in RV. That is, ORV only amplifies or attenuates values of RV depending on the parameters of the option. Regarding regression estimates, we observe that the individual hypothesis that $\gamma_1 = 1$, $\gamma_2 = 2\sigma\rho = 0$, and $\gamma_3 = \sigma^2 = 0.25$ cannot be rejected with a confidence level of 95%, suggesting that this specification follows Equation (10) closely with the assumption of constant option derivatives. This last remark supports the sampling technique used in the filter to compute particles of ORV with few intraday samples, as option derivatives vary little between days.

Table 4: Information Content of ORV when Jumps are Absent.

	Coefficient	Standard error
γ_1	1.0136	0.0156
γ_2	-0.0234	0.0674
γ_3	0.4356	0.2552
R^2	0.9891	

[1] The following regression is applied to ORV:

$$ORV_i = \gamma_1 \left(\frac{\partial O_i}{\partial y}\right)^2 RV_i + \gamma_2 \left(2\frac{\partial O_i}{\partial y}\frac{\partial O_i}{\partial v}\right) RV_i + \gamma_3 \left(\frac{\partial O_i}{\partial v}\right)^2 RV_i + \varepsilon_i.$$

The derivatives are computed based on beginning-of-the-day information.
[2] Values in bold are statistically different (at a confidence level of 95%) from their theoretical values (i.e. 1, 0, and 0.25 respectively).
[3] We use a simulated sample of 1000 observations.

We now proceed to analyze the impact that jumps in the underlying process might have on the information content of ORV. The experiment is run this time by taking into account the specificity of the option contract. To do this, we fix in advance the option type (call or put) and the call-equivalent delta (0.20, 0.35, 0.50, 0.65, and 0.8), and then the daily ORV is computed from the path generated by the simulation algorithm. The following regression is run separately for each type of contract and moneyness:

$$\log(ORV_i) = \beta_0 + \beta_1 \log(RV_i) + \beta_2 \Delta N_{Y,i} + \beta_3 \Delta N_{V,i} + \varepsilon_i \tag{13}$$

where $\Delta N_{Y,i}$ and $\Delta N_{V,i}$ are variables that capture the number of log-equity price jumps and variance jumps during day i, respectively.

Table 5 presents two specifications of the previous regression model. The first one includes information about log-return jumps and the second one adds to this specification information about volatility jumps. Taking R-squared as a measure of redundancy, we observe that RV and ORV are more redundant when the option is in-the-money (delta higher than 0.5 for calls and lower than 0.5 for puts). As the option becomes out-of-the-money, redundancy decreases. A closer look at the coefficients in this regression show the sensitiveness of ORV to different types of information. Whereas the coefficient associated to RV increases with the moneyness of the option, those associated with jump activity do so (in absolute value) when the moneyness decreases. These two pieces of evidence show that the ORV of OTM options provides complementary information not contained in RV.

4.3 Option quadratic variation increments approximation

One of the key features of the filter proposed in Section 3 is that a few number of intraday prices are required to compute ORV. We test this approximation by studying the impact of M on the computation of ORV.

Using the parameters given in Table 1, we simulate 500 paths at a frequency of $1/1,560$ over a day and compute the option realized variance for a call along each path. Next, the simulated ORV is compared to approximations of this quantity, denoted by ΔOQV, which are computed with a lower number of intraday observations $M \in \{1; 2; 3; 5; 10; 1,560\}$. The maturity of the options used in this exercise is 30 days. As a measure of the quality of the approximation, we compute the RMSE and relative RMSE that result from comparing the ORV computed at the highest frequency with that of the approximation. We also regress ΔOQV on ORV and employ the R-squared of this regression as a measure of the quality of the fit.[25]

Table 6 shows the root mean square errors (RMSE), relative RMSE, and regression R-squareds for different levels of moneyness. As expected, we find that errors decrease as M becomes larger and that with as few as $M = 5$ observations per day the approximation provides satisfactory results. Note that the presence of jumps has an apparent impact on the performance of the approximation, which is not surprising as these rare events introduce more variation in the estimation.

[25] We run the following regression: $\Delta OQV_i = \beta_0 + \beta_1 ORV_i + \varepsilon_i$ and compute the R-squared associated with it. The higher the R-squared, the better the quality of the approximation.

Table 5: Information Content of ORV when Jumps are Present.

		Call					Put			
Δ^e		(1)		(2)			(1)		(2)	
		Coefficient	SE	Coefficient	SE		Coefficient	SE	Coefficient	SE
0.20	β_0	13.945	(0.383)	11.161	(0.327)	β_0	14.149	(0.080)	13.811	(0.080)
	β_1	1.333	(0.041)	1.045	(0.035)	β_1	1.079	(0.008)	1.044	(0.008)
	β_2	-1.064	(0.086)	-0.582	(0.071)	β_2	-0.111	(0.018)	-0.052	(0.017)
	β_3			1.067	(0.045)	β_3			0.129	(0.011)
	R^2	0.627		0.763		R^2	0.978		0.981	
0.35	β_0	13.796	(0.285)	11.805	(0.249)	β_0	14.757	(0.138)	14.018	(0.132)
	β_1	1.199	(0.030)	0.994	(0.026)	β_1	1.187	(0.015)	1.111	(0.014)
	β_2	-0.726	(0.064)	-0.382	(0.054)	β_2	-0.265	(0.031)	-0.137	(0.029)
	β_3			0.763	(0.034)	β_3			0.283	(0.018)
	R^2	0.742		0.829		R^2	0.943		0.954	
0.50	β_0	13.681	(0.215)	12.278	(0.194)	β_0	15.303	(0.192)	14.177	(0.179)
	β_1	1.119	(0.023)	0.974	(0.020)	β_1	1.297	(0.020)	1.181	(0.019)
	β_2	-0.497	(0.048)	-0.255	(0.042)	β_2	-0.426	(0.043)	-0.231	(0.039)
	β_3			0.538	(0.026)	β_3			0.432	(0.024)
	R^2	0.833		0.882		R^2	0.903		0.926	
0.65	β_0	13.548	(0.141)	12.740	(0.133)	β_0	15.910	(0.258)	14.272	(0.235)
	β_1	1.048	(0.015)	0.964	(0.014)	β_1	1.448	(0.027)	1.278	(0.025)
	β_2	-0.282	(0.031)	-0.142	(0.029)	β_2	-0.648	(0.058)	-0.364	(0.051)
	β_3			0.310	(0.018)	β_3			0.628	(0.032)
	R^2	0.922		0.940		R^2	0.853		0.894	
0.80	β_0	13.470	(0.083)	13.079	(0.082)	β_0	16.273	(0.323)	14.136	(0.288)
	β_1	1.004	(0.009)	0.964	(0.009)	β_1	1.596	(0.034)	1.375	(0.030)
	β_2	-0.131	(0.019)	-0.064	(0.018)	β_2	-0.883	(0.072)	-0.514	(0.063)
	β_3			0.150	(0.011)	β_3			0.819	(0.039)
	R^2	0.972		0.976		R^2	0.806		0.865	

[1] The following regression is applied to ORV:

$$\log(ORV_i) = \beta_0 + \beta_1 \log(RV_i) + \beta_2 \Delta N_{Y,i} + \beta_3 \Delta N_{V,i} + \varepsilon_i$$

where $\Delta N_{Y,i}$ is the number of log-equity price jumps jump during day i and $\Delta N_{V,i}$ is the number of variance jumps jump during day i.
[2] We estimate two versions of Equation (13): Regression (1) we force $\beta_3 = 0$, and Regression (2) we let β_3 be different than zero.
[3] R^2 and Newey and West (1987) standard errors (SE, in parentheses) are reported. All coefficients estimated are statistically significant at a confidence level of 95%.

To visualize the performance of the approximation, Figure 2 plots ORV and their approximations ΔOQV for days without (top panels) and with jumps (bottom panels), respectively. If ΔOQV constitutes a good approximation of ORV, all the points should be aligned on the diagonal, as it is the case for $M = 1,560$. Note that ΔOQV approaches to ORV for values of $M = 3$ and higher.

5 Exploring option realized variances empirically

In this section, we first present our datasets. Next, we analyze nonparametrically the information contained in option realized variances. This is done by constructing surfaces of these variations. We complement this investigation with a principal component analysis (PCA) of option realized variances. Finally, we provide evidence of the economic relationship between option realized variances and index return variability using predictive regressions.

Table 6: RMSE, relative RMSE and regression R-squared for ΔOQV approximation across 500 days.

Panel A: RMSE

	Days without jumps					Days with jumps				
Δ^e	0.2	0.35	0.5	0.65	0.8	0.2	0.35	0.5	0.65	0.8
1	0.867	1.851	2.794	1.295	0.563	21.925	35.893	55.659	62.941	30.808
2	0.458	1.006	1.599	0.713	0.295	16.286	28.140	45.653	58.119	28.371
3	0.311	0.711	1.191	0.560	0.220	14.131	22.775	32.613	37.994	20.383
5	0.232	0.559	0.987	0.449	0.169	11.956	15.303	20.103	20.851	12.772
10	0.172	0.462	0.855	0.381	0.137	8.960	13.258	18.675	19.392	11.282
1560	0.146	0.433	0.806	0.348	0.126	0.725	1.714	2.924	1.890	0.787

Panel B: Relative RMSE

	Days without jumps					Days with jumps				
Δ^e	0.2	0.35	0.5	0.65	0.8	0.2	0.35	0.5	0.65	0.8
1	0.205	0.151	0.121	0.141	0.175	0.289	0.240	0.205	0.176	0.199
2	0.109	0.081	0.068	0.076	0.089	0.209	0.179	0.158	0.144	0.159
3	0.077	0.058	0.052	0.059	0.065	0.141	0.118	0.103	0.108	0.120
5	0.057	0.046	0.043	0.046	0.049	0.111	0.091	0.077	0.077	0.089
10	0.043	0.039	0.038	0.040	0.040	0.091	0.079	0.069	0.070	0.078
1560	0.038	0.038	0.036	0.037	0.038	0.026	0.027	0.027	0.025	0.024

Panel C: Regression R-squareds

	Days without jumps					Days with jumps				
Δ^e	0.2	0.35	0.5	0.65	0.8	0.2	0.35	0.5	0.65	0.8
1	0.439	0.475	0.532	0.585	0.573	0.915	0.892	0.864	0.916	0.918
2	0.867	0.861	0.855	0.889	0.899	0.953	0.935	0.910	0.926	0.928
3	0.944	0.933	0.922	0.930	0.941	0.964	0.957	0.952	0.960	0.956
5	0.967	0.957	0.946	0.954	0.963	0.977	0.981	0.981	0.988	0.981
10	0.978	0.968	0.958	0.965	0.973	0.987	0.985	0.984	0.989	0.985
1560	0.981	0.970	0.960	0.969	0.976	1.000	1.000	1.000	1.000	1.000

[1] The real ORV value is computed using option prices at a frequency of 1/1,560. The error corresponds to the difference between ΔOQV and ORV.
[2] 0.20, 0.35, 0.50, 0.65 and 0.80 correspond to the different call-equivalent deltas considered.
[3] The OTM option maturity is 30 business days. ORVs are compared to six different values for which various M are used (i.e. 1, 2, 3, 5, 10 and 1,560).
[4] To compute the R-squared, we run the following regression: $\Delta OQV_i = \beta_0 + \beta_1 ORV_i + \varepsilon_i$.

5.1 Data

The sample period employed in this study is from July 2004 to December 2012. This period offers several empirical features such as periods of high economic uncertainty, which makes it appealing for studying different empirical features of equity index returns and volatility.

We start by constructing a time series measure of the option realized variance at the daily level. We employ tick-by-tick Level I quote data provided by Tick Data for European options written on the S&P 500 index. Tick Data prices come from the Options Price Reporting Authority (OPRA), the national market system that provides information about last sale reports and quotation information. We employ midquote prices instead of trade prices to mitigate the effect of bid-ask spread bounces in the total variation of the option price. For each trading day, we start with 390 one-minute prices from 9:30 AM to 4:00 PM. Next, we construct five different grids with five-minute prices and compute the daily variation according to Equation (11) over each grid. The average of these five values provides an estimate of the option daily variation. This procedure helps to mitigate the presence of microstructure noise, as suggested by Zhang et al. (2005) for the case of realized volatility estimation. For a quote to be included in the dataset, we require its bid price to be higher than zero and the quote not to have any condition code or be eligible for automatic execution.[26,27] Each day,

[26] Our final ORV dataset contains 682,380 data points, for an average of 286 option realized variance per day.
[27] Errors in the option quote dataset could artificially increase the computed ORV. To discard such outliers, the last permille (0.1%) of the ORV sample (i.e. largest values) is removed.

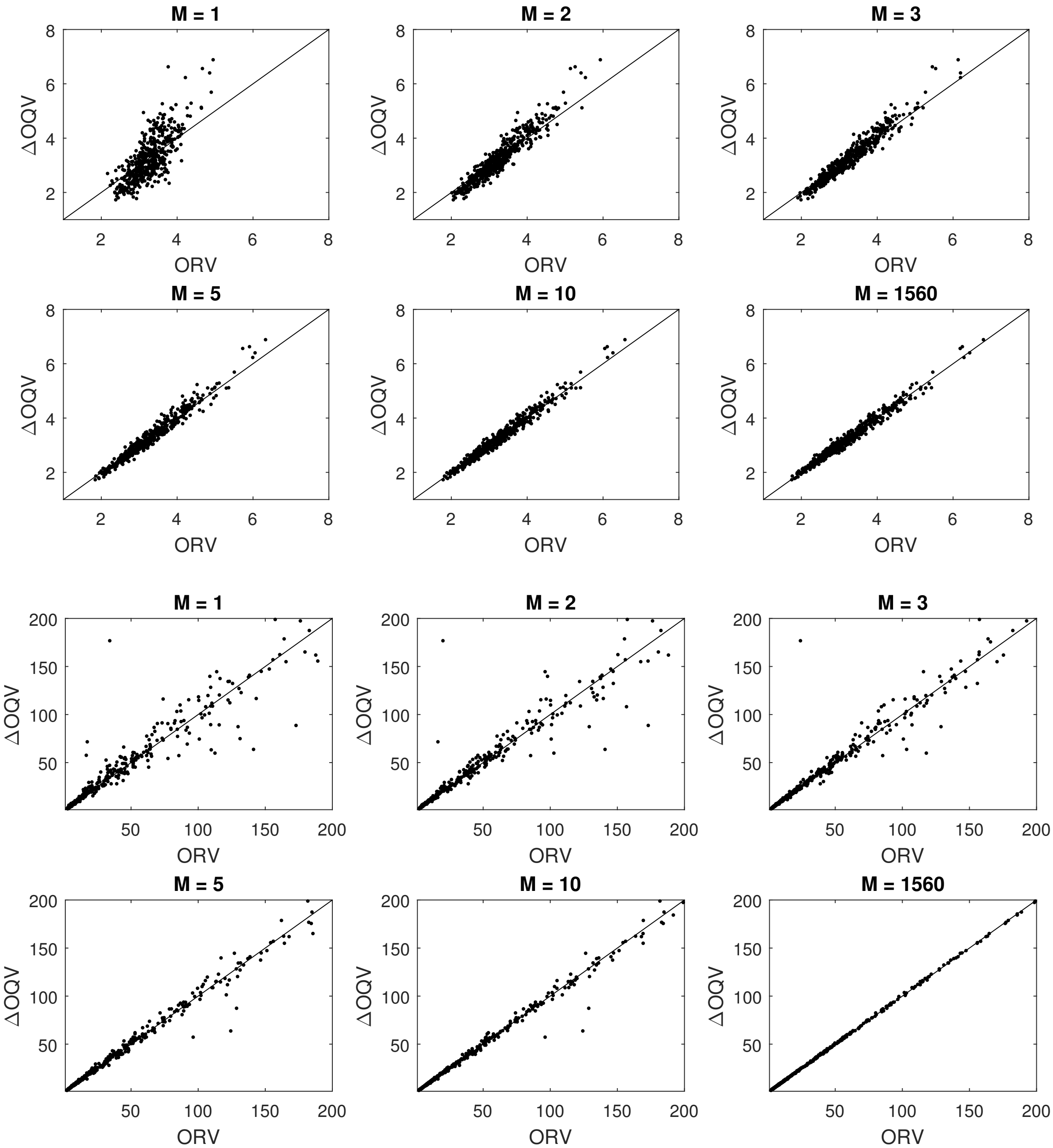

Figure 2: Option realized variance against option quadratic variance increments for a call-equivalent delta of 0.50 and a maturity of 30 business days, on days without (top panels) and without jumps (bottom panels). This figure is generated using 500 simulated paths of one day and a European call option that has a call-equivalent delta of 0.50 and a maturity of 30 business days. These paths contain no jump. ORVs are compared to six different values for which various M are used (i.e 1, 2, 3, 5, 10 and 1,560). Parameters of Table 1 are used.

we restrict our attention to a representative sample set composed of OTM and ATM options with maturities closest to 30 and 90 business days. As was argued in Section 2.2, ORVs for ITM options yield equivalent information to that of RV, so we exclude these options from our sample. Only options with positive volume and bid prices are included in the sample, as well as those satisfying the no-arbitrage conditions of Bakshi et al. (1997).

Additional to the option's price variation, we compute several variables that capture different aspects of market activity for each day in the sample. The first is the daily Black-Scholes implied volatility (IV), which is computed for the option with a forward-to-strike ratio closest to 1 (ATM option) and a maturity closest to 30 business days. The second is the realized variance RV of index returns, constructed from one-minute returns of the E-mini S&P futures contract prices. Finally, the third variable is the bipower variation BV, which accounts for the variability of the diffusive component governing the return process. These last two variables are constructed with five sub-grids, following Zhang et al. (2005) sub-sampling methodology. Descriptive statistics about these variables and the panel of option realized variances are provided in the Internet appendix D.

Figure 3 presents the time series associated with some of these variables. It shows in the first three panels the daily time series of the previous three variables and in the last panel the option realized variance time series for the ATM option with a maturity of 30 business days. We observe that all series increase during the financial crisis period and exhibit sporadic spikes across the sample following the flash crash episode (May 6, 2010) and the downgrade of U.S. debt (August 5, 2011). This commonality shows the degree of interdependence across different markets in response to important events. We now proceed to explore in more detail the full panel of option realized variances.

5.2 Understanding option realized variances

The surfaces (indexed by time) constitute a parsimonious way to study and understand the behaviour of option prices, as shown in Andersen et al. (2015b). In opposition to previous authors who studied implied volatilities, we analyze the behaviour of option realized variances. To interpret the large cross section of option data that spans distinct maturities and moneynesses, we construct a sequence of option realized variance surfaces across these two dimensions. For a given day, we collect the ORVs for all the ATM and OTM options in our dataset and perform a locally weighted scatter plot smoothing across moneynesses and maturities.[28] Figure 4 shows the surface induced by option realized variances on July 6, 2004. As it is clear from the figure, the surface has an inverted U-shape, in which the highest values are observed for options that are at-the-money and the lowest for those that are out-of-the-money.

Following Andersen et al. (2015b), Figure 5 presents specific ORV surface characteristics such as its level, term structure, skew, and skew term structure across time. The ORV level comes from the ATM option ($\Delta^{\mathrm{e}} = 0.5$) with 30 days to maturity. The ORV term structure (TS) is defined as the difference between the ORV of the ATM with 90 days to maturity minus the ORV of the ATM option with 30 days to maturity. The ORV skew represents the difference between shorter dated OTM put options (i.e. $\Delta^{\mathrm{e}} = 0.9$) and OTM call options (i.e. $\Delta^{\mathrm{e}} = 0.1$), both with 30 days to maturity. Finally, the ORV skew term structure (Skew TS) is the difference between longer and shorter dated skew, with the longer dated (i.e. 90 business days) skew defined analogously to the shorter one.

The surface level presents sporadic spikes that generate some persistence after their occurrence (top-left panel of Figure 5). ATM options exhibit realized variations that mimic the behaviour of the underlying realized variance (top-left and bottom-middle panels of Figure 5, as well as Table 7 showing that the correlation coefficient between the level and RV is 92%). Consequently, ATM option realized variance brings little new information when RV or BV are part of the sample. The sporadic spikes are also observed at the same times in the other characteristics of the surface (top-middle, top-right and bottom-left panels of Figure 5), showing a level of commonality associated with large shocks. Since the other surface characteristics present no sign of persistence and fluctuate around zero, this behaviour reveals that these characteristics are particularly elevated during turbulent market periods. More precisely, ORV term structure (top-middle panel of Figure 5) shows that shocks are more important for short-dated options. Its low correlation with RV and $\max(RV - BV, 0)$ (see Table 7) indicates that the ORV term structure is a non-redundant information source. Regarding the ORV skew (top-right panel of Figure 5), this characteristic generally takes positive values, which means that OTM puts are more responsive to shocks than OTM calls. This type of responsiveness is observed more for short dated options than for longer dated ones, as evidenced from the negative sign associated with values of the skew term structure (bottom-left panel of Figure 5).

Figure 5 also presents realized volatility and realized jump variation, defined as $\max(RV - BV, 0)$, of index returns. Realized jump variation captures the variability induced by discontinuous activity in the index return, which explains its erratic spikes and less persistent behaviour. Sparks in different characteristics of

[28] The locally smoothing quadratic regression is performed using Matlab procedure Lowess on $\log(ORV)$, and then transformed back to ORV. The Matlab procedure performs a local regression using weighted linear least squares with a 2nd degree polynomial model.

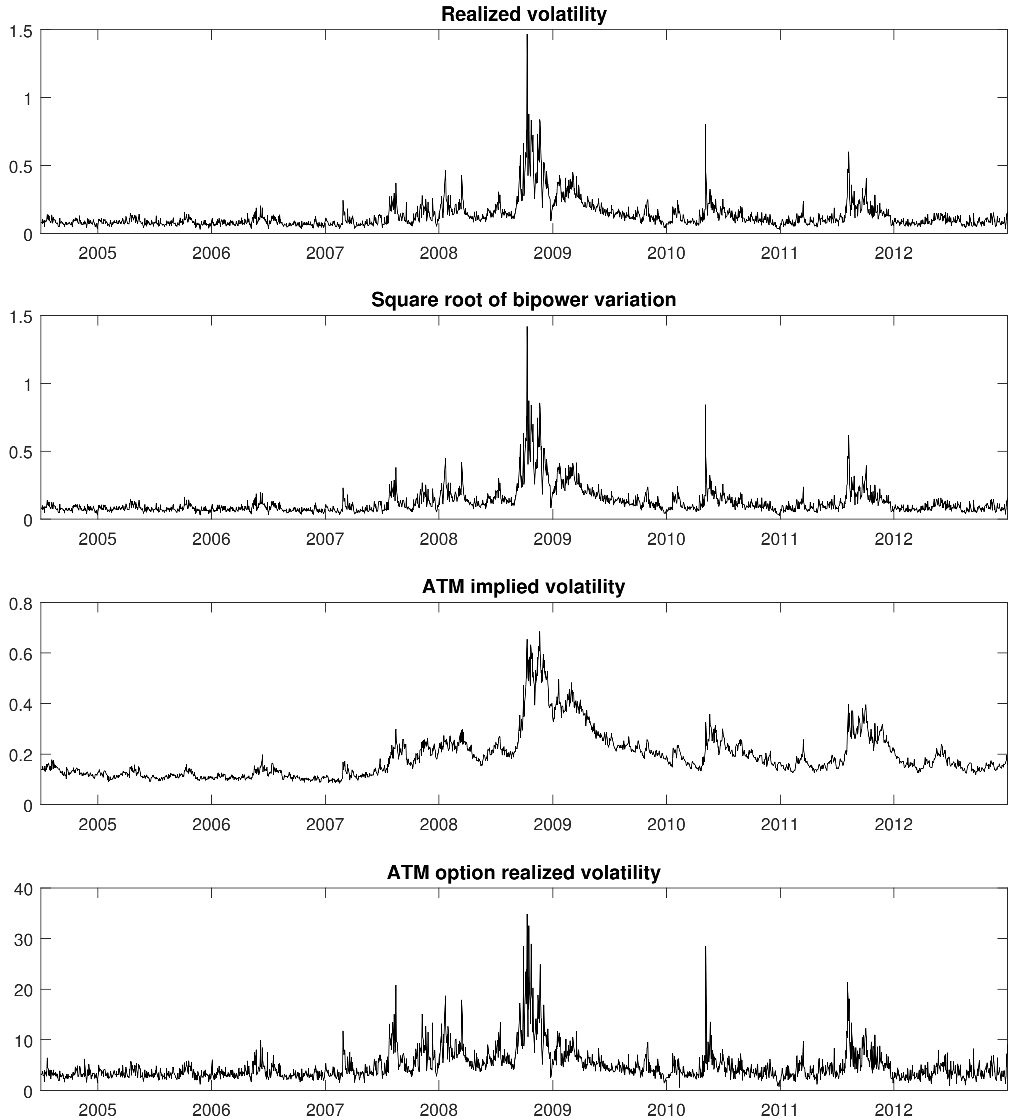

Figure 3: Realized volatility, square root of the bipower variation, ATM option implied volatility for options with maturity closest to 30 business days and ATM option realized volatility (square root of ORV) for options with maturity closest to 30 business days. Annualized realized variance and bipower variation are computed from intraday S&P futures prices. Since futures are quarterly contracts, we build a time series from these data by rolling contracts two weeks before expiration. We follow Zhang et al. (2005) and compute a microstructure-noise robust estimate of the daily realized variance as the average of RV and BV estimates based on different subsets of prices. To compute the daily realized variance of an option, we employ tick-by-tick Level I quote data from options provided by Tick Data. From the data, we construct one-minute midquote series and compute the daily variation according to Equation (11). We again follow Zhang et al. (2005) and compute a microstructure-noise robust estimate of the daily option realized variance. Each time series is displayed from July 2004 to December 2012.

the ORV surface are associated with shocks to realized variance and jump activity of the option's underlying asset (Figure 5 and Table 7).

We now employ the principal component analysis (PCA) of the ORV surface to look more closely at different aspects of the commonality among ORV surface characteristics, realized variance, and jump activity of the S&P index. We extract from the ORV surface 18 values per day and conduct a PCA over these values for the full sample. More precisely, we take nine equally spaced points over the call-equivalent delta dimension between 0.1 and 0.9 for maturities of 30 and 90 business days.

Figure 6 shows the first six in-sample principal components (PCs) of the option realized variance surface. Similar to what is observed for the implied volatility surface in Andersen et al. (2015b), the ORV surface displays a dominant level type effect, as the first PC accounts for 94.44% of the total variation and displays a high degree of commonality with the surface level (top-left panel of Figure 6). The second PC captures 4.73%

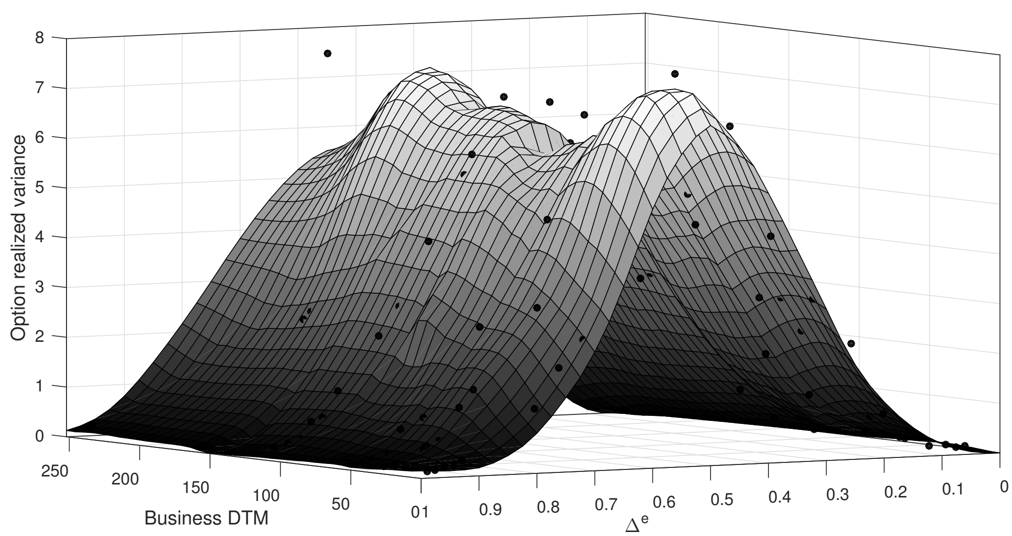

Figure 4: Option realized variances and fitted surface as a function of both the option Black and Scholes (1973) call-equivalent delta and business days to maturity. Option realized variances are computed using the daily variation according to Equation (11). The example is given for July 6, 2004. The fitted surface uses the locally smoothing quadratic regression method.

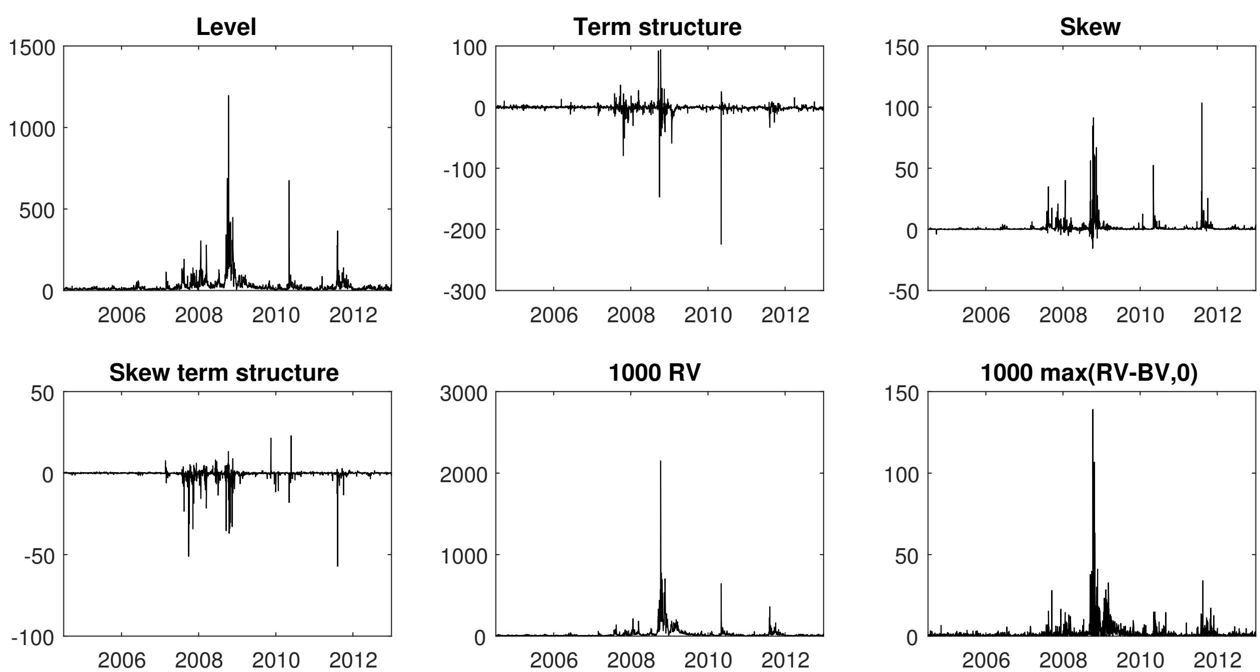

Figure 5: Option realized variance surface characteristics and realized measures. The option realized variance level is the option realized volatility for ATM options (i.e. $\Delta^e = 0.5$ and 30 business days). The option realized volatility term structure is the difference between long- and short-dated ATM options (i.e. 90 and 30 business days in our case). The option realized variance skew is the difference between short-dated OTM put options (i.e. $\Delta^e = 0.9$, 30 business days) and OTM call options (i.e. $\Delta^e = 0.1$, 30 business days). The option realized volatility skew term structure is the difference between long- and short-dated skew, with the long-dated (i.e. 90 business days) skew defined analogously to the short one. The realized volatility and the bipower variation are computed using Zhang, Mykland, and Aït-Sahalia's (2005) microstructure-noise robust estimate.

Table 7: Correlation matrix for option realized variance characteristics and realized measures.

	Level	TS	Skew	Skew TS	RV	$\max(RV - BV, 0)$
Level	1.000					
TS	-0.260	1.000				
Skew	0.630	0.049	1.000			
Skew TS	-0.384	-0.098	-0.763	1.000		
RV	0.920	-0.099	0.675	-0.390	1.000	
$\max(RV - BV, 0)$	0.626	-0.008	0.423	-0.217	0.703	1.000

[1] The option realized variance level is the option realized variance for ATM options (i.e. $\Delta^e = 0.5$).
[2] The option realized variance term structure (TS) is the difference between longer and shorter dated ATM options (i.e. 90 and 30 business days in our case).
[3] The option realized variance skew is the difference between shorter dated OTM put options (i.e. $\Delta^e = 0.9$, 30 business days) and OTM call options (i.e. $\Delta^e = 0.1$, 30 business days).
[4] The option realized variance skew term structure (Skew TS) is the difference between longer and shorter dated skew, with the longer dated (i.e. 90 business days) skew defined analogously to the shorter one.
[5] The realized variance and the bipower variation are computed using Zhang, Mykland, and Aït-Sahalia's (2005) microstructure-noise robust estimate and are multiplied by 1000.

of the total variation, while the following ones account for 0.32%, 0.18%, 0.11%, and 0.05%, respectively (all the panels of Figure 6, except for the top-left panel).

We now turn to the question of how much information is shared between ORV surface characteristics (or variations of the index returns) and the principal components. The aim of this exercise is to determine whether the ORV surface can be summarized in one simple specification (e.g. the first component of a PCA) or whether different ORV measures are needed to appropriately capture the nonlinear changes in the surface. Indeed, we have no guarantee that extracted PCs would represent the whole surface adequately as nonlinear behaviour cannot be captured efficiently by a few summaries of the said surface.

This analysis is performed by computing in-sample regressions of these variables on PCs as follows:

$$\mathrm{Char}_t = \beta_0 + \beta_1 \mathrm{PC}_{1,t} + \beta_2 \mathrm{PC}_{2,t} + \beta_3 \mathrm{PC}_{3,t} + \beta_4 \mathrm{PC}_{4,t} + \beta_5 \mathrm{PC}_{5,t} + \beta_6 \mathrm{PC}_{6,t} + \varepsilon_t,$$

where Char_t is the characteristic of interest at time t (i.e. Level, TS, Skew, Skew TS, RV and $\max(RV - BV, 0)$) and $\mathrm{PC}_{n,t}$ represents the n^{th} principal component at time t. Newey and West (1987) regressions are run to account for heteroskedasticity and autocorrelation.

Table 8 displays regression coefficients, standard errors, R-squares, and autocorrelations in the residuals. Observe that PCs are associated with surface characteristics and index return variations, as well, providing further evidence of the commonality existing between these two sets of variables. This commonality effect is largely driven by the first PC, as other PCs are not always statistically significant at explaining index return variations. Notice also that PCs are successful at capturing the behaviour of index return variations, as evidenced from R-square values of 90% for realized variance and 45% for realized jump variation. However, PCs impact these variables differently, suggesting that the information contained in the surface is impounded differently in these variations. This difference is also evidenced by looking at the persistence of regression residuals, which have different autocorrelation patterns. Persistent residuals in the realized variance regression suggest that either the relation is nonlinear, or that there are missing factors in the model (e.g. lag values of RV). On the other hand, the jump realized variation regression exhibits low persistent residuals.

What can we learn from these results? First, option realized variations are intertwined with measures of index return variation, revealing an important degree of commonality that is useful for analyzing index return dynamics such as variances and sporadic shocks. Notwithstanding, option realized variations also exhibit information that is not shared with index return variations, suggesting their pertinence as an alternative source of information about the dynamics of the underlying generating process. Second, the fact that different characteristics of the ORV surface cannot be summarized in one simple specification of PCs suggests that various option realized variances should be used in parametric studies; given the large number of options available at a given point in time, a well-selected subset of option realized variance should be employed for empirical analyses.

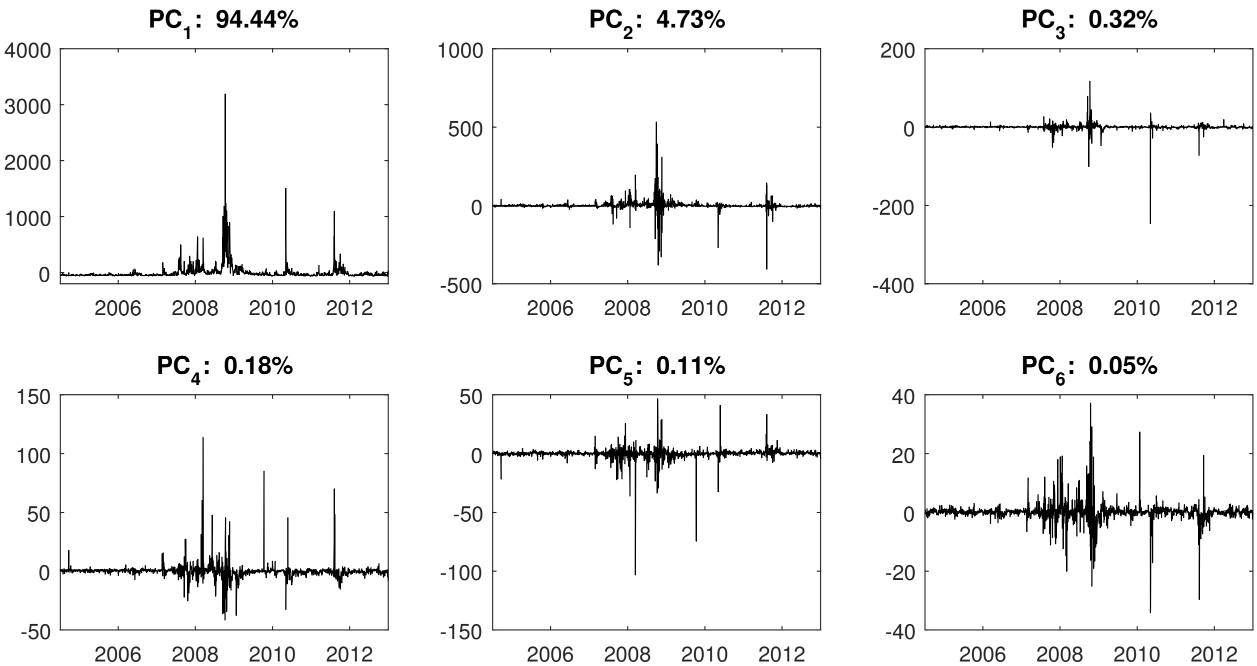

Figure 6: Principal components of the option realized volatility surface. The figure shows the first six principal components extracted from the S&P 500 option realized variance surface from July 2004 to December 2012. On each day, option realized variances are interpolated from a locally smoothing quadratic regression surface estimated on every available option realized volatility. Over the call-equivalent delta dimension, we use the grid of values 0.1, 0.2, ..., 0.9; over the tenor dimension, we employ maturities of 30 and 90 business days. These partitions require a total of 18 option realized volatilities per day.

Table 8: Option realized volatility characteristics, realized measures, and principal component regressions.

	Level	TS	Skew	Skew TS	RV	$\max(RV-BV,0)$
PC_1	**0.395**	**-0.009**	**0.029**	**-0.011**	**0.515**	**0.025**
	(0.001)	(0.002)	(0.002)	(0.002)	(0.036)	(0.003)
PC_2	**0.268**	**-0.072**	**-0.107**	**0.051**	-0.060	0.004
	(0.005)	(0.006)	(0.007)	(0.007)	(0.074)	(0.010)
PC_3	**-0.434**	**0.938**	-0.014	-0.005	0.697	0.070
	(0.016)	(0.034)	(0.046)	(0.043)	(0.358)	(0.041)
PC_4	**-0.360**	**0.230**	0.048	-0.066	-0.536	-0.088
	(0.016)	(0.028)	(0.031)	(0.046)	(0.445)	(0.057)
PC_5	0.027	**-0.126**	-0.028	**0.170**	**1.203**	0.079
	(0.029)	(0.045)	(0.032)	(0.044)	(0.575)	(0.086)
PC_6	**-0.427**	**0.375**	**0.101**	-0.050	0.988	0.207
	(0.043)	(0.057)	(0.050)	(0.056)	(0.642)	(0.111)
R^2	1.000	0.950	0.928	0.537	0.901	0.445
AC(1)	0.065	0.234	0.129	0.051	0.623	0.025
AC(2:10)	0.053	0.109	0.070	0.038	0.479	0.074
AC(11:20)	-0.009	0.000	0.036	0.015	0.320	0.051

[1] The following linear regressions are performed:

$$\mathrm{Char}_t = \beta_0 + \beta_1 \mathrm{PC}_{1,t} + \beta_2 \mathrm{PC}_{2,t} + \beta_3 \mathrm{PC}_{3,t} + \beta_4 \mathrm{PC}_{4,t} + \beta_5 \mathrm{PC}_{5,t} + \beta_6 \mathrm{PC}_{6,t} + \varepsilon_t,$$

where Char_t is the characteristic of interest at time t (i.e. Level, TS, Skew, Skew TS, RV and $\max(RV-BV,0)$) and $\mathrm{PC}_{n,t}$ represents the n-th principal component at time t.

[2] R^2 and Newey and West (1987) standard errors (in parentheses) are reported. Values in bold are statistically significant at a confidence level of 95%.

[3] The first six principal components extracted from the S&P 500 option realized volatility surface from July 2004 to December 2012.

[4] The first sample autocorrelation coefficient and the average sample autocorrelation over two to ten and eleven to twenty lags of the regression residuals are exhibited.

[5] The values of RV and $\max(RV-BV,0)$ are multiplied by 1000 in the regressions.

5.3 Predicting index return variations

The economic relationship between option realized variations and index return variations is now studied with predictive regressions. The motivation behind this exercise is to look at the role of option realized variations as economic variables that predict different types of index return variability.

The first model consists of explaining one-day ahead index return realized variances. We employ the logarithm of realized variance as a dependent variable and estimate the following model:

$$\log(RV_{t+1}) = \beta_0+\beta_1\log(RV_t)+\beta_2\max(RV_t-BV_t,0)+\beta_3 IV^{\mathrm{ATM}}_{\log,\perp,t}+\beta_4 ORV^{\Delta^{\mathrm{e}}=0.1}_{\log,\perp,t}+\beta_5 ORV^{\Delta^{\mathrm{e}}=0.9}_{\log,\perp,t}+\varepsilon_t \quad (14)$$

The variables of interest in this model are lagged values of jump realized variation ($\max(RV_t - BV_t, 0)$), ATM implied volatility (IV^{ATM}), and option realized variances of OTM options with call-equivalent deltas (Δ^{e}) of 0.1 and 0.9. The maturity of all options is 30 days. To remove potential collinearity issues across the regressors (see Table 9), we employ the orthogonal component that results from the projection of a given measure on RV in our regressions.

Table 9: Correlation matrix of realized values used in the predictive regressions.

	$\log(RV)$	$\max(RV-BV,0)$	$\log(IV^{\mathrm{ATM}})$	$\log(ORV^{\Delta^{\mathrm{e}}=0.1})$	$\log(ORV^{\Delta^{\mathrm{e}}=0.9})$
$\log(RV)$	1.0000				
$\max(RV-BV,0)$	0.4876	1.0000			
$\log(IV^{\mathrm{ATM}})$	0.8511	0.4121	1.0000		
$\log(ORV^{\Delta^{\mathrm{e}}=0.1})$	0.8470	0.3961	0.7116	1.0000	
$\log(ORV^{\Delta^{\mathrm{e}}=0.9})$	0.8691	0.3993	0.7202	0.8194	1.0000

Panel A of Table 10 presents estimates and t-statistics of six specifications of the regression in Equation (14). The first four specifications show that only the orthogonal components of IV^{ATM} and $ORV^{\Delta^{\mathrm{e}}=0.1}$ are statistically significant explaining the one-day ahead realized variation of index returns after controlling for the lagged value of the dependent variable. They enter in the regression model with positive signs, which confirms the forward-looking nature of IV^{ATM}. Interestingly, it is the residual component of ORV associated with OTM calls that predicts the subsequent realized variance, even after controlling for IV^{ATM}. As discussed in Section 2.2, the ORV for an OTM option is related to jump activity in the log-equity price and variance processes. Thus, the explanation power of this variable might come from two sources. The first one is the high persistence of the variance process, so that volatility jumps lead to higher activity in subsequent periods. The second possibility is that positive jumps induce future variability by arriving in clusters or by increasing the volatility directly. Fulop et al. (2014) provide evidence of self-exciting jump clustering during turbulent market periods.

The second model we consider consists of explaining one-day ahead jump activity on the index return realized variances. This time we run the regression:

$$\max(0, RV_{t+1} - BV_{t+1}) = \beta_0 + \beta_1\log(RV_t) + \beta_2\max(0, RV_t - BV_t) + \beta_3 IV^{\mathrm{ATM}}_{\log,\perp,t} + \beta_4 ORV^{\Delta^{\mathrm{e}}=0.1}_{\log,\perp,t} + \beta_5 ORV^{\Delta^{\mathrm{e}}=0.9}_{\log,\perp,t} + \varepsilon_t. \quad (15)$$

Panel B of Table 10 shows that lagged values of RV and jump realized variance have explanatory power over future jump activity. This relationship provides evidence in favour of the parametric model we are considering in Section 2, since the intensity of the counting process governing jump returns is a function of volatility. Regarding IV, its residual component also has a positive effect on jump realized variance. Contrary to what was observed in the RV regression, it is the ORV of the OTM put that now has a significant relation with the dependent variable. However, this time, the coefficient of the relationship is negative. Given that jump activity is measured as the difference between total and diffusive variance, the negative sign might indicate that the jump activity driving the ORV of OTM puts exerts more influence over future diffusive variance than return jumps. Notwithstanding, if we compare the magnitude of this coefficient with the one of OTM calls in Equation (14), we note that the significance of the relationship is more important in the latter case.

Lastly, we emphasize that the regression models (14) and (15) are of predictive nature, so our analysis focuses on the identification of variables that are important in the determination of future realized variances. The fact that R-squareds in Panel A are higher than those reported in Panel B just shows how much easier it is to predict future total variance than to predict variance induced by jump activity.

Table 10: Predictive regressions.

Panel A: Logarithm of realized variance							
Regression	β_0	β_1	β_2	β_3	β_4	β_5	R^2
(1)	**-0.5493**	**0.8733**	-3.2276				0.7490
	(0.0981)	(0.0199)	(3.6529)				
(2)	**-0.2279**	**0.9425**	-2.9616	**0.9432**			0.7839
	(0.0932)	(0.0193)	(3.2157)	(0.0705)			
(3)	**-0.8316**	**0.8128**	-2.8130		**0.1197**		0.7515
	(0.1101)	(0.0228)	(3.6017)		(0.0257)		
(4)	**-0.3872**	**0.9081**	-3.4894			-0.0438	0.7494
	(0.1391)	(0.0289)	(3.6881)			(0.0238)	
(5)	**-0.5424**	**0.8750**	-2.4922	**0.9529**	**0.1347**		0.7871
	(0.1003)	(0.0216)	(3.1548)	(0.0723)	(0.0280)		
(6)	**-0.1785**	**0.9531**	-3.0435	**0.9408**		-0.0136	0.7839
	(0.1270)	(0.0269)	(3.2375)	(0.0705)		(0.0238)	

Panel B: Maximum between 0 and the difference between realized variance and bipower variation							
Regression	β_0	β_1	β_2	β_3	β_4	β_5	R^2
(1)	**0.0102**	**0.0019**	**0.0963**				0.1885
	(0.0019)	(0.0004)	(0.0460)				
(2)	**0.0110**	**0.0021**	**0.0969**	**0.0023**			0.1963
	(0.0019)	(0.0004)	(0.0457)	(0.0004)			
(3)	**0.0100**	**0.0019**	**0.0966**		0.0001		0.1885
	(0.0020)	(0.0004)	(0.0462)		(0.0003)		
(4)	**0.0126**	**0.0024**	**0.0924**			**-0.0007**	0.1921
	(0.0024)	(0.0005)	(0.0455)			(0.0002)	
(5)	**0.0107**	**0.0020**	**0.0974**	**0.0023**	0.0001		0.1964
	(0.0020)	(0.0004)	(0.0460)	(0.0004)	(0.0003)		
(6)	**0.0131**	**0.0026**	**0.0934**	**0.0022**		**-0.0006**	0.1992
	(0.0024)	(0.0005)	(0.0453)	(0.0004)		(0.0002)	

[1] Variations of following linear regression are performed:

$$\mathrm{X}_{t+1} = \beta_0 + \beta_1 \log(RV_t) + \beta_2 \max(RV_t - BV_t, 0) + \beta_3 IV^{\mathrm{ATM}}_{\log,\perp,t} + \beta_4 ORV^{\Delta^e=0.1}_{\log,\perp,t} + \beta_5 ORV^{\Delta^e=0.9}_{\log,\perp,t} + \varepsilon_t,$$

where $\mathrm{X}_{t+1} \in \{RV_{t+1}, \max(RV_{t+1} - BV_{t+1}, 0)\}$, RV_t is the realized variance at time t, BV_t is the bipower variation at time t, $IV^{\mathrm{ATM}}_{\log,\perp,t}$ is the residual of the following regression

$$\log\left(IV^{\mathrm{ATM}}_t\right) = \alpha_1 \log(RV_t) + IV^{\mathrm{ATM}}_{\log,\perp,t},$$

where IV^{ATM}_t is the ATM implied volatility (with maturity of 30 days). The variables $ORV^{\Delta^e=0.1}_{\log,\perp,t}$ and $ORV^{\Delta^e=0.9}_{\log,\perp,t}$ are computed similarly from the option realized variance for OTM calls with call-equivalent delta of 0.1 and the option realized variance for OTM calls with call-equivalent delta of 0.9.
[2] We compute Newey-West standard errors. These are in parentheses in the above table. Values in bold are statistically significant at a confidence level of 95%.
[3] Results for bipower variation are both qualitatively and quantitatively similar to those of realized variance.

6 Option pricing implications

This section provides empirical results using the model introduced in Section 2. We start by analyzing parameter estimates of the model with different sets of information. We then use these parameters to disentangle latent variables and analyze the information content of option realized variances. Finally, we look at the fitting performance using in- and out-of-sample analyses.

6.1 Parameter estimates

We obtain model parameters using the estimation procedure described in Section 3.2. As explained in Section 2.2, this procedure combines several observables into a likelihood function that is computed using a Monte Carlo based approximation. The first set of observable variables are related to S&P 500 returns. We use daily log returns, realized variance, and bipower variation.[29] The second set is composed of daily option prices and their realized variances (ORVs). Option prices come from OptionMetrics and correspond

[29]The computation of these last two variables is explained in Section 5.1.

to European S&P 500 index option contracts. As argued in Bates (2000), the daily overabundance of option data becomes a hurdle for estimation routines, so we use a representative sample of options by restricting our attention to OTM or ATM options with maturities closest to 30 and 90 days, and call-equivalent deltas closest to 0.2, 0.35, 0.5, 0.65 and 0.8. Options with positive volume and bid price are included in the sample, as well as those satisfying the no-arbitrage conditions of Bakshi et al. (1997).[30] Thus, the final sample of options is composed of a panel of 21,400 contracts.

Table 11: S&P 500 parameter estimates.

Panel A: With *ORV*								
Log-price process			Variance process			Standard deviations of error terms		
η_Y	0.7635	(0.000230)	η_V	-0.2199	(0.000013)	η_1	0.2160	(0.000023)
γ_Y	0.0058	(0.000010)	Γ_V	0.5811	(0.000019)	η_2	0.2296	(0.000023)
ρ	-0.4336	(0.000011)	κ	5.7808	(0.000061)	η_3	0.2471	(0.000018)
$\lambda_{Y,0}$	2.1530	(0.000498)	θ	0.0085	(0.000177)	η_4	0.4600	(0.000028)
$\lambda_{Y,1}$	29.0744	(0.000682)	σ	0.8935	(0.000007)			
μ_Y	-0.0050	(0.000018)	$\lambda_{V,0}$	7.6498	(0.000090)			
σ_Y	0.0163	(0.000129)	μ_V	0.0214	(0.000101)			
			V_0	0.0118	(0.000174)			
Panel B: Without *ORV*								
Log-price process			Variance process			Standard deviations of error terms		
η_Y	1.8734	(0.000311)	η_V	-1.5870	(0.000033)	η_1	0.2407	(0.000034)
γ_Y	0.0009	(0.000004)	Γ_V	0.7061	(0.000016)	η_2	0.2288	(0.000022)
ρ	-0.3912	(0.000015)	κ	4.7614	(0.000107)	η_3	0.2453	(0.000018)
$\lambda_{Y,0}$	0.0045	(0.025987)	θ	0.0030	(0.000825)	η_4	-	-
$\lambda_{Y,1}$	30.0106	(0.000992)	σ	0.9121	(0.000010)			
μ_Y	-0.0062	(0.000049)	$\lambda_{V,0}$	11.4438	(0.000065)			
σ_Y	0.0189	(0.000464)	μ_V	0.0174	(0.000041)			
			V_0	0.0114	(0.000242)			

[1] The index parameters are estimated using daily index returns, realized variances, bipower variations, daily option prices, and option realized variances (in the first case), from July 2004 to December 2012.
[2] Parameters are estimated using multiple simplex search method optimizations (fminsearch in Matlab).
[3] Robust standard errors are computed from the outer product of the gradient at optimal parameter values.
[4] Each day, we restrict our attention to OTM or ATM options with maturities closest to 30 and 90 days, and call-equivalent deltas closest to 0.2, 0.35, 0.5, 0.65 and 0.8.

To assess the information contained in ORVs, we first estimate the model excluding these variables from the set of observables and then re-estimate it using the complete set. Table 11 reports parameter estimates and standard errors (in parentheses) obtained with and without information from option realized variances. We first consider parameters governing the jump process intensities. We observe a decrease in the intensity of the jump process governing volatility jumps, $\lambda_{V,0}$, when ORVs are introduced, but an increase in the parameter governing the size of the jumps, μ_V. This suggests that ORV is detecting less frequent jumps with higher magnitudes in the volatility process. Regarding jumps in the log-equity price process, we observe an increase in the base intensity, $\lambda_{Y,0}$, as well as in the average size of jumps, μ_Y, in absolute value. These values show that ORV is favouring more frequent negative jumps with lower magnitudes, which is also observed from the average intensity – 0.0112 for the estimation with ORV and 0.0028 without.

We now look at compensation for bearing different types of risk. Jump return risk, or crash risk, is captured in this model by the parameter γ_Y times λ_{Y,t^-}, as shown in Equation (3). Since ORV is favouring more frequent negative jumps, compensation for bearing this type of risk increases with the addition of this new source of information (i.e. 0.06% without ORV vs. 1.63% with ORV, on average). The diffusive risk premium parameter η_Y captures the risk premium associated with diffusive shocks when multiplied by V_{t^-}. To find the compensation for this type of risk, we multiply the filtered instantaneous variance by η_Y and observe that this value is higher when ORV is not included in the estimation, on average (It is 4.41% when ORV is excluded and 1.75% when ORV is used). Therefore, in total, the average risk premiums calculated using both models are similar, although the breakdown between diffusive and jump risks is different. These findings suggest that the risk premiums of discontinuous risk is underestimated when information about intraday evolution of option prices is not accounted for during the estimation. Estimates for jump risk are

[30] Option realized variances are computed following the procedure explained in Section 5.1.

close but somewhat lower than those reported in Broadie et al. (2007), Christoffersen et al. (2012b), and Ornthanalai (2014).[31]

6.2 Informativeness of data sources

Next, we focus on the informativeness of ORV about different latent variables of the model. Using the set of parameters estimated in Table 11, we filter different latent quantities using all data sources and compare the average standard deviations of these quantities with those obtained when filtering without ORV. Table 12 shows the posterior standard deviation (PSD) of these latent quantities under the two filtering procedures.[32] The PSD of variance jumps decreases approximately five times when ORVs are added. This dramatic decrease confirms our simulated results that show how ORV embeds vital information about the presence of variance jumps. Note also, as it is the case in the simulation results, the PSDs of the instantaneous variances, quadratic variations, and integrated variances also fall when ORVs are included. Regarding the slight increase in the PSD for log-return jumps, this could be associated with the fact that these jumps are less frequent than jumps in volatility, which increases the estimation uncertainty about this value.

Table 12: Posterior standard deviation of filtered quantities with and without ORV.

	With ORV	Without ORV
Instantaneous variance	4.821×10^{-03}	5.961×10^{-03}
Quadratic variation	1.252×10^{-05}	1.410×10^{-05}
Integrated variance	1.088×10^{-05}	1.255×10^{-05}
Log-equity price jumps	2.886×10^{-04}	1.804×10^{-04}
Variance jumps	7.038×10^{-04}	3.297×10^{-03}

[1] The posterior standard deviation is calculated from the particles generated in the particle filtering scheme.
[2] Parameters from Table 11 are used to infer the filtered values and their posterior standard deviation.

We next provide visual evidence of the informativeness of ORVs for disentangling jumps. Figure 7 displays filtered price jumps and variance jumps excluding ORVs (first row) and with all data sources (second row). The dynamics of both jump processes consistently differ across sources, showing that jumps for log-prices are sporadic and largely negative on average and that jumps in volatility are more frequent and tend to be small on average. ORV plays an important role identifying jumps in volatility. Note the striking decrease in the number and sizes of volatility jumps when ORV is employed in the filtering process. This result, coupled with the fact that jump risk premiums vary depending on the data source employed, show the economic gains from including intraday option prices in the analysis of option pricing models.

6.3 In- and out-of-sample assessment

We now investigate the goodness of fit of the two parameter sets under analysis. We start with an in-sample analysis that employs data over the same period the parameters were estimated. Then, we employ the parameters obtained over the period from July 2004 to December 2012 to perform out-of-sample comparisons using 2013 option data.

6.3.1 In-sample

We first asses the ability of both parameter sets to fit historical implied volatilities. To perform this exercise, we use the relative implied volatility root mean square error (RIVRMSE), defined as follows:

$$\text{RIVRMSE} = \sqrt{\left(\frac{1}{\sum_k \mathcal{O}_k}\right) \sum_k \sum_{i=1}^{\mathcal{O}_k} \left(\frac{IV_{k\Delta,i}(Y_{\Delta k}, \hat{V}_{\Delta k}) - \sigma^{\text{BS}}_{k\Delta,i}}{\sigma^{\text{BS}}_{k\Delta,i}}\right)^2}, \tag{16}$$

where IV is the model implied volatility, $\hat{V}_{\Delta k}$ is the filtered instantaneous variance on day k, and $\mathcal{O}_k$ represents the number of options in a subset of all the options available on day k. Here, σ^{BS} denotes the Black-Scholes implied volatility associated with the observed option price.

[31] Variations in the sampling period or the datasets could also explain these small differences, to some extent.
[32] The posterior standard deviation is the standard deviation of the posterior density (as given by the particle filter). It allows us to assess the uncertainty around estimated latent variables.

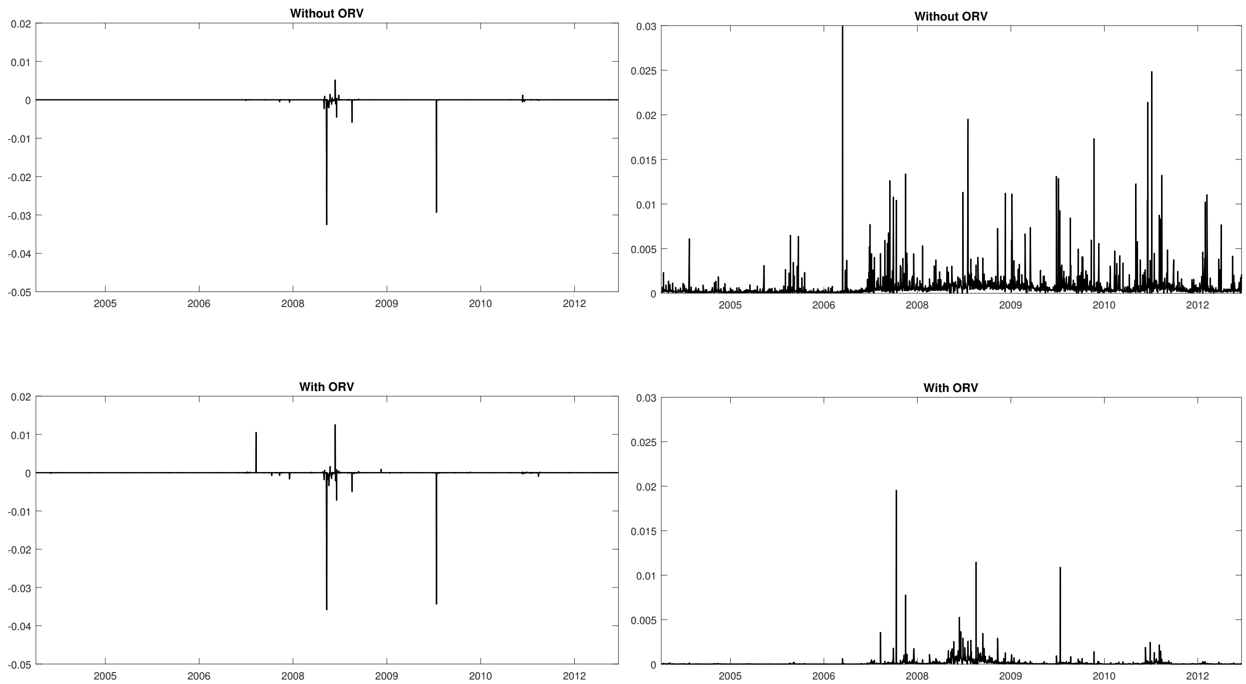

Figure 7: Filtered log-equity price jumps (left panels) and variance jumps (right panels). The figure shows the log-equity price jumps (left panels) and variance jumps (right panels). The top panels show the filtered jumps based on returns, option implied volatilities, realized variances and bipower variations. The bottom panels also include option realized variances as a new source of information.

The leftmost columns of Panel A (Table 13) show the RIVRMSE for the panel of 21,400 options employed in the estimation. We observe that the fit provided by the parameter set without ORVs is more accurate on average than the one that includes these variances – an RIVRMSE of 24.56 with ORV vs. 23.45 without. This result stems from the fact that maximization of the likelihood in the former case backs parameters that better fit IVs. However, the average fit is not that different, so the addition of ORVs does not substantially deteriorate the overall fit of option prices.

In order to identify which contracts would benefit more from the inclusion of ORVs, we assess the goodness of fit of both parameter sets for these variances. To this end, we use a criterion similar to the RIVRMSE in Equation (16) and compute the relative option realized variance root mean square error (RORVRMSE), defined as:

$$\text{RORVRMSE} = \sqrt{\left(\frac{1}{\sum_k \mathcal{O}_k}\right) \sum_k \sum_{i=1}^{\mathcal{O}_k} \left(\frac{\Delta OQV_{(k-1)\Delta,k\Delta,i} - ORV_{(k-1)\Delta,k\Delta,i}}{ORV_{(k-1)\Delta,k\Delta,i}}\right)^2},$$

where ΔOQV is the option quadratic variation increment computed from the model and ORV is the observed option realized variance.

Rightmost columns of Panel A (Table 13) exhibit the RORVRMSE by moneyness and maturity. As expected, the average fit of these quantities is lower when ORVs are included in the information set. Nonetheless, it is remarkable to observe that the overall RORVRMSE is about 3 times lower when ORV is included and that there are significant differences across contracts. Whereas error differences for call options are almost fourfold, those differences for put options are about twofold. The differences across contracts suggest that ORVs bring more information from OTM calls than from OTM puts, which goes in line with the importance of the coefficient associated with call contracts in explaining future index variation as discussed in Section 5.3.

We continue with the in-sample analysis by looking at one-day ahead predicted option prices from both sets of parameters. To analyse the fit of implied volatilities, we enlarge our estimation sample of 21,400 options to include all OTM options available for the S&P 500 index in OptionMetrics between July 2004

Table 13: In-sample performance (2004–2012).

Panel A: In-sample option pricing and option realized variance performances, in terms of RIVRMSE and RORVRMSE

	RIVRMSE		RORVRMSE	
	With ORV	Without ORV	With ORV	Without ORV
DTM = 30, $\Delta^{\mathrm{e}} = 0.20$	19.13	17.62	50.17	152.95
DTM = 30, $\Delta^{\mathrm{e}} = 0.35$	25.05	23.04	36.29	103.59
DTM = 30, $\Delta^{\mathrm{e}} = 0.50$	28.51	27.93	41.81	90.90
DTM = 30, $\Delta^{\mathrm{e}} = 0.65$	27.27	25.94	55.26	106.11
DTM = 30, $\Delta^{\mathrm{e}} = 0.80$	25.03	23.16	61.43	95.19
DTM = 90, $\Delta^{\mathrm{e}} = 0.20$	21.97	26.01	61.02	272.48
DTM = 90, $\Delta^{\mathrm{e}} = 0.35$	23.37	22.90	40.78	145.63
DTM = 90, $\Delta^{\mathrm{e}} = 0.50$	25.23	23.16	40.77	101.02
DTM = 90, $\Delta^{\mathrm{e}} = 0.65$	25.17	22.40	44.92	122.24
DTM = 90, $\Delta^{\mathrm{e}} = 0.80$	23.57	20.69	53.56	137.20
All	24.56	23.45	49.34	142.17

Panel B: One-day ahead in-sample performances, in terms of RIVRMSE and RORVRMSE

	RIVRMSE		RORVRMSE	
	With ORV	Without ORV	With ORV	Without ORV
DTM ¡ 60	26.78	25.39	233.08	286.97
60 $\leq$ DTM ¡ 120	26.20	24.24	230.46	337.40
120 $\leq$ DTM ¡ 180	26.07	25.08	203.42	335.05
180 $\leq$ DTM	51.76	55.28	180.71	270.46
$\Delta^{\mathrm{e}} < 0.20$	23.25	28.56	358.69	512.51
$0.20 \leq \Delta^{\mathrm{e}} < 0.35$	29.55	31.11	216.98	302.68
$0.35 \leq \Delta^{\mathrm{e}} < 0.50$	34.52	35.51	152.92	198.51
$0.50 \leq \Delta^{\mathrm{e}} < 0.65$	41.42	41.24	188.62	239.69
$0.65 \leq \Delta^{\mathrm{e}} < 0.80$	37.41	36.83	200.04	267.02
$0.80 \leq \Delta^{\mathrm{e}}$	31.74	29.62	210.69	285.87
2004	25.73	28.52	204.64	268.17
2005	28.44	33.71	270.87	348.78
2006	26.58	32.05	316.43	407.00
2007	29.29	31.87	220.31	290.46
2008	31.17	30.56	77.09	92.51
2009	38.47	35.74	79.21	93.69
2010	34.99	33.49	188.20	284.60
2011	35.33	34.38	193.82	274.96
2012	31.68	31.39	314.55	437.40
All	32.79	32.87	221.94	303.31

[1] In Panel A, only options used for estimation are employed.
[2] In Panel B, the sample of S&P 500 options is acquired via OptionMetrics. Options violating arbitrage conditions were discarded.
[3] In Panel C, the sample of S&P 500 options is acquired via Tick Data. Options violating arbitrage conditions were discarded.
[4] Model prices and ORVs are calculated by using the parameters of Table 11.
[5] The relative implied volatility root mean square error (RIVRMSE) is computed as follows:

$$\text{RIVRMSE} = \sqrt{\left(\frac{1}{\sum_k \mathcal{O}_k}\right) \sum_k \sum_{i=1}^{\mathcal{O}_k} \left(\frac{IV_{k\Delta,i}(Y_{\Delta k}, \hat{V}_{\Delta k}) - \sigma^{\text{BS}}_{k\Delta,i}}{\sigma^{\text{BS}}_{k\Delta,i}}\right)^2},$$

where IV is the model implied volatility, $\hat{V}_{\Delta k}$ is the filtered instantaneous variance on day k, and $\mathcal{O}_k$ represents the number of options in a subset of all the options available on day k. The relative option realized variance root mean square error (RORVRMSE) is computed similarly: $IV_{k\Delta,i}(Y_{\Delta k}, \hat{V}_{\Delta k})$ is replaced by $\Delta OQV_{(k-1)\Delta,k\Delta,i}$ and $\sigma^{\text{BS}}_{k\Delta,i}$ by $ORV_{(k-1)\Delta,k\Delta,i}$.
[6] RIVRMSEs and RORVRMSEs are given in percentage.

and December 2012.[33] We restrict our analysis to maturities of at least one week and at most one year. As before, observations violating no-arbitrage restrictions are excluded. Our new sample is composed of a total of 401,081 contracts. Option prices are converted to implied volatilities with the Black and Scholes's (1973) pricing formula. To compute model-predicted implied volatilities on day t, we calculate one-day ahead

[33] We continue using OTM options to keep a comparable sample with that employed in our previous analyses.

expectations of model variables for day t using the filter's predictive distribution resulting from day $t-1$. Using observed and predicted implied volatilities, we compute RIVRMSEs according to maturity, moneyness, and year, which provides a better picture of the fit associated with each parameter set.

The overall RIVRMSEs (leftmost columns of Panel B in Table 13) are very close on average for both parameter sets, with lower values of RIVRMSE observed when ORVs are included (32.79 against 32.87). We use the Diebold and Mariano (1995, DM) test to see if the apparent predictive superiority of ORV-based forecasts is not particular to this sample. Using both RIVRMSE time series, we compare their forecasting accuracy and test for:[34]

$$H_0 : \mathbb{E}\left[d_t\right] = 0,\, \forall t \qquad H_1 : \mathbb{E}\left[d_t\right] > 0,\, \forall t$$

where $d_t = \mathrm{RIVRMSE}_{\mathrm{without},t} - \mathrm{RIVRMSE}_{\mathrm{with},t}$ is the time-t loss differential between the forecast produced without ORV and the one including it. The DM test statistic is 5.32 and is significant at a 1% level, confirming that there exists a differential between the two forecasts and that the one based on ORV information produces more accurate results on average. A closer scrutiny of the data reveals that including ORVs is especially helpful in the pricing of options with long maturities, OTM calls, and options for the years before 2008.

Finally, we carry out a similar exercise with option realized variances and analyse one-day ahead forecasts for both parameter sets. For this exercise, we restrict our enlarged sample to those options for which ORV data is available in the TickData database. Out of 401,081 options, 282,534 contracts were included in our analysis. As reported in the rightmost columns of Panel B, Table 13, we observe again that, across different option characteristics and years, RORVRMSE are lower for the parameter set that was obtained with ORVs. Similar to the RIVRMSE case, we apply the DM test to both RORVRMSE series and obtain a value of 13.63, confirming statistically the important differences between the two sets of parameters.[35]

6.3.2 Out-of-sample

We provide further evidence on the forecast differences of both parameter sets by constructing out-of-sample errors. We employ the parameters obtained over the sample period between July 2004 and December 2012, and use daily information between January 2013 and December 2013 to compute one-day ahead forecast errors. As in the previous section, we employ the filter's predictive distribution resulting from day $t-1$ to compute expectations for day t. Regarding the sample, we employ all OTM options available in OptionMetrics for 2013 to compute RIVRMSE, yielding a total of 77,310 contracts. To compute RORVRMSEs, we employed a dataset of 68,857 OTM options for which ORVs were available.

Table 14 shows RIVRMSE and RORVRMSE by moneyness and maturity. The parameter set based on ORVs produces the lowest forecast errors, as shown by the average means for the whole sample. This is also confirmed with the DM test, which gives a value of 8.09 for RIVRMSE and 16.17 for RORVRMSE, both significant at a 1% level. When we look at the RIVRMSE across maturities, we observe that ORV-based forecasts consistently outperform those forecasts that do not employ the information of ORVs. Regarding performance by type of contract, it is still the case that the largest gains are obtained for OTM calls. Nonetheless, OTM puts that are close to the money also exhibit lower RIVRMSE.

The above evidence is consistent with the view of ORV as a new source of information to disentangle jumps in volatility and prices. The parameter set obtained with the addition of ORV supports a variance process that has less frequent jumps with higher magnitudes and a price process that has more frequent negative jumps with lower magnitudes. This set also has a different attribution of risk premiums between diffusive and discontinuous innovations. It seems most likely that these features are important in the pricing of options, as they consistently produce lower forecasting errors of implied volatilities in-sample and out-of-sample.

[34] The lag in the Diebold and Mariano (1995) is selected as the first partial autocorrelation that is within confidence bounds. The estimated lag in this exercise is 2.

[35] We repeated our analysis of RIVRMSE with the sample of 282,534 contracts and found similar results.

Table 14: One-day ahead out-of-sample performances, in terms of RIVRMSE and RORVRMSE (2013)

	RIVRMSE		**RORVRMSE**	
	With ORV	Without ORV	With ORV	Without ORV
DTM ¡ 60	18.85	19.09	512.96	635.93
60 $\leq$ DTM ¡ 120	18.62	20.75	559.93	810.20
120 $\leq$ DTM ¡ 180	22.50	27.59	431.52	691.71
180 $\leq$ DTM	50.14	55.54	390.10	585.19
$\Delta^e < 0.20$	34.97	45.40	871.92	1214.42
$0.20 \leq \Delta^e < 0.35$	33.16	39.70	465.52	617.28
$0.35 \leq \Delta^e < 0.50$	36.38	41.39	275.85	361.76
$0.50 \leq \Delta^e < 0.65$	37.38	38.37	357.39	464.95
$0.65 \leq \Delta^e < 0.80$	30.85	31.08	526.85	701.61
$0.80 \leq \Delta^e$	21.18	19.61	433.91	573.80
All	28.94	31.95	504.30	680.05

[1] The sample of S&P 500 options is acquired via OptionMetrics. Options violating arbitrage conditions were discarded. The IV sample size is 77,310.
[2] The sample of S&P 500 options is acquired via Tick Data. Options violating arbitrage conditions were discarded. The ORV sample size is 68,857.
[3] Model prices and ORVs are calculated by using the parameters of Table 11.
[4] RIVRMSEs and RORVRMSEs are given in percentages.

7 Concluding remarks

The observable variables used in this paper provide a portrait of the incremental information of these variables for the identification of latent features governing dynamics of asset prices. The paper proposes the option realized variance as a new observable quantity. This variable provides evidence of the usefulness of high frequency option prices to infer characteristics such as instantaneous variance, as well as jumps in returns and the variance process.

One of the reasons behind the information gains of this measure is its ability to capture different properties of the DGP depending on the moneyness of the option employed. Whereas ITM and OTM options provide ORVs that are responsive to discontinuous and diffusive innovations, the ORV of OTM puts are sensitive to changes in the discontinuous part of the variance and the return process.

The paper empirically documents how option realized variance behaves for options on the S&P 500 and studies its relationship with the realized variance of the index. For instance, using a principal component analysis for the surface of option realized variances, we find that ORV contains additional information when compared to the one embedded in realized variance. The paper further explores the economic implications of not using high frequency option prices for model estimation. Model parameters estimated without this information are not able to correctly disentangle diffusive and discontinuous innovations, which produces an incorrect attribution of risk premiums among these two competitive sources of risk.

Appendix

A Pricing

A.1 Radon-Nikodym derivative

Let $\mathcal{F}_t = \sigma\left\{W_{V,u}, W_{\perp,u}, J_{Y,u}, J_{V,u}\right\}_{0\leq u\leq t}$ be the $\sigma-$field generated by the past and actual noise terms. The market being incomplete, there are infinitely many equivalent martingale measures. We restrict the choice among those that have a Radon-Nikodym derivative of the form

$$\left.\frac{d\mathbb{Q}}{d\mathbb{P}}\right|_{\mathcal{F}_t} = \frac{\exp\left(-\int_0^t \Lambda_{V,u^-} dW_{V,u} - \int_0^t \Lambda_{\perp,u^-} dW_{\perp,u} + \Gamma_Y J_{Y,t} + \Gamma_V J_{V,t}\right)}{\mathrm{E}^{\mathbb{P}}\left[\exp\left(-\int_0^t \Lambda_{V,u^-} dW_{V,u} - \int_0^t \Lambda_{\perp,u^-} dW_{\perp,u} + \Gamma_Y J_{Y,t} + \Gamma_V J_{V,t}\right)\right]}, \tag{17}$$

the latter being an extended version of the Girsanov theorem. The predictable process $\left\{\Lambda_{V,t^-}\right\}_{t\geq 0}$ and $\left\{\Lambda_{\perp,t^-}\right\}_{t\geq 0}$ and the constants Γ_Y and Γ_V characterize the risk premiums embedded in this framework by linking the $\mathbb{P}-$ and $\mathbb{Q}-$parameters together.

This approach is different from the one proposed in Duffie et al. (2000), Pan (2002), and Broadie et al. (2007) in which the $\mathbb{P}-$ and $\mathbb{Q}-$ parameters are allow to vary independently. However, it shares similarities to Christoffersen et al. (2012b) and Ornthanalai (2014) that consider GARCH models with jumps. It is also related to Bates (2000): in the latter, the author restricts the value of certain parameters to be consistent with the time series behaviour of returns.

Building on the properties of exponential martingales,[36]

$$\begin{aligned}
&\mathrm{E}^{\mathbb{P}}\left[\exp\left(-\int_0^t \Lambda_{V,u^-} dW_{V,u} - \int_0^t \Lambda_{\perp,u^-} dW_{\perp,u} + \Gamma_Y J_{Y,t} + \Gamma_V J_{V,t}\right)\right]\\
= \quad &\exp\left(\frac{1}{2}\int_0^t \left(\Lambda^2_{V,u^-} + \Lambda^2_{\perp,u^-}\right) du + \left(\varphi^{\mathbb{P}}_{Z_Y}\left(\Gamma_Y\right) - 1\right)\int_0^t \lambda_{Y,u^-} du + \left(\varphi^{\mathbb{P}}_{Z_V}\left(\Gamma_v\right) - 1\right)\int_0^t \lambda_{V,u^-} du\right)
\end{aligned}$$

where $\varphi^{\mathbb{P}}_{Z_Y}\left(\Gamma_Y\right)$ and $\varphi^{\mathbb{P}}_{Z_V}\left(\Gamma_V\right)$ represent the moment generating functions of the log-equity price and variance jump size,[37]

$$\varphi^{\mathbb{P}}_{Z_Y}\left(\Gamma_Y\right) = \exp\left(\mu_Y\Gamma_Y + \frac{1}{2}\sigma_Y^2\Gamma_Y^2\right) \quad \text{and} \quad \varphi^{\mathbb{P}}_{Z_V}\left(\Gamma_V\right) = \left(1 - \Gamma_V\mu_V\right)^{-1}. \tag{18}$$

A.2 Model under the risk-neutral measure $\mathbb{Q}$

For the diffusion components of the model, the risk-neutral Brownian motion are constructed in the usual way:

$$W^{\mathbb{Q}}_{V,t} = W_{V,t} + \int_0^t \Lambda_{V,u^-} du, \qquad W^{\mathbb{Q}}_{\perp,t} = W_{\perp,t} + \int_0^t \Lambda_{\perp,u^-} du \tag{19}$$

and $W^{\mathbb{Q}}_{Y,t} = \rho W_{V,t} + \sqrt{1-\rho^2}W_{\perp,t} = W_{Y,t} + \int_0^t \Lambda_{Y,u^-} du$ where $\Lambda_{Y,u^-} = \rho\Lambda_{V,u^-} + \sqrt{1-\rho^2}\Lambda_{\perp,u^-}$.

[36] It is required that $\mathrm{E}^{\mathbb{P}}\left[\int_0^t \Lambda^2_{V,u^-} du\right] < \infty$ and $\mathrm{E}^{\mathbb{P}}\left[\int_0^t \Lambda^2_{\perp,u^-} du\right] < \infty$. Details are provided in Lemmas 4 and 6 of the Internet appendix.

[37] Provided that $\Gamma_V < \frac{1}{\mu_V}$.

The risk-neutral jump component are obtained from a direct comparison of the $\mathbb{P}-$ and $\mathbb{Q}-$versions of the moment generating functions of the jump increments ($J_{Y,t} - J_{Y,s}$ and $J_{V,t} - J_{V,s}$).[38] Indeed, the change of measure affects the parameters:

$$J^{\mathbb{Q}}_{Y,t} = \sum_{n=1}^{N^{\mathbb{Q}}_{Y,t}} Z^{\mathbb{Q}}_{Y,n}, \text{ and } J^{\mathbb{Q}}_{V,t} = \sum_{n=1}^{N^{\mathbb{Q}}_{V,t}} Z^{\mathbb{Q}}_{V,n},$$

where $\left(N^{\mathbb{Q}}_{Y,t}\right)_{t\geq 0}$ is a Cox process with predictable intensity $\left(\lambda_{Y,t^-}\right)_{t\geq 0}$, $\left(N^{\mathbb{Q}}_{V,t}\right)_{t\geq 0}$ is a Poisson process of intensity $\lambda^{\mathbb{Q}}_{V,0}$ and

$$\begin{array}{lll} \lambda^{\mathbb{Q}}_{Y,t^-} = \varphi^{\mathbb{P}}_{Z_Y}\left(\Gamma_Y\right)\lambda_{Y,t^-}, & \mu^{\mathbb{Q}}_Y = \mu_Y + \Gamma_Y \sigma^2_Y, & \sigma^{\mathbb{Q}}_Y = \sigma_Y, \\ \lambda^{\mathbb{Q}}_{V,0} = \varphi^{\mathbb{P}}_{Z_V}\left(\Gamma_V\right)\lambda_{V,0}, & \mu^{\mathbb{Q}}_V = \varphi^{\mathbb{P}}_{Z_V}\left(\Gamma_V\right)\mu_V. & \end{array}$$

The risk-neutral dynamics of the log-price process is established by imposing the discounted price process $\{\exp\left(\left(q-r\right)t\right)\exp\left(Y_t\right)\}_{t\geq 0}$ to be a $\mathbb{Q}-$ martingale where r is the risk-free rate and q is the dividend rate.[39] To get a semi-closed form for option prices, the risk-neutral stochastic differential equation (SDE) of the variance process is assumed to have a mean reverting behaviour, as in Heston (1993) among others. Implicitly, it constraints [40]

$$\Lambda_{V,t^-} = \eta_V \sqrt{V_{t^-}} \tag{20}$$

and the model under the risk-neutral measure is thus

$$dY_t = \alpha^{\mathbb{Q}}_{t^-} dt + \sqrt{V_{t^-}} dW^{\mathbb{Q}}_{Y,t} + dJ^{\mathbb{Q}}_{Y,t}, \tag{21}$$

$$dV_t = \kappa^{\mathbb{Q}}\left(\theta^{\mathbb{Q}} - V_{t^-}\right)dt + \sigma\sqrt{V_{t^-}} dW^{\mathbb{Q}}_{V,t} + dJ^{\mathbb{Q}}_{V,t}, \tag{22}$$

where the correspondence between the $\mathbb{P}-$ and $\mathbb{Q}-$ parameters is

$$\begin{array}{ll} \alpha^{\mathbb{Q}}_{t^-} = r - q - \frac{1}{2}V_{t^-} - \left(\varphi^{\mathbb{P}}_{Z_Y}\left(1\right) - 1\right)\lambda^{\mathbb{Q}}_{Y,t^-}, & \kappa^{\mathbb{Q}} = \kappa + \sigma\eta_V, \\ \lambda^{\mathbb{Q}}_{Y,t^-} = \varphi^{\mathbb{P}}_{Z_Y}\left(\Gamma_Y\right)\lambda_{Y,t^-}, & \theta^{\mathbb{Q}} = \frac{\kappa\theta}{\kappa+\sigma\eta_V}. \end{array}$$

A.3 Pricing

The price of a European call option with strike price K and maturity T is

$$C_t(Y_t, V_t) = \exp(Y_t)\exp\left(-q(T-t)\right)P_1(Y_t,V_t) - K\exp\left(-r(T-t)\right)P_2(Y_t,V_t) \tag{23}$$

[38] Lemma 8 of the Internet appendix shows that

$$\begin{aligned} \varphi^{\mathbb{P}}_{J_{Y,t}-J_{Y,s}}(a) &= \mathrm{E}^{\mathbb{P}}_{\mathcal{F}_s}\left[\left(\exp\left(\mu_Y a + \frac{1}{2}\sigma^2_Y a^2\right) - 1\right)\exp\left(\int_s^t \lambda_{Y,u^-} du\right)\right], \\ \varphi^{\mathbb{Q}}_{J_{Y,t}-J_{Y,s}}(a) &= \mathrm{E}^{\mathbb{P}}_{\mathcal{F}_s}\left[\left(\exp\left(\left(\mu_Y + \Gamma_Y\sigma^2_Y\right)a + \frac{1}{2}a^2\sigma^2_Y\right) - 1\right)\exp\left(\varphi^{\mathbb{P}}_{Z_Y}\left(\Gamma_Y\right)\int_s^t \lambda_{Y,u^-} du\right)\right], \\ \varphi^{\mathbb{P}}_{J_{V,t}-J_{V,s}}(a) &= \mathrm{E}^{\mathbb{P}}_{\mathcal{F}_s}\left[\exp\left(\left(\left(1-a\mu_V\right)^{-1} - 1\right)\int_s^t \lambda_{V,u^-} du\right)\right], \\ \varphi^{\mathbb{Q}}_{J_{V,t}-J_{V,s}}(a) &= \mathrm{E}^{\mathbb{P}}_{\mathcal{F}_s}\left[\exp\left(\left(\left(1-a\varphi^{\mathbb{P}}_{Z_V}\left(\Gamma_V\right)\mu_V\right)^{-1} - 1\right)\varphi^{\mathbb{P}}_{Z_V}\left(\Gamma_V\right)\int_s^t \lambda_{Y,u^-} du\right)\right]. \end{aligned}$$

[39] Details are provided in Lemma 9 of the Internet appendix.

[40] Indeed,

$$\begin{aligned} dV_t &= \kappa\left(\theta - V_{t^-}\right)dt + \sigma\sqrt{V_{t^-}} dW_{V,t} + dJ_{V,t} \\ &= \kappa\left(\theta - V_{t^-}\right) - \sigma\sqrt{V_{t^-}}\Lambda_{V,u^-} dt + \sigma\sqrt{V_{t^-}} dW^{\mathbb{Q}}_{V,t} + dJ^{\mathbb{Q}}_{V,t} \\ &= \left(\kappa + \sigma\eta_V\right)\left(\frac{\kappa\theta}{\kappa+\sigma\eta_V} - V_{t^-}\right)dt + \sigma\sqrt{V_{t^-}} dW^{\mathbb{Q}}_{V,t} + dJ^{\mathbb{Q}}_{V,t}. \end{aligned}$$

where

$$P_1(y,v) = \frac{1}{2} + \frac{1}{\pi}\int_0^\infty \mathrm{Re}\left(\frac{\exp(-\mathrm{i}uk - y)\,\varphi^{\mathbb{Q}}_{Y_T|Y_t,V_t}(u\mathrm{i}+1,y,v)}{u\mathrm{i}}\right) du,$$
$$P_2(y,v) = \frac{1}{2} + \frac{1}{\pi}\int_0^\infty \mathrm{Re}\left(\frac{\exp(-\mathrm{i}uk)\,\varphi^{\mathbb{Q}}_{Y_T|Y_t,V_t}(u\mathrm{i},y,v)}{u\mathrm{i}}\right) du.$$

and $\varphi^{\mathbb{Q}}_{Y_T|Y_t,V_t}(u,y,v) = \mathrm{E}^{\mathbb{Q}}_t\left[\exp(uY_T)\,|Y_t = y, V_t = v\right]$ is the moment generating function of Y_T conditional on time t information. More precisely,

$$\varphi^{\mathbb{Q}}_{Y_T|Y_t,V_t}(u,Y_t,V_t) = \exp\left(\mathcal{A}(u,t,T) + uY_t + \mathcal{C}(u,t,T)\,V_t\right)$$

where

$$\begin{aligned}
\mathcal{C}(u,t,T) &= \frac{2C_0(\exp(-C_2(T-t)) - 1)}{C_2(\exp(-C_2(T-t)) + 1) - C_1(\exp(-C_2(T-t)) - 1)}, \qquad (24)\\
C_0 &= \lambda^{\mathbb{Q}}_{Y,1}\left(\varphi^{\mathbb{Q}}_{Z_Y}(1) - 1\right)u - \lambda^{\mathbb{Q}}_{Y,1}\left(\varphi^{\mathbb{Q}}_{Z_Y}(u) - 1\right) + \frac{u-u^2}{2},\\
C_1 &= \kappa^{\mathbb{Q}} - \rho\sigma u,\\
C_2 &= \sqrt{C_1^2 + 2\sigma^2 C_0},
\end{aligned}$$

and

$$\begin{aligned}
\mathcal{A}(u;t,T) &= D_0(T-t) + \theta^{\mathbb{Q}}\kappa^{\mathbb{Q}} g_1(t,T) + \lambda^{\mathbb{Q}}_{V,0} g_2(t,T) \qquad (25)\\
D_0 &= -r + (r-q)u + \lambda^{\mathbb{Q}}_{Y,0}\left(\varphi^{\mathbb{Q}}_{Z_Y}(u) - 1\right) - \lambda^{\mathbb{Q}}_{Y,0}\left(\varphi^{\mathbb{Q}}_{Z_Y}(1) - 1\right)u\\
g_1(t,T) &= \frac{2\log(2C_2) - 2\log\left(C_1\left(e^{C_2(T-t)} - 1\right) + C_2\left(e^{C_2(T-t)} + 1\right)\right) + (C_1 + C_2)(T-t)}{-\sigma^2}\\
g_2(t,T) &= \frac{\mu^{\mathbb{Q}}_V}{2}\frac{2\log(2C_2) - 2\log\left(C_1\left(e^{C_2(T-t)} - 1\right) + C_2\left(e^{C_2(T-t)} + 1\right) + 2C_0\mu^{\mathbb{Q}}_V\left(e^{C_2(T-t)} - 1\right)\right)}{C_0\left(\mu^{\mathbb{Q}}_V\right)^2 + C_1\mu^{\mathbb{Q}}_V - \frac{\sigma^2}{2}}\\
&\quad + \frac{\mu^{\mathbb{Q}}_V}{2}\frac{2C_0\mu^{\mathbb{Q}}_V + C_1 - C_2}{C_0\left(\mu^{\mathbb{Q}}_V\right)^2 + C_1\mu^{\mathbb{Q}}_V - \frac{\sigma^2}{2}}(T-t)
\end{aligned}$$

The approach is inspired from Heston (1993) that relies on an inversion similar to the one of Gil-Pelaez (1951). The explicit form of the moment generating function is similar to the ones found by Filipovic and Mayerhofer (2009) and Duffie et al. (2000).[41]

B Estimation

B.1 Drift term

The drift term process of Equation (1) is

$$\begin{aligned}
\alpha^{\mathbb{P}}_{u^-} &= r - q - \frac{1}{2}V_{u^-} + \sqrt{V_{u^-}}\Lambda_{Y,u^-} + \left(\varphi^{\mathbb{P}}_{Z_Y}(\Gamma_Y) - \varphi^{\mathbb{P}}_{Z_Y}(1+\Gamma_Y)\right)\lambda_{Y,u^-}\\
&= r - q - \frac{1}{2}V_{u^-} + \sqrt{V_{u^-}}\Lambda_{Y,u^-} + \left(\gamma_Y - \left(\varphi^{\mathbb{P}}_{Z_Y}(1) - 1\right)\right)\lambda_{Y,u^-}
\end{aligned}$$

[41] Details are available in the Internet appendix B.

where the moment generating functions, $\varphi^{\mathbb{P}}_{Z_Y}(\Gamma_Y)$ and $\varphi^{\mathbb{P}}_{Z_V}(\Gamma_V)$, of the log-equity price and variance jump size are defined at Equation (18). To obtain a drift term that depends on the instantaneous variance only, it is assumed that

$$\Lambda_{\perp,u^-} = \eta_\perp \sqrt{V_{t^-}}. \tag{26}$$

Consequently, letting $\eta_Y = \rho\eta_V + \sqrt{1-\rho^2}\eta_\perp$ yields $\Lambda_{Y,u^-} = \left(\rho\eta_V + \sqrt{1-\rho^2}\eta_\perp\right)\sqrt{V_{t^-}}$ and

$$\alpha^{\mathbb{P}}_{u^-} = r - q + \left(\eta_Y - \frac{1}{2}\right) V_{u^-} + \left(\gamma_Y - \left(\varphi^{\mathbb{P}}_{Z_Y}(1) - 1\right)\right)\lambda_{Y,u^-}. \tag{27}$$

Sketch of the proof. Let

$$Z_t = \left(\begin{array}{l} -\int_0^t \Lambda_{V,u^-} dW_{V,u} - \int_0^t \Lambda_{\perp,u^-} dW_{\perp,u} - \frac{1}{2}\int_0^t \left(\Lambda^2_{V,u^-} + \Lambda^2_{\perp,u^-}\right) du \\ +\Gamma_Y J_{Y,t} - \left(\varphi^{\mathbb{P}}_{Z_Y}(\Gamma_Y) - 1\right)\int_0^t \lambda_{Y,u^-} du + \Gamma_V J_{V,t} - \left(\varphi^{\mathbb{P}}_{Z_V}(\Gamma_V) - 1\right)\int_0^t \lambda_{V,u^-} du \end{array} \right)$$

be associated to the Radon-Nikodym derivative of Equation (17) and $D_t = \exp(-(r-q)t)$ be the combination of the discount factor and the dividend yield. Since the discounted price have to be a $\mathbb{Q}-$martingale, then for all $0 < s < t$,

$$1 = \mathrm{E}^{\mathbb{Q}}_s \left[\frac{D_t \exp(Y_t)}{D_s \exp(Y_s)}\right] = \mathrm{E}^{\mathbb{P}}_s \left[\frac{D_t \exp(Y_t + Z_t)}{D_s \exp(Y_s + Z_s)}\right],$$

which means that $\{D_t \exp(Y_t + Z_t)\}_{t\geq 0}$ is a $\mathbb{P}-$martingale. The computation of this last expectation leads to the final result.[42] □

B.2 Filtering procedure

B.2.1 Intraday simulation

In what follows, h is set to Δ/M implying that the path simulation is performed with M steps per day. Assuming that Y_t and V_t are known, V_{t+h}, $\Delta I_{t,t+h}$ and Y_{t+h} are generated as follows:

1. The jump indicator functions $\mathbf{1}_{\{N_{Y,t+h}-N_{Y,t}=1\}}$ and $\mathbf{1}_{\{N_{V,t+h}-N_{V,t}=1\}}$ are generated from independent Bernouilli random variables with a success probabilities of $\lambda_{Y,t}h$ and $\lambda_{V,t}h$ respectively.[43]
2. If needed, $Z_{Y,t+h} \sim \mathcal{N}(\mu_Y;\sigma^2_Y)$ and $Z_{V,t+h} \sim \mathrm{Exp}(\mu_V)$ are simulated.
3. Time $t+h$ variance V_{t+h} is simulated according to

$$\begin{aligned} V_{t+h} &\cong V_t + \kappa(\theta - V_t)h + \sigma\sqrt{V_t}\left(W_{V,t+h} - W_{V,t}\right) + Z_{V,t+h}\mathbf{1}_{\{N_{V,t+h}-N_{V,t}=1\}}. \\ &= V_{(t+h)^-} + Z_{V,t+h}\mathbf{1}_{\{N_{V,t+h}-N_{V,t}=1\}} \end{aligned} \tag{28}$$

   where $\mathbf{1}_{\{N_{V,t+h}-N_{V,t}=1\}}$ is an indicator function that is worth 1 if there is a jump during the interval and 0 otherwise. Indeed, it corresponds to the Euler approximation of the variance process (2).
4. The integrated variance increment $\Delta I_{t,t+h} = \int_t^{t+h} V_{u^-}\, du$ is simulated conditionally on V_t and $V_{(t+h)^-}$. More precisely, the cumulant generating function of $\Delta I_{t,t+h}$ is

$$\begin{aligned} \log\left(\mathrm{E}^{\mathbb{P}}\left[\exp(a\Delta I_{t,t+h})\,|V_t, V_{(t+h)^-}\right]\right) &= \log\left(1 + \sum_{m=1}^{\infty} \mathrm{E}^{\mathbb{P}}\left[(\Delta I_{t,t+h})^m|V_t, V_{(t+h)^-}\right]\frac{a^m}{m!}\right) \\ &\cong \mathrm{E}^{\mathbb{P}}\left[\Delta I_{t,t+h}|V_t, V_{(t+h)^-}\right]a + \mathrm{Var}^{\mathbb{P}}\left[\Delta I_{t,t+h}|V_t, V_{(t+h)^-}\right]\frac{a^2}{2}, \end{aligned}$$

[42] Lemma 10 of the Internet appendix provides all details.

[43] Because of the Poisson process properties, the probability of observing a single jump is approximately $\lambda_{\cdot,t}$ when h is small.

which is the cumulant generating function of a Gaussian distribution. The conditional density function of $\Delta I_{t,t+h}$ is approximated by

$$\frac{1}{\sqrt{2\pi \mathrm{Var}^{\mathbb{P}}\left[\Delta I_{t,t+h}|V_t, V_{(t+h)^-}\right]}} \exp\left(-\frac{1}{2}\frac{\left(x - \mathrm{E}^{\mathbb{P}}\left[\Delta I_{t,t+h}|V_t, V_{(t+h)^-}\right]\right)^2}{\mathrm{Var}^{\mathbb{P}}\left[\Delta I_{t,t+h}|V_t, V_{(t+h)^-}\right]}\right).$$

The first two centred moments of $\Delta I_{t,t+h}$ are available in closed form in Tse and Wan (2013).

5. The log-price is simulated according to [44,45,46]

$$\begin{aligned} Y_{t+h} &= Y_t + c_1 h + c_2 \Delta I_{t,t+h} + \rho\sigma^{-1}\left(V_{(t+h)^-} - V_t\right) \\ &+ \sqrt{1-\rho^2}\int_t^{t+h}\sqrt{V_{u^-}}\,dW_{\perp,u} - \frac{\rho}{\sigma}\left(\sum_{n=N_{V,t}+1}^{N_{V,t+h}} Z_{V,n}\right) + \sum_{n=N_{Y,t}+1}^{N_{Y,t+h}} Z_{Y,n}. \end{aligned} \tag{29}$$

where

$$\begin{aligned} c_1 &= r - q + \left(\varphi^{\mathbb{P}}_{Z_Y}\left(\Gamma_Y\right) - \varphi^{\mathbb{P}}_{Z_Y}\left(\left(1+\Gamma_Y\right)\right)\right)\lambda_{Y,0} - \frac{\rho\kappa\theta}{\sigma} \\ c_2 &= \eta_Y - \frac{1}{2} + \left(\varphi^{\mathbb{P}}_{Z_Y}\left(\Gamma_Y\right) - \varphi^{\mathbb{P}}_{Z_Y}\left(\left(1+\Gamma_Y\right)\right)\right)\lambda_{Y,1} + \frac{\rho}{\sigma}\kappa. \end{aligned}$$

In fact, from the integral version of Equation (2),

$$\int_t^{t+h}\sqrt{V_{u^-}}\,dW_{V,u} = \sigma^{-1}\left(V_{(t+h)^-} - V_t - \kappa\theta h + \kappa\int_t^{t+h} V_{u^-}\,du - \sum_{n=N_{V,t}+1}^{N_{V,t+h}} Z_{V,n}\right).$$

Replacing back in the integral form of the log-equity price (1), substituing the drift term of Equation (27) and noting that $\lambda_{Y,t^-} = \lambda_{Y,0} + \lambda_{Y,1}V_{t^-}$ completes the construction.

B.2.2 Time aggregation

Let $t = (k-1)\Delta$. Once Steps 1 to 5 of Appendix B.2.1 have been executed for each intraday periods $\{t+jh\}_{j=1}^{M}$, the integrated variance and quadratic variation increments are approximated by the aggregation of the simulated variables:

$$\Delta I_{t,t+\Delta} \cong \sum_{j=1}^{M}\Delta I_{t+(j-1)h,t+jh} \text{ and } \Delta QV_{t,t+\Delta} \cong \Delta I_{t,t+\Delta} + \sum_{j=1}^{M} Z_{Y,t+jh}\mathbf{1}_{\left\{N_{Y,t+jh}-N_{Y,t+(j-1)h}=1\right\}}.$$

Note that a time aggregation of Equation (29) suggests the approximation

$$Y_{t+\Delta} - Y_t = \sum_{j=1}^{M}\left(Y_{t+jh} - Y_{t+(j-1)h}\right) \cong \mu_{t+\Delta} + \sigma^2_{t+\Delta}\varepsilon_{t+h}$$

[44] Again, for small $h>0$, the two last terms may be approximated with

$$-\frac{\rho}{\sigma}Z_{V,t+h}\mathbf{1}_{\left\{N_{V,t+h}-N_{V,t}=1\right\}} + Z_{Y,t+h}\mathbf{1}_{\left\{N_{Y,t+h}-N_{Y,t}=1\right\}}.$$

[45] As in Broadie and Kaya (2006), $\int_t^{t+h}\sqrt{V_{u^-}}\,dW_{\perp,u}$ is approximated with a Gaussian distribution of mean zero and variance $\Delta I_{t,t+h}$. Indeed, since the instantaneous variance is stochastic, the distribution of $\int_t^{t+h}\sqrt{V_{u^-}}\,dW_{\perp,u}$ is not truly Gaussian. Though, it would have been the case if the variance was a deterministic function of time. The variance of $\int_t^{t+h}\sqrt{V_{u^-}}dW_{\perp,u}$ is $\mathrm{E}^{\mathbb{P}}_t\left[\int_t^{t+h}V_{u^-}du\right] = \mathrm{E}^{\mathbb{P}}_t[\Delta I_{t,t+h}]$.

[46] Note that the log-prices are simulated intraday but the oberved log-price is used whenever it is available, that is at the end of each day. These intermediary log-prices are required in the computation of ΔOQV_{t-h}.

where ε_{t+h} is a standard normal random variable,

$$\begin{aligned}\mu_{t+\Delta} &= c_1\Delta + c_2\Delta I_{t,t+\Delta} + \frac{\rho}{\sigma}\left(V_{t+\Delta} - V_t\right) \\ &\quad -\frac{\rho}{\sigma}\sum_{j=1}^{M} Z_{V,t+jh}\mathbf{1}_{\left\{N_{V,t+jh}-N_{V,t+(j-1)h}=1\right\}} + \sum_{j=1}^{M} Z_{Y,t+jh}\mathbf{1}_{\left\{N_{Y,t+jh}-N_{Y,t+(j-1)h}=1\right\}}\end{aligned} \tag{30}$$

and $\sigma^2_{t+\Delta} = \left(1-\rho^2\right)\Delta I_{t,t+\Delta}$. The model option implied volatility $IV_{t+\Delta}(Y_{t+\Delta}, V_{t+\Delta})$ is calculated based on Equation (23).[47] Finally, the Euler discretization of Equation (10) provides an approximation of the option quadratic variation:[48]

$$\begin{aligned}\Delta OQV_{t,t+\Delta} = h\sum_{j=0}^{M-1}&\left(\left(\frac{\partial O_{t+jh}}{\partial y}\left(Y_{t+jh}, V_{t+jh}\right)\right)^2 + \sigma^2\left(\frac{\partial O_{t+jh}}{\partial v}\left(Y_{t+jh}, V_{t+jh}\right)\right)^2\right. \\ &\left. +2\sigma\rho\frac{\partial O_{t+jh}}{\partial y}\left(Y_{t+jh}, V_{t+jh}\right)\frac{\partial O_{t+jh}}{\partial v}\left(Y_{t+jh}, V_{t+jh}\right)\right)\Delta I_{t+(j-1)h,t+jh} \\ &+\sum_{j=1}^{M}\left\{O_{t+jh}\left(Y_{t+jh}, V_{t+jh}\right) - O_{t+jh}\left(Y_{(t+jh)^-}, V_{(t+jh)^-}\right)\right\}^2.\end{aligned} \tag{31}$$

Internet appendix B.2.1 provides details about how these derivatives are computed. At the end of this stage, a simulated vector

$$x_{t+\Delta} = \left(Y_{t+\Delta}, V_{t+\Delta}, \Delta I_{t,t+\Delta}, QV_{t,t+\Delta}, O^{(i)}_{t+\Delta}(Y_{t+\Delta}, V_{t+\Delta}), \Delta OQV^{(i)}_{t,t+\Delta} : i \in \{1,2,...,n_t\}\right)$$

is obtained at the end of the day.

[47] $IV_{t+\Delta}(Y_{t+\Delta}, V_{t+\Delta})$ is the Black-Scholes implied volatility obtained from the model option price $O^{(i)}_{t,t+\Delta}(Y_{t,t+\Delta}, V_{t,t+\Delta})$.

[48] The log-equity process is only observable on a daily basis. However, $\Delta OQV^{(i)}_{t+(j-1)h,t+jh}$ requires intraday log-equity values. Therefore, it is convenient to treat intraday log-equity values as latent variables.

Internet appendix

A Model construction

A.1 General properties of moment generating functions

The jumps component are model using Cox processes. Moment generating function for such processes are involved in many proofs.

Lemma 1 *Let $\varphi_X^{\mathbb{P}}(a) = \mathrm{E}^{\mathbb{P}}[\exp(aX)]$ be the moment generating function of the random variable X. Assume that $\{X_k\}_{k=1}^{\infty}$ is a sequence of independent and identically distributed random variables. Then*

$$\varphi^{\mathbb{P}}_{\sum_{i=1}^{n} X_i}(a) = \prod_{i=1}^{n} \mathrm{E}^{\mathbb{P}}[\exp(aX_i)] = \left(\varphi^{\mathbb{P}}_{X_1}(a)\right)^n. \tag{32}$$

If N is a Poisson distributed random variable of expectation λ, then the law of iterated expectation implies that

$$\begin{aligned}\varphi^{\mathbb{P}}_{\sum_{i=1}^{N} X_i}(a) &= \mathrm{E}^{\mathbb{P}}\left[\mathrm{E}^{\mathbb{P}}\left[\exp\left(a\sum_{k=1}^{N} X_i\right)\middle| N\right]\right] \\ &= \sum_{n=0}^{\infty}\left(\varphi^{\mathbb{P}}_{X_1}(a)\right)^n \exp(-\lambda)\frac{\lambda^n}{n!} = \exp\left(\lambda\left(\varphi^{\mathbb{P}}_{X_1}(a)-1\right)\right). \end{aligned} \tag{33}$$

If $\{N_t\}_{t\geq 0}$ is a Cox process with predictible intensity $\{\lambda_t\}_{t\geq 0}$, then

$$\begin{aligned}\varphi^{\mathbb{P}}_{\sum_{i=1}^{N_t} X_i}(a) &= \mathrm{E}^{\mathbb{P}}\left[\mathrm{E}^{\mathbb{P}}\left[\exp\left(a\sum_{i=1}^{N_t} X_i\right)\middle| \int_0^t \lambda_u du\right]\right] \\ &= \mathrm{E}^{\mathbb{P}}\left[\exp\left(\left(\int_0^t \lambda_u du\right)\left(\varphi^{\mathbb{P}}_{X_1}(a)-1\right)\right)\right]. \end{aligned} \tag{34}$$

Lemma 2 *If $X \sim \mathcal{N}(\mu, \sigma^2)$, then $\varphi_X^{\mathbb{P}}(a) = \exp\left(\mu a + \frac{1}{2}a^2\sigma^2\right)$.*

Lemma 3 *If X is exponentially distributed of expectation μ, then $\varphi_X^{\mathbb{P}}(a) = (1-a\mu)^{-1}$ provided that $a < \frac{1}{\mu}$.*

A.2 Exponential martingales

Many proofs are based on properties of exponential martingales. The following three lemmas are the central pivots of many proofs.

Lemma 4 *If $E^{\mathbb{P}}\left[\int_0^t \Lambda^2_{V,u^-} du\right] < \infty$ and $E^{\mathbb{P}}\left[\int_0^t \Lambda^2_{\perp,u^-} du\right] < \infty$, then*

$$\left\{\exp\left(-\int_0^t \Lambda_{V,u^-} dW_{V,u} - \int_0^t \Lambda_{\perp,u^-} dW_{\perp,u} - \frac{1}{2}\int_0^t \left(\Lambda^2_{V,u^-} + \Lambda^2_{\perp,u^-}\right) du\right)\right\}_{t\geq 0}$$

is a $\mathbb{P}-$martingale of expectation 1.

Lemma 5 *For $Z \in \{Y, V\}$, $\left\{J_{Z,t} - \mu_Z \int_0^t \lambda_{Z,s^-} ds\right\}_{t\geq 0}$ is a $\mathbb{P}-$martingale.*

Lemma 6 *For $X \in \{Y, V\}$, $\left\{\exp\left(\Gamma_X J_{X,t} - \left(\varphi^{\mathbb{P}}_{Z_X}(\Gamma_X) - 1\right)\int_0^t \lambda_{X,u^-} du\right)\right\}_{t\geq 0}$ is a $\mathbb{P}-$martingale where $\varphi^{\mathbb{P}}_{Z_X}$ is the moment generating function of the jump size Z_X.*

A.2.1 Proofs

Proof of Lemma 4. The continuous process $\{X_t\}_{t\geq 0}$ where

$$X_t = -\int_0^t \Lambda_{V,u^-} dW_{V,u} - \int_0^t \Lambda_{\perp,u^-} dW_{\perp,u}$$

is a $\mathbb{P}-$martingale. Its quadratic variation is $[X,X]_t = \int_0^t \left(\Lambda^2_{V,u^-} + \Lambda^2_{\perp,u^-}\right) du$. Using Itō's lemma,

$$\begin{aligned} & d\exp\left(X_t - \frac{1}{2}[X,X]_t\right) \\ = \; & \exp\left(X_t - \frac{1}{2}[X,X]_t\right)\left(dX_t - \frac{1}{2}d[X,X]_t\right) + \frac{1}{2}\exp\left(X_t - \frac{1}{2}[X,X]_t\right) d[X,X]_t \\ = \; & \exp\left(X_t - \frac{1}{2}[X,X]_t\right) dX_t. \end{aligned}$$

Because $\exp\left(X_t - \frac{1}{2}[X,X]_t\right)$ is a stochastic integral with respect to a martingale, $\left\{\exp\left(X_t - \frac{1}{2}[X,X]_t\right)\right\}_{t\geq 0}$ is a $\mathbb{P}-$martingale. Since $X_0 = 0$, then

$$\mathrm{E}^{\mathbb{P}}\left[\exp\left(X_t - \frac{1}{2}[X,X]_t\right)\right] = \mathrm{E}^{\mathbb{P}}\left[\exp\left(X_0 - \frac{1}{2}[X,X]_0\right)\right] = 1.$$

□

Proof of Lemma 5.

$$\begin{aligned} & \mathrm{E}^{\mathbb{P}}_{\mathcal{F}_s}\left[J_{Z,t} - J_{Z,s} - \mu_Z \int_0^t \lambda_{Z,u^-} du\right] \\ & = \mathrm{E}^{\mathbb{P}}_{\mathcal{F}_s}\left[\mathrm{E}^{\mathbb{P}}_{\mathcal{F}_s}\left[J_{Z,t} - J_{Z,s} - \mu_Z \int_0^t \lambda_{Z,u^-} du \middle| \int_0^t \lambda_{Z,u^-} du\right]\right] \\ & = \mathrm{E}^{\mathbb{P}}_{\mathcal{F}_s}\left[\mathrm{E}^{\mathbb{P}}_{\mathcal{F}_s}\left[\sum_{n=N_{Z,s}+1}^{N_{Z,t}} Z_{Y,n} - \mu_Z \int_0^t \lambda_{Z,u^-} du \middle| \int_0^t \lambda_{Z,u^-} du\right]\right] \\ & = \mathrm{E}^{\mathbb{P}}_{\mathcal{F}_s}\left[\mathrm{E}^{\mathbb{P}}_{\mathcal{F}_s}\left[\mathrm{E}^{\mathbb{P}}_{\mathcal{F}_s}\left[\sum_{n=N_{Z,s}+1}^{N_{Z,t}} Z_{Y,n} \middle| \int_0^t \lambda_{Z,u^-} du, N_{Z,t} - N_{Z,s}\right] - \mu_Z \int_0^t \lambda_{Z,u^-} du \middle| \int_0^t \lambda_{Z,u^-} du\right]\right] \\ & = \mathrm{E}^{\mathbb{P}}_{\mathcal{F}_s}\left[\mathrm{E}^{\mathbb{P}}_{\mathcal{F}_s}\left[\sum_{n=0}^{\infty} n\mu_Z \exp\left(-\int_0^t \lambda_{Z,u^-} du\right) \frac{\left(\int_0^t \lambda_{Z,u^-} du\right)^n}{n!} - \mu_Z \int_0^t \lambda_{Z,u^-} du \middle| \int_0^t \lambda_{Z,u^-} du\right]\right] \\ & = \mathrm{E}^{\mathbb{P}}_{\mathcal{F}_s}\left[\mathrm{E}^{\mathbb{P}}_{\mathcal{F}_s}\left[\mu_Z \int_0^t \lambda_{Z,u^-} du - \mu_Z \int_0^t \lambda_{Z,u^-} du \middle| \int_0^t \lambda_{Z,u^-} du\right]\right] \\ & = 0. \end{aligned}$$

Proof of Lemma 6. From the moment generating function of a compound Poisson process with stochastic jump intensity of Equation (34),

$$\begin{aligned} & \mathrm{E}^{\mathbb{P}}_{\mathcal{F}_s}\left[\exp\left(\Gamma_X\left(J_{X,t} - J_{X,s}\right) - \left(\int_s^t \lambda_{X,u^-} du\right)\left(\varphi^{\mathbb{P}}_{Z_X}\left(\Gamma_X\right) - 1\right)\right)\right] \\ = \; & \mathrm{E}^{\mathbb{P}}_{\mathcal{F}_s}\left[\exp\left(\Gamma_X\left(\sum_{n=N_{X,s}+1}^{N_{X,t}} Z_{X,n}\right) - \left(\int_s^t \lambda_{X,u^-} du\right)\left(\varphi^{\mathbb{P}}_{Z_X}\left(\Gamma_X\right) - 1\right)\right)\right] \end{aligned}$$

$$= \quad \mathrm{E}^{\mathbb{P}}_{\mathcal{F}_s}\left[\exp\left(\left(\left(\int_s^t \lambda_{X,u^-}du\right)\left(\varphi^{\mathbb{P}}_{Z_X}\left(\Gamma_X\right)-1\right)-\left(\int_s^t \lambda_{X,u^-}du\right)\left(\varphi^{\mathbb{P}}_{Z_X}\left(\Gamma_X\right)-1\right)\right)\right]=0.$$

For the log-equity price jumps,

$$\varphi^{\mathbb{P}}_{Z_Y}\left(\Gamma_Y\right)-1=\exp\left(\mu_Y\Gamma_Y+\frac{1}{2}\sigma_Y^2\Gamma_Y^2\right)-1,$$

while for the variance jumps,

$$\varphi^{\mathbb{P}}_{Z_V}\left(\Gamma_V\right)-1=\left(1-\Gamma_V\mu_V\right)^{-1}-1$$

provided that $\Gamma_V<\mu_V^{-1}$. □

A.3 Risk-neutral innovations

Lemma 7 justifies Equation (19). Lemma 8 determines the jump dynamics under $\mathbb{Q}$. These are components of the risk-neutral version of the model presented in Appendices A.1 and A.2.

Lemma 7 *For $X\in\{Y,\perp\}$, the risk-neutral moment generating function of the Brownian increments $W_{X,t}-W_{X,s}$ satisfies*

$$\varphi^{\mathbb{Q}}_{W_{X,t}-W_{X,s}}\left(a\right)=\mathrm{E}^{\mathbb{P}}_{\mathcal{F}_s}\left[\exp\left(-a\int_s^t\Lambda_{X,u^-}du+\frac{a^2\left(t-s\right)}{2}\right)\right]$$

which is the moment generating function of a Gaussian distribution of expectation $\mathrm{E}^{\mathbb{P}}_{\mathcal{F}_s}\left[-a\int_s^t\Lambda_{X,u^-}du\right]$ and variance $t-s$.

Lemma 8 *For $X\in\{Y,V\}$, the risk-neutral moment generating function of the jump increments $J_{Y,t}-J_{Y,s}$ is given by*

$$\mathrm{E}^{\mathbb{Q}}_{\mathcal{F}_s}\left[\exp\left(a\left(J_{X,t}-J_{X,s}\right)\right)\right]=\mathrm{E}^{\mathbb{P}}_{\mathcal{F}_s}\left[\exp\left(\left(\varphi^{\mathbb{P}}_{Z_X}\left(a+\Gamma_X\right)-\varphi^{\mathbb{P}}_{Z_X}\left(\Gamma_X\right)\right)\int_s^t\lambda_{X,u^-}du\right)\right].$$

In particular

$$\begin{aligned}&\varphi^{\mathbb{Q}}_{J_{Y,t}-J_{Y,s}}\left(a\right)=\mathrm{E}^{\mathbb{Q}}_{\mathcal{F}_s}\left[\exp\left(a\left(J_{Y,t}-J_{Y,s}\right)\right)\right]\\ =\;&\mathrm{E}^{\mathbb{P}}_{\mathcal{F}_s}\left[\exp\left(\left(\exp\left(\mu_Y\left(a+\Gamma_Y\right)+\frac{1}{2}\left(a+\Gamma_Y\right)^2\sigma_Y^2\right)-\exp\left(\mu_Y\Gamma_Y+\frac{1}{2}\Gamma_Y^2\sigma_Y^2\right)\right)\int_s^t\lambda_{Y,u^-}du\right)\right]\end{aligned}$$

and

$$\begin{aligned}&\varphi^{\mathbb{Q}}_{J_{V,t}-J_{V,s}}\left(a\right)=\mathrm{E}^{\mathbb{Q}}_{\mathcal{F}_s}\left[\exp\left(a\left(J_{V,t}-J_{V,s}\right)\right)\right]\\ =\;&\mathrm{E}^{\mathbb{P}}_{\mathcal{F}_s}\left[\exp\left(\left(\left(1-\left(a+\Gamma_V\right)\mu_{\mu_V}\right)^{-1}-\left(1-\Gamma_V\mu_{\mu_V}\right)^{-1}\right)\int_s^t\lambda_{Y,u^-}du\right)\right]\end{aligned}$$

provided that $\Gamma_V<\mu_{\mu_V}^{-1}$ and $a+\Gamma_V<\mu_{\mu_V}^{-1}$.

A comparison of the $\mathbb{P}-$ and the $\mathbb{Q}-$versions of the between the $\mathbb{P}-$ and $\mathbb{Q}-$parameters:

$$\begin{aligned}\varphi^{\mathbb{P}}_{J_{Y,t}-J_{Y,s}}\left(a\right)&=\mathrm{E}^{\mathbb{P}}_{\mathcal{F}_s}\left[\exp\left(\int_s^t\lambda_{Y,u^-}du\left(\exp\left(\mu_Ya+\frac{1}{2}\sigma_Y^2a^2\right)-1\right)\right)\right],\\ \varphi^{\mathbb{Q}}_{J_{Y,t}-J_{Y,s}}\left(a\right)&=\mathrm{E}^{\mathbb{P}}_{\mathcal{F}_s}\left[\exp\left(\exp\left(\mu_Y\Gamma_Y+\frac{1}{2}\Gamma_Y^2\sigma_Y^2\right)\int_s^t\lambda_{Y,u^-}du\left(\frac{\exp\left(\mu_Y\left(a+\Gamma_Y\right)+\frac{1}{2}\left(a+\Gamma_Y\right)^2\sigma_Y^2\right)}{\exp\left(\mu_Y\Gamma_Y+\frac{1}{2}\Gamma_Y^2\sigma_Y^2\right)}-1\right)\right)\right]\\ &=\mathrm{E}^{\mathbb{P}}_{\mathcal{F}_s}\left[\exp\left(\exp\left(\mu_Y\Gamma_Y+\frac{1}{2}\Gamma_Y^2\sigma_Y^2\right)\int_s^t\lambda_{Y,u^-}du\left(\exp\left(\left(\mu_Y+\Gamma_Y\sigma_Y^2\right)a+\frac{1}{2}a^2\sigma_Y^2\right)-1\right)\right)\right],\end{aligned}$$

$$\begin{aligned}
\varphi^{\mathbb{P}}_{J_{V,t}-J_{V,s}}(a) &= \mathrm{E}^{\mathbb{P}}_{\mathcal{F}_s}\left[\exp\left(\int_s^t \lambda_{V,u^-}du\left(\left(1-a\mu_V\right)^{-1}-1\right)\right)\right],\\
\varphi^{\mathbb{Q}}_{J_{V,t}-J_{V,s}}(a) &= \mathrm{E}^{\mathbb{P}}_{\mathcal{F}_s}\left[\exp\left(\left(1-\Gamma_V\mu_V\right)^{-1}\int_s^t \lambda_{Y,u^-}du\left(\frac{1-\Gamma_V\mu_V}{1-\left(a+\Gamma_V\right)\mu_V}-1\right)\right)\right]\\
&= \mathrm{E}^{\mathbb{P}}_{\mathcal{F}_s}\left[\exp\left(\left(1-\Gamma_V\mu_V\right)^{-1}\int_s^t \lambda_{Y,u^-}du\left(\left(1-a\frac{\mu_V}{1-\Gamma_V\mu_V}\right)^{-1}-1\right)\right)\right].
\end{aligned}$$

A.3.1 Proofs

Proof of Lemma 7. The moment generating function of $W_{X,t}-W_{X,s}$ under $\mathbb{Q}$ is

$$\begin{aligned}
&\varphi^{\mathbb{Q}}_{W_{X,t}-W_{X,s}}(a) = \mathrm{E}^{\mathbb{Q}}_{\mathcal{F}_s}\left[\exp\left(a\left(W_{X,t}-W_{X,s}\right)\right)\right]\\
=\;& \mathrm{E}^{\mathbb{P}}_{\mathcal{F}_s}\left[\exp\left(a\left(W_{X,t}-W_{X,s}\right)\right)\exp\left(\begin{array}{l} -\int_s^t \Lambda_{V,u^-}dW_{V,u}-\int_s^t \Lambda_{\perp,u^-}dW_{\perp,u}-\frac{1}{2}\int_s^t\left(\Lambda^2_{V,u^-}+\Lambda^2_{\perp,u^-}\right)du\\ +\Gamma_Y\left(J_{Y,t}-J_{Y,s}\right)-\left(\exp\left(\mu_Y\Gamma_Y+\frac{1}{2}\sigma_Y^2\Gamma_Y^2\right)-1\right)\int_s^t\lambda_{Y,u^-}du\\ +\Gamma_V\left(J_{V,t}-J_{V,s}\right)-\left(\left(1-\mu_V\Gamma_V\right)^{-1}-1\right)\int_s^t\lambda_{V,u^-}du \end{array}\right)\right].
\end{aligned}$$

Because the variance jump intensity is independent of the other components inside the exponential function, the last expression is equal to

$$\begin{aligned}
&\mathrm{E}^{\mathbb{P}}_{\mathcal{F}_s}\left[\exp\left(a\left(W_{X,t}-W_{X,s}\right)\right)\exp\left(\begin{array}{l} -\int_s^t \Lambda_{V,u^-}dW_{V,u}-\int_s^t \Lambda_{\perp,u^-}dW_{\perp,u}-\frac{1}{2}\int_s^t\left(\Lambda^2_{V,u^-}+\Lambda^2_{\perp,u^-}\right)du\\ +\Gamma_Y\left(J_{Y,t}-J_{Y,s}\right)-\left(\exp\left(\mu_Y\Gamma_Y+\frac{1}{2}\sigma_Y^2\Gamma_Y^2\right)-1\right)\int_s^t\lambda_{Y,u^-}du \end{array}\right)\right]\\
&\times\mathrm{E}^{\mathbb{P}}_{\mathcal{F}_s}\left[\exp\left(\Gamma_V\left(J_{V,t}-J_{V,s}\right)-\left(\left(1-\mu_V\Gamma_V\right)^{-1}-1\right)\int_s^t\lambda_{V,u^-}du\right)\right].
\end{aligned}$$

Lemma 6 implies that the last expectation is 1. Using the tower property of conditional expectations, conditioning on the log-equity price intensity, the previous expression becomes

$$\begin{aligned}
&\mathrm{E}^{\mathbb{P}}_{\mathcal{F}_s}\left[\begin{array}{l}\mathrm{E}^{\mathbb{P}}_{\mathcal{F}_s}\left[\begin{array}{c}\exp\left(a\left(W_{X,t}-W_{X,s}\right)\right)\\ \exp\left(-\int_s^t \Lambda_{V,u^-}dW_{V,u}-\int_s^t \Lambda_{\perp,u^-}dW_{\perp,u}-\frac{1}{2}\int_s^t\left(\Lambda^2_{V,u^-}+\Lambda^2_{\perp,u^-}\right)du\right)\end{array}\middle|\int_s^t\lambda_{Y,u^-}du\right]\\ \times\mathrm{E}^{\mathbb{P}}_{\mathcal{F}_s}\left[\exp\left(\Gamma_Y\left(J_{Y,t}-J_{Y,s}\right)-\left(\exp\left(\mu_Y\Gamma_Y+\frac{1}{2}\sigma_Y^2\Gamma_Y^2\right)-1\right)\int_s^t\lambda_{Y,u^-}du\right)\middle|\int_s^t\lambda_{Y,u^-}du\right]\end{array}\right]\\
=\;&\mathrm{E}^{\mathbb{P}}_{\mathcal{F}_s}\left[\mathrm{E}^{\mathbb{P}}_{\mathcal{F}_s}\left[\begin{array}{c}\exp\left(a\left(W_{X,t}-W_{X,s}\right)\right)\\ \exp\left(-\int_s^t \Lambda_{V,u^-}dW_{V,u}-\int_s^t \Lambda_{\perp,u^-}dW_{\perp,u}-\frac{1}{2}\int_s^t\left(\Lambda^2_{V,u^-}+\Lambda^2_{\perp,u^-}\right)du\right)\end{array}\middle|\int_s^t\lambda_{Y,u^-}du\right]\right].
\end{aligned}$$

Finally, from Lemma 4,

$$\begin{aligned}
&\varphi^{\mathbb{Q}}_{W_{X,t}-W_{X,s}}(a) = \mathrm{E}^{\mathbb{P}}_{\mathcal{F}_s}\left[\exp\left(a\left(W_{X,t}-W_{X,s}\right)\right)\exp\left(-\int_s^t\Lambda_{X,u^-}dW_{X,u}-\frac{1}{2}\int_s^t\Lambda^2_{X,u^-}du\right)\right]\\
=\;&\mathrm{E}^{\mathbb{P}}_{\mathcal{F}_s}\left[\exp\left(\int_s^t\left(a-\Lambda_{X,u^-}\right)dW_{V,u}-\frac{1}{2}\int_s^t\Lambda^2_{X,u^-}du\right)\right]\\
=\;&\mathrm{E}^{\mathbb{P}}_{\mathcal{F}_s}\left[\exp\left(\int_s^t\left(a-\Lambda_{X,u^-}\right)dW_{V,u}-\frac{1}{2}\int_s^t\left(a-\Lambda_{X,u^-}\right)^2du-\frac{1}{2}\int_s^t\Lambda^2_{X,u^-}du+\frac{1}{2}\int_s^t\left(a-\Lambda_{X,u^-}\right)^2du\right)\right]\\
=\;&\mathrm{E}^{\mathbb{P}}_{\mathcal{F}_s}\left[\exp\left(-a\int_s^t\Lambda_{X,u^-}du+\frac{a^2\left(t-s\right)}{2}\right)\right].
\end{aligned}$$

$\square$

Proof of Lemma 8.

$$
\begin{aligned}
& \mathrm{E}^{\mathbb{Q}}_{\mathcal{F}_s}\left[\exp\left(a\left(J_{X,t}-J_{X,s}\right)\right)\right] \\
= \quad & \mathrm{E}^{\mathbb{P}}_{\mathcal{F}_s}\left[\exp\left(\begin{array}{c} a\left(J_{X,t}-J_{X,s}\right) \\ -\int_s^t \Lambda_{V,u^-}dW_{V,u}-\int_s^t \Lambda_{\perp,u^-}dW_{\perp,u}-\frac{1}{2}\int_s^t\left(\Lambda^2_{V,u^-}+\Lambda^2_{\perp,u^-}\right)du \\ +\Gamma_X\left(J_{Y,t}-J_{Y,s}\right)-\left(\varphi^{\mathbb{P}}_{Z_Y}\left(\Gamma_Y\right)-1\right)\int_s^t \lambda_{Y,u^-}du \\ +\Gamma_V\left(J_{V,t}-J_{V,t}\right)-\left(\varphi^{\mathbb{P}}_{Z_Y}\left(\Gamma_V\right)-1\right)\int_s^t \lambda_{V,u^-}du \end{array}\right)\right].
\end{aligned}
$$

Using the tower property of conditional expectations, the last expression becomes

$$
\begin{aligned}
& \mathrm{E}^{\mathbb{P}}_{\mathcal{F}_s}\left[\mathrm{E}^{\mathbb{P}}_{\mathcal{F}_s}\left[\exp\left(-\int_s^t \Lambda_{V,u^-}dW_{V,u}-\int_s^t \Lambda_{\perp,u^-}dW_{\perp,u}-\frac{1}{2}\int_s^t\left(\Lambda^2_{V,u^-}+\Lambda^2_{\perp,u^-}\right)du\right)\middle|\int_s^t \lambda_{Y,u^-}du\right]\right] \\
& \times\mathrm{E}^{\mathbb{P}}_{\mathcal{F}_s}\left[\mathrm{E}^{\mathbb{P}}_{\mathcal{F}_s}\left[\begin{array}{c} \exp\left(a\left(J_{X,t}-J_{X,s}\right)\right) \\ \exp\left(\begin{array}{c} +\Gamma_X\left(J_{Y,t}-J_{Y,s}\right)-\left(\varphi^{\mathbb{P}}_{Z_Y}\left(\Gamma_Y\right)-1\right)\int_s^t \lambda_{Y,u^-}du \\ +\Gamma_V\left(J_{V,t}-J_{V,t}\right)-\left(\varphi^{\mathbb{P}}_{Z_Y}\left(\Gamma_V\right)-1\right)\int_s^t \lambda_{V,u^-}du \end{array}\right)\end{array}\middle|\int_s^t \lambda_{Y,u^-}du\right]\right].
\end{aligned}
$$

Lemma 4 implies that the first term vanishes. Therefore,

$$
\begin{aligned}
& \mathrm{E}^{\mathbb{Q}}_{\mathcal{F}_s}\left[\exp\left(a\left(J_{X,t}-J_{X,s}\right)\right)\right]=\mathrm{E}^{\mathbb{P}}_{\mathcal{F}_s}\left[\exp\left(\left(a+\Gamma_X\right)\left(J_{X,t}-J_{X,s}\right)-\left(\varphi^{\mathbb{P}}_{Z_{X,1}}\left(\Gamma_X\right)-1\right)\int_s^t \lambda_{X,u^-}du\right)\right] \\
= \quad & \mathrm{E}^{\mathbb{P}}_{\mathcal{F}_s}\left[\exp\left(\begin{array}{c}\left(a+\Gamma_X\right)\left(J_{X,t}-J_{X,s}\right)-\left(\varphi^{\mathbb{P}}_{Z_X}\left(a+\Gamma_X\right)-1\right)\int_s^t \lambda_{X,u^-}du \\ +\left(\varphi^{\mathbb{P}}_{Z_X}\left(a+\Gamma_X\right)-1\right)\int_s^t \lambda_{X,u^-}du-\left(\varphi^{\mathbb{P}}_{Z_X}\left(\Gamma_X\right)-1\right)\int_s^t \lambda_{X,u^-}du\end{array}\right)\right] \\
= \quad & \mathrm{E}^{\mathbb{P}}_{\mathcal{F}_s}\left[\mathrm{E}^{\mathbb{P}}_{\mathcal{F}_s}\left[\exp\left(\begin{array}{c}\left(a+\Gamma_X\right)\left(J_{X,t}-J_{X,s}\right)-\left(\varphi^{\mathbb{P}}_{Z_X}\left(a+\Gamma_X\right)-1\right)\int_s^t \lambda_{X,u^-}du \\ +\left(\varphi^{\mathbb{P}}_{Z_X}\left(a+\Gamma_X\right)-1\right)\int_s^t \lambda_{X,u^-}du-\left(\varphi^{\mathbb{P}}_{Z_X}\left(\Gamma_X\right)-1\right)\int_s^t \lambda_{X,u^-}du\end{array}\right)\middle|\int_s^t \lambda_{X,u^-}du\right]\right] \\
= \quad & \mathrm{E}^{\mathbb{P}}_{\mathcal{F}_s}\left[\exp\left(\left(\varphi^{\mathbb{P}}_{Z_X}\left(a+\Gamma_X\right)-\varphi^{\mathbb{P}}_{Z_X}\left(\Gamma_X\right)\right)\int_s^t \lambda_{X,u^-}du\right)\right].
\end{aligned}
$$

□

A.4 Log-equity price drift

This section provides a detailed proof of the log-equity price drift term described in Appendix B.1.

Lemma 9 *Under the risk-neutral measure, the log-equity price is characterized by*

$$
\begin{aligned}
dY_t &= \alpha^{\mathbb{Q}}_{t^-}dt+\sqrt{V_{t^-}}dW^{\mathbb{Q}}_{Y,t}+dJ^{\mathbb{Q}}_{Y,t}, \\
\alpha^{\mathbb{Q}}_{t^-} &= r-q-\frac{1}{2}V_{t^-}-\xi^{\mathbb{Q}}_Y\lambda^{\mathbb{Q}}_{Y,t^-}, \\
\xi^{\mathbb{Q}}_Y &= \varphi^{\mathbb{Q}}_{Z_Y}(1)-1=\exp\left(\mu^{\mathbb{Q}}_Y+\frac{1}{2}\sigma^2_Y\right)-1, \\
\lambda^{\mathbb{Q}}_{Y,t^-} &= \varphi^{\mathbb{Q}}_{Z_Y}\left(\Gamma_Y\right)\lambda^{\mathbb{P}}_{Y,t^-}=\exp\left(\mu_Y\Gamma_Y+\frac{1}{2}\Gamma^2_Y\sigma^2_Y\right)\lambda^{\mathbb{P}}_{Y,t^-}.
\end{aligned}
$$

Proof of Lemma 9 . Using Itō's lemma,

$$
\begin{aligned}
\exp\left(Y_t\right)-\exp\left(Y_0\right) &= \int_0^t \exp\left(Y_{u^-}\right)dY_u+\frac{1}{2}\int_0^t \exp\left(Y_{u^-}\right)d\left[Y,Y\right]^c_u \\
&+\sum_{0<u\le t}\left\{\exp\left(Y_u\right)-\exp\left(Y_{u^-}\right)-\exp\left(Y_{u^-}\right)\Delta Y_u\right\}.
\end{aligned}
$$

The last term is equal to

$$
\begin{aligned}
& \sum_{0<u\le t} \exp\left(Y_{u^-}\right)\left\{\exp\left(Y_u - Y_{u^-}\right) - 1\right\} - \sum_{0<u\le t} \left\{\exp\left(Y_{u^-}\right)\left(J^{\mathbb{Q}}_{Y,u} - J^{\mathbb{Q}}_{Y,u^-}\right)\right\} \\
= & \sum_{0<u\le t} \exp\left(Y_{u^-}\right)\left\{\exp\left(J^{\mathbb{Q}}_{Y,u} - J^{\mathbb{Q}}_{Y,u^-}\right) - 1\right\} - \sum_{0<u\le t} \left\{\exp\left(Y_{u^-}\right)\left(J^{\mathbb{Q}}_{Y,u} - J^{\mathbb{Q}}_{Y,u^-}\right)\right\} \\
= & \sum_{0<u\le t} \exp\left(Y_{u^-} - J^{\mathbb{Q}}_{Y,u^-}\right)\left\{\exp\left(J^{\mathbb{Q}}_{Y,u}\right) - \exp\left(J^{\mathbb{Q}}_{Y,u^-}\right)\right\} \\
& - \sum_{0<u\le t} \left\{\exp\left(Y_{u^-}\right)\left(J^{\mathbb{Q}}_{Y,u} - J^{\mathbb{Q}}_{Y,u^-}\right)\right\}.
\end{aligned}
$$

Therefore, by substituing Equation (21) in the first term of $\exp(Y_t) - \exp(Y_0)$, we obtain

$$
\begin{aligned}
& \exp\left(Y_t\right) - \exp\left(Y_0\right) \\
= & \int_0^t \exp\left(Y_{u^-}\right)\alpha^{\mathbb{Q}}_{u^-}du + \int_0^t \exp\left(Y_{u^-}\right)\sqrt{V_{u^-}}dW^{\mathbb{Q}}_{Y,u} + \int_0^t \exp\left(Y_{u^-}\right)dJ^{\mathbb{Q}}_{Y,u} \\
& + \frac{1}{2}\int_0^t \exp\left(Y_{u^-}\right)V_{u^-}du + \int_0^t \exp\left(Y_{u^-} - J^{\mathbb{Q}}_{Y,u^-}\right)d\exp\left(J^{\mathbb{Q}}_{Y,u}\right) - \int_0^t \exp\left(Y_{u^-}\right)dJ^{\mathbb{Q}}_{Y,u} \\
= & \int_0^t \exp\left(Y_{u^-}\right)\left(\alpha^{\mathbb{Q}}_{u^-} + \frac{1}{2}V_{u^-}\right)du + \int_0^t \exp\left(Y_{u^-}\right)\sqrt{V_{u^-}}dW^{\mathbb{Q}}_{Y,u} \\
& + \int_0^t \exp\left(Y_{u^-} - J^{\mathbb{Q}}_{Y,u^-}\right)d\exp\left(J^{\mathbb{Q}}_{Y,u}\right).
\end{aligned}
$$

Lemma 6 states that $\left\{\exp\left(J^{\mathbb{Q}}_{Y,t} - \left(\varphi^{\mathbb{Q}}_{Z_Y}(1) - 1\right)\int_0^t \lambda^{\mathbb{Q}}_{Y,u^-}du\right)\right\}_{t\ge 0}$ is a $\mathbb{Q}-$martingale, where $\varphi^{\mathbb{Q}}_{Z_Y}$ is the moment generating function of the log-equity price jump size. Therefore, if

$$
\xi^{\mathbb{Q}}_Y = \varphi^{\mathbb{Q}}_{Z_Y}(1) - 1 = \exp\left(\mu^{\mathbb{Q}}_Y + \frac{1}{2}\sigma^2_Y\right) - 1,
$$

then

$$
\begin{aligned}
& \exp\left(Y_t\right) - \exp\left(Y_0\right) \\
= & \int_0^t \exp\left(Y_{u^-}\right)\left(\alpha^{\mathbb{Q}}_{u^-} + \frac{1}{2}V_{u^-}\right)du + \int_0^t \exp\left(Y_{u^-}\right)\sqrt{V_{u^-}}dW^{\mathbb{Q}}_{Y,u} \\
& + \int_0^t \exp\left(Y_{u^-} - J^{\mathbb{Q}}_{Y,u^-}\right)d\left(\exp\left(J^{\mathbb{Q}}_{Y,u} - \xi^{\mathbb{Q}}_Y\int_0^u \lambda^{\mathbb{Q}}_{Y,s^-}\,ds\right)\exp\left(\xi^{\mathbb{Q}}_Y\int_0^u \lambda^{\mathbb{Q}}_{Y,s^-}\,ds\right)\right) \\
= & \int_0^t \exp\left(Y_{u^-}\right)\left(\alpha^{\mathbb{Q}}_{u^-} + \frac{1}{2}V_{u^-}\right)du + \int_0^t \exp\left(Y_{u^-}\right)\sqrt{V_{u^-}}dW^{\mathbb{Q}}_{Y,u} \\
& + \int_0^t \exp\left(Y_{u^-} - J^{\mathbb{Q}}_{Y,u^-}\right)\exp\left(\xi^{\mathbb{Q}}_Y\int_0^u \lambda^{\mathbb{Q}}_{Y,s^-}\,ds\right)d\exp\left(J^{\mathbb{Q}}_{Y,u} - \xi^{\mathbb{Q}}_Y\int_0^u \lambda^{\mathbb{Q}}_{Y,s^-}\right) \\
& + \int_0^t \exp\left(Y_{u^-} - J^{\mathbb{Q}}_{Y,u^-}\right)\exp\left(J^{\mathbb{Q}}_{Y,u^-} - \xi^{\mathbb{Q}}_Y\int_0^u \lambda^{\mathbb{Q}}_{Y,s^-}du\right)\xi^{\mathbb{Q}}_Y\lambda^{\mathbb{Q}}_{Y,u^-}\exp\left(\xi^{\mathbb{Q}}_Y\int_0^u \lambda^{\mathbb{Q}}_{Y,s^-}ds\right)du \\
= & \int_0^t \exp\left(Y_{u^-}\right)\left(\alpha^{\mathbb{Q}}_{u^-} + \frac{1}{2}V_{u^-} + \xi^{\mathbb{Q}}_Y\lambda^{\mathbb{Q}}_{Y,u^-}\right)du + \int_0^t \exp\left(Y_{u^-}\right)\sqrt{V_{u^-}}dW^{\mathbb{Q}}_{Y,u} \\
& + \int_0^t \exp\left(Y_{u^-} - J^{\mathbb{Q}}_{Y,u^-}\right)\exp\left(\xi^{\mathbb{Q}}_Y\int_0^u \lambda^{\mathbb{Q}}_{Y,s^-}du\right)d\exp\left(J^{\mathbb{Q}}_{Y,u} - \xi^{\mathbb{Q}}_Y\int_0^u \lambda^{\mathbb{Q}}_{Y,s^-}du\right).
\end{aligned}
$$

Note that the last two terms are martingales. Because the discount factor and the dividend correction are both continuous, i.e.

$$
D_t = \exp\left(-(r-q)t\right), \tag{35}
$$

integration by part implies that

$$
\begin{aligned}
& D_t \exp(Y_t) - D_0 \exp(Y_0) \\
= & \int_0^t D_u d\exp(Y_u) - \int_0^t (r-q) D_u \exp(Y_{u^-})\, du \\
= & \int_0^t D_u \exp(Y_{u^-}) \left(\alpha^{\mathbb{Q}}_{u^-} + \frac{1}{2} V_{u^-} + \xi^{\mathbb{Q}}_Y \lambda^{\mathbb{Q}}_{Y,u^-} - r + q \right) du \\
& + \int_0^t D_u \exp(Y_{u^-}) \sqrt{V_{u^-}} dW^{\mathbb{Q}}_{Y,u} \\
& + \int_0^t D_u \exp\left(Y_{u^-} - J^{\mathbb{Q}}_{Y,u^-} \right) \exp\left(\xi^{\mathbb{Q}}_Y \int_0^u \lambda^{\mathbb{Q}}_{Y,s^-} du \right) d\exp\left(J^{\mathbb{Q}}_{Y,u} - \xi^{\mathbb{Q}}_Y \int_0^t \lambda^{\mathbb{Q}}_{Y,u^-} du \right).
\end{aligned}
$$

The pricing theory implied that $\{D_t \exp(Y_t)\}_{t\geq 0}$ must be a $\mathbb{Q}$-martingale. Therefore, the drift component must be nil, that is

$$
\alpha^{\mathbb{Q}}_{u^-} = r - q - \frac{1}{2} V_{u^-} - \xi^{\mathbb{Q}}_Y \lambda^{\mathbb{Q}}_{Y,u^-}.
$$

□

Lemma 10 *Under the $\mathbb{P}-$measure, the returns' are characterized by*

$$
\begin{aligned}
dY_t &= \alpha^{\mathbb{P}}_{t^-} dt + \sqrt{V_{t^-}} dW_{Y,t} + dJ_{Y,t}, \\
\alpha^{\mathbb{P}}_{u^-} &= r - q - \frac{1}{2} V_{u^-} + \sqrt{V_{u^-}} \Lambda_{Y,u^-} + \left(\xi^{\mathbb{P}}_Y - \zeta^{\mathbb{P}}_Y \right) \lambda_{Y,u^-} + \left(\xi^{\mathbb{P}}_V - \zeta^{\mathbb{P}}_V \right) \lambda_{V,u^-} \\
&= r - q - \frac{1}{2} V_{u^-} + \sqrt{V_{u^-}} \Lambda_{Y,u^-} + \left(\varphi^{\mathbb{P}}_{Z_Y}(\Gamma_Y) - \varphi^{\mathbb{P}}_{Z_Y}(1+\Gamma_Y) \right) \lambda_{Y,u^-}, \\
\xi^{\mathbb{P}}_Y &= \varphi^{\mathbb{P}}_{Z_Y}(\Gamma_Y) - 1, \\
\xi^{\mathbb{P}}_V &= \varphi^{\mathbb{P}}_{Z_V}(\Gamma_V) - 1, \\
\zeta^{\mathbb{P}}_Y &= \varphi^{\mathbb{P}}_{Z_Y}(1+\Gamma_Y) - 1, \\
\zeta^{\mathbb{P}}_V &= \varphi^{\mathbb{P}}_{Z_V}(\Gamma_V) - 1,
\end{aligned}
$$

Proof of Lemma 10. Let

$$
Z_t = \begin{pmatrix} -\int_0^t \Lambda_{V,u^-} dW_{V,u} - \int_0^t \Lambda_{\perp,u^-} dW_{\perp,u} - \frac{1}{2}\int_0^t \left(\Lambda^2_{V,u^-} + \Lambda^2_{\perp,u^-} \right) du \\ + \Gamma_Y J_{Y,t} - \xi^{\mathbb{P}}_Y \int_0^t \lambda_{Y,u^-} du + \Gamma_V J_{V,t} - \xi^{\mathbb{P}}_V \int_0^t \lambda_{V,u^-} du \end{pmatrix}
$$

be associated to the Radon-Nikodym derivative (17) and $D_t \exp(-(r-q)t)$ be the combination of the discount factor and the dividend yield. Since the discounted price must be a $\mathbb{Q}-$martingale,

$$
1 = \mathrm{E}^{\mathbb{Q}}_s \left[\frac{D_t \exp(Y_t)}{D_s \exp(Y_s)} \right] = \mathrm{E}^{\mathbb{P}}_s \left[\frac{D_t \exp(Y_t + Z_t)}{D_s \exp(Y_s + Z_s)} \right]
$$

which means that $\{D_t \exp(Y_t + Z_t)\}_{t\geq 0}$ is a $\mathbb{P}-$martingale. Note that

$$
\begin{aligned}
Y_t + Z_t = & \; Y_0 + Z_0 + \int_0^t \left(\alpha^{\mathbb{P}}_{u^-} - \frac{1}{2}\left(\Lambda^2_{V,u^-} + \Lambda^2_{\perp,u^-} \right) - \xi^{\mathbb{P}}_Y \lambda_{Y,u^-} - \xi^{\mathbb{P}}_V \lambda_{V,u^-} \right) du \\
& + \int_0^t \left(\rho \sqrt{V_{u^-}} - \Lambda_{V,u^-} \right) dW_{V,u} + \int_0^t \left(\sqrt{1-\rho^2}\sqrt{V_{u^-}} - \Lambda_{\perp,u^-} \right) dW_{\perp,u} \\
& + (1+\Gamma_Y) \int_0^t dJ_{Y,u} + \Gamma_V \int_0^t dJ_{V,u}.
\end{aligned}
$$

Itō's lemma implies that

$$\begin{aligned}
&\exp\left(Y_t+Z_t\right)-\exp\left(Y_0+Z_0\right)=\int_0^t \exp\left(Y_{u^-}+Z_{u^-}\right)d\left(Y_u+Z_u\right)\\
&+\frac{1}{2}\int_0^t \exp\left(Y_{u^-}+Z_{u^-}\right)\left(V_{u^-}-2\sqrt{V_{u^-}}\Lambda_{Y,u^-}+\Lambda_{V,u^-}^2+\Lambda_{\perp,u^-}^2\right)du\\
&+\sum_{0<u\le t}\left\{\exp\left(Y_u+Z_u\right)-\exp\left(Y_{u^-}+Z_{u^-}\right)-\exp\left(Y_{u^-}+Z_{u^-}\right)\Delta\left(Y_u+Z_u\right)\right\}
\end{aligned}$$

Replacing the first expression in the second one leads to

$$\begin{aligned}
&\exp\left(Y_t+Z_t\right)-\exp\left(Y_0+Z_0\right)\\
=&\int_0^t \exp\left(Y_{u^-}+Z_{u^-}\right)\left(\alpha_{u^-}^{\mathbb{P}}-\frac{1}{2}\left(\Lambda_{V,u^-}^2+\Lambda_{\perp,u^-}^2\right)-\xi_Y^{\mathbb{P}}\lambda_{Y,u^-}-\xi_V^{\mathbb{P}}\lambda_{V,u^-}\right)du\\
&+\int_0^t \exp\left(Y_{u^-}+Z_{u^-}\right)\left(\rho\sqrt{V_{u^-}}-\Lambda_{V,u^-}\right)dW_{V,u}\\
&+\int_0^t \exp\left(Y_{u^-}+Z_{u^-}\right)\left(\sqrt{1-\rho^2}\sqrt{V_{u^-}}-\Lambda_{\perp,u^-}\right)dW_{\perp,u}\\
&+\int_0^t \exp\left(Y_{u^-}+Z_{u^-}\right)\left(1+\Gamma_Y\right)dJ_{Y,u}+\int_0^t \exp\left(Y_{u^-}+Z_{u^-}\right)\Gamma_V dJ_{V,u}\\
&+\frac{1}{2}\int_0^t \exp\left(Y_{u^-}+Z_{u^-}\right)\left(V_{u^-}-2\sqrt{V_{u^-}}\Lambda_{Y,u^-}+\Lambda_{V,u^-}^2+\Lambda_{\perp,u^-}^2\right)du\\
&+\sum_{0<u\le t}\left\{\exp\left(Y_u+Z_u\right)-\exp\left(Y_{u^-}+Z_{u^-}\right)-\exp\left(Y_{u^-}+Z_{u^-}\right)\Delta\left(Y_u+Z_u\right)\right\}.
\end{aligned}$$

The last term can be rewritten as

$$\begin{aligned}
&\sum_{0<u\le t}\exp\left(Y_{u^-}+Z_{u^-}\right)\left\{\exp\left(\Delta Y_u+\Delta Z_u\right)-1-\Delta\left(Y_u+Z_u\right)\right\}\\
=&\sum_{0<u\le t}\exp\left(Y_{u^-}+Z_{u^-}\right)\left\{\exp\left(\left(1+\Gamma_Y\right)\Delta J_{Y,u}+\Gamma_V\Delta J_{V,u}\right)-1-\left(1+\Gamma_Y\right)\Delta J_{Y,u}-\Gamma_V\Delta J_{V,u}\right\}\\
=&\sum_{0<u\le t}\left[\begin{array}{c}\exp\left(Y_{u^-}+Z_{u^-}-\left(1+\Gamma_Y\right)J_{Y,u^-}-\Gamma_V J_{V,u^-}\right)\\ \times\left\{\exp\left(\left(1+\Gamma_Y\right)J_{Y,u}+\Gamma_V J_{V,u}\right)-\exp\left(\left(1+\Gamma_Y\right)J_{Y,u^-}+\Gamma_V J_{V,u^-}\right)\right\}\end{array}\right]\\
&-\sum_{0<u\le t}\exp\left(Y_{u^-}+Z_{u^-}\right)\left\{\left(1+\Gamma_Y\right)\Delta J_{Y,u}+\Gamma_V\Delta J_{V,u}\right\}\\
=&\int_0^t \exp\left(Y_{u^-}+Z_{u^-}-\left(1+\Gamma_Y\right)J_{Y,u^-}-\Gamma_V J_{V,u^-}\right)d\exp\left(\left(1+\Gamma_Y\right)J_{Y,u}+\Gamma_V J_{V,u}\right)\\
&-\int_0^t \exp\left(Y_{u^-}+Z_{u^-}\right)\left(1+\Gamma_Y\right)dJ_{Y,u}-\int_0^t \exp\left(Y_{u^-}+Z_{u^-}\right)\Gamma_V dJ_{V,u}.
\end{aligned}$$

Therefore,

$$\begin{aligned}
&\exp\left(Y_t+Z_t\right)-\exp\left(Y_0+Z_0\right)\\
=&\int_0^t \exp\left(Y_{u^-}+Z_{u^-}\right)\left(\alpha_{u^-}^{\mathbb{P}}-\xi_Y^{\mathbb{P}}\lambda_{Y,u^-}-\xi_V^{\mathbb{P}}\lambda_{V,u^-}+\frac{1}{2}V_{u^-}-\sqrt{V_{u^-}}\Lambda_{Y,u^-}\right)du\\
&+\int_0^t \exp\left(Y_{u^-}+Z_{u^-}\right)\left(\rho\sqrt{V_{u^-}}-\Lambda_{V,u^-}\right)dW_{V,u}\\
&+\int_0^t \exp\left(Y_{u^-}+Z_{u^-}\right)\left(\sqrt{1-\rho^2}\sqrt{V_{u^-}}-\Lambda_{\perp,u^-}\right)dW_{\perp,u}
\end{aligned}$$

$$+\int_0^t \exp\left(Y_{u^-}+Z_{u^-}-(1+\Gamma_Y)\,J_{Y,u^-}-\Gamma_V J_{V,u^-}\right)d\exp\left((1+\Gamma_Y)\,J_{Y,u}+\Gamma_V J_{V,u}\right).$$

We need to construct a martingale out of the last term. From Lemma 6, $\{M_t\}_{t\geq 0}$ is a $\mathbb{P}-$martingale where

$$M_t=\exp\left((1+\Gamma_Y)\,J_{Y,t}+\Gamma_V J_{V,t}-\zeta_Y^{\mathbb{P}}\int_0^t\lambda_{Y,u^-}du-\zeta_V^{\mathbb{P}}\int_0^t\lambda_{V,u^-}du\right).$$

Indeed,

$$\begin{aligned}
&\mathrm{E}^{\mathbb{P}}_{\mathcal{F}_s}\left[\exp\left((1+\Gamma_Y)\,(J_{Y,t}-J_{Y,s})+\Gamma_V\,(J_{V,t}-J_{V,s})-\zeta_Y^{\mathbb{P}}\left(\int_s^t\lambda_{Y,u^-}du\right)-\zeta_V^{\mathbb{P}}\left(\int_s^t\lambda_{V,u^-}du\right)\right)\right]\\
=\ &\mathrm{E}^{\mathbb{P}}_{\mathcal{F}_s}\left[\mathrm{E}^{\mathbb{P}}_{\mathcal{F}_s}\left[\exp\left(\begin{array}{c}(1+\Gamma_Y)\,(J_{Y,t}-J_{Y,s})+\Gamma_V\,(J_{V,t}-J_{V,s})\\ -\zeta_Y^{\mathbb{P}}\left(\int_s^t\lambda_{Y,u^-}du\right)-\zeta_V^{\mathbb{P}}\left(\int_s^t\lambda_{V,u^-}du\right)\end{array}\right)\middle|\int_s^t\lambda_{Y,u^-}du,\int_s^t\lambda_{V,u^-}du\right]\right]=1.
\end{aligned}$$

Moreover,

$$\begin{aligned}
&d\exp\left((1+\Gamma_Y)\,J_{Y,t}+\Gamma_V J_{V,t}\right)\\
=\ &dM_t\exp\left(\zeta_Y^{\mathbb{P}}\int_0^t\lambda_{Y,u^-}du+\zeta_V^{\mathbb{P}}\int_0^t\lambda_{V,u^-}du\right)\\
=\ &M_{t^-}\,d\exp\left(\zeta_Y^{\mathbb{P}}\int_0^t\lambda_{Y,u^-}du+\zeta_V^{\mathbb{P}}\int_0^t\lambda_{V,u^-}du\right)+\exp\left(\zeta_Y^{\mathbb{P}}\int_0^t\lambda_{Y,u^-}du+\zeta_V^{\mathbb{P}}\int_0^t\lambda_{V,u^-}du\right)dM_t\\
=\ &\left(\zeta_Y^{\mathbb{P}}\lambda_{Y,t^-}+\zeta_V^{\mathbb{P}}\lambda_{V,t^-}\right)M_{t^-}\exp\left(\zeta_Y^{\mathbb{P}}\int_0^t\lambda_{Y,u^-}du+\zeta_V^{\mathbb{P}}\int_0^t\lambda_{V,u^-}du\right)dt\\
&+\exp\left(\zeta_Y^{\mathbb{P}}\int_0^t\lambda_{Y,u^-}du+\zeta_V^{\mathbb{P}}\int_0^t\lambda_{V,u^-}du\right)dM_t\\
=\ &\left(\zeta_Y^{\mathbb{P}}\lambda_{Y,t^-}+\zeta_V^{\mathbb{P}}\lambda_{V,t^-}\right)\exp\left((1+\Gamma_Y)\,J_{Y,t^-}+\Gamma_V J_{V,t^-}\right)dt\\
&+\exp\left(\zeta_Y^{\mathbb{P}}\int_0^t\lambda_{Y,u^-}du+\zeta_V^{\mathbb{P}}\int_0^t\lambda_{V,u^-}du\right)dM_t.
\end{aligned}$$

Therefore,

$$\begin{aligned}
&\exp\left(Y_t+Z_t\right)-\exp\left(Y_0+Z_0\right)\\
=\ &\int_0^t\exp\left(Y_{u^-}+Z_{u^-}\right)\left(\alpha_{u^-}^{\mathbb{P}}-\xi_Y^{\mathbb{P}}\lambda_{Y,u^-}-\xi_V^{\mathbb{P}}\lambda_{V,u^-}+\frac{1}{2}V_{u^-}-\sqrt{V_{u^-}}\Lambda_{Y,u^-}\right)du\\
&+\int_0^t\exp\left(Y_{u^-}+Z_{u^-}\right)\left(\rho\sqrt{V_{u^-}}-\Lambda_{V,u^-}\right)dW_{V,u}\\
&+\int_0^t\exp\left(Y_{u^-}+Z_{u^-}\right)\left(\sqrt{1-\rho^2}\sqrt{V_{u^-}}-\Lambda_{\perp,u^-}\right)dW_{\perp,u}\\
&+\int_0^t\left(\zeta_Y^{\mathbb{P}}\lambda_{Y,u^-}+\zeta_V^{\mathbb{P}}\lambda_{V,u^-}\right)\exp\left(Y_{u^-}+Z_{u^-}\right)du\\
&+\int_0^t\exp\left(Y_{u^-}+Z_{u^-}-(1+\Gamma_Y)\,J_{Y,u^-}-\Gamma_V J_{V,u^-}+\zeta_Y^{\mathbb{P}}\int_0^u\lambda_{Y,s^-}ds+\zeta_V^{\mathbb{P}}\int_0^u\lambda_{V,s^-}ds\right)dM_u\\
=\ &\int_0^t\exp\left(Y_{u^-}+Z_{u^-}\right)\left(\alpha_{u^-}^{\mathbb{P}}-\xi_Y^{\mathbb{P}}\lambda_{Y,u^-}-\xi_V^{\mathbb{P}}\lambda_{V,u^-}+\frac{1}{2}V_{u^-}-\sqrt{V_{u^-}}\Lambda_{Y,u^-}+\zeta_Y^{\mathbb{P}}\lambda_{Y,u^-}+\zeta_V^{\mathbb{P}}\lambda_{V,u^-}\right)du\\
&+\int_0^t\exp\left(Y_{u^-}+Z_{u^-}\right)\left(\rho\sqrt{V_{u^-}}-\Lambda_{V,u^-}\right)dW_{V,u}\\
&+\int_0^t\exp\left(Y_{u^-}+Z_{u^-}\right)\left(\sqrt{1-\rho^2}\sqrt{V_{u^-}}-\Lambda_{\perp,u^-}\right)dW_{\perp,u}
\end{aligned}$$

$$+\int_0^t \exp\left(Y_{u^-}+Z_{u^-}-(1+\Gamma_Y)\,J_{Y,u^-}-\Gamma_V J_{V,u^-}+\zeta_Y^{\mathbb{P}}\int_0^u \lambda_{Y,s^-}ds+\zeta_V^{\mathbb{P}}\int_0^u \lambda_{V,s^-}ds\right)dM_u.$$

Since

$$D_t\exp(Y_t+Z_t)-D_0\exp(Y_0+Z_0)=\int_0^t D_u d\exp(Y_u+Z_u)+\int_0^t (q-r)\,D_u\exp(Y_{u^-}+Z_{u^-})\,du,$$

then

$$\begin{aligned}
& D_t\exp(Y_t+Z_t)-D_0\exp(Y_0+Z_0)\\
= & \int_0^t D_u\exp(Y_{u^-}+Z_{u^-})\begin{pmatrix}\alpha_{u^-}^{\mathbb{P}}-\xi_Y^{\mathbb{P}}\lambda_{Y,u^-}-\xi_V^{\mathbb{P}}\lambda_{V,u^-}+\frac{1}{2}V_{u^-}-\sqrt{V_{u^-}}\Lambda_{Y,u^-}\\ +\zeta_Y^{\mathbb{P}}\lambda_{Y,u^-}+\zeta_V^{\mathbb{P}}\lambda_{V,u^-}+q-r\end{pmatrix}du\\
& +\int_0^t D_u\exp(Y_{u^-}+Z_{u^-})\left(\rho\sqrt{V_{u^-}}-\Lambda_{V,u^-}\right)dW_{V,u}\\
& +\int_0^t D_u\exp(Y_{u^-}+Z_{u^-})\left(\sqrt{1-\rho^2}\sqrt{V_{u^-}}-\Lambda_{\perp,u^-}\right)dW_{\perp,u}\\
& +\int_0^t D_u\exp\left(Y_{u^-}+Z_{u^-}-(1+\Gamma_Y)\,J_{Y,u^-}-\Gamma_V J_{V,u^-}+\zeta_Y^{\mathbb{P}}\int_0^u \lambda_{Y,s^-}ds+\zeta_V^{\mathbb{P}}\int_0^u \lambda_{V,s^-}ds\right)dM_u.
\end{aligned}$$

Finally, as $\{D_t\exp(Y_t+Z_t)\}_{t\geq 0}$ needs to be a $\mathbb{P}-$martingale, the drift term must be nil, implying that

$$\alpha_{u^-}^{\mathbb{P}}=r-q-\frac{1}{2}V_{u^-}+\sqrt{V_{u^-}}\Lambda_{Y,u^-}+\left(\xi_Y^{\mathbb{P}}-\zeta_Y^{\mathbb{P}}\right)\lambda_{Y,u^-}+\left(\xi_V^{\mathbb{P}}-\zeta_V^{\mathbb{P}}\right)\lambda_{V,u^-}.$$

□

Corollary 1

$$\mathrm{E}_t^{\mathbb{P}}[\exp(Y_T)]=\exp(Y_t)\,\mathrm{E}_t^{\mathbb{P}}\left[\exp\left(\int_t^T m_{u^-}^{\mathbb{P}}du\right)\right]$$

where

$$\begin{aligned}
m_{u^-}^{\mathbb{P}} &= \alpha_{u^-}^{\mathbb{P}}+\frac{1}{2}V_{u^-}du+\left(\varphi_{Z_Y}^{\mathbb{P}}(1)-1\right)\lambda_{Y,u^-}\\
&= r-q+\sqrt{V_{u^-}}\Lambda_{Y,u^-}+\left(\xi_Y^{\mathbb{P}}-\zeta_Y^{\mathbb{P}}\right)\lambda_{Y,u^-}+\left(\varphi_{Z_Y}^{\mathbb{P}}(1)-1\right)\lambda_{Y,u^-}\\
&= r-q+\sqrt{V_{u^-}}\Lambda_{Y,u^-}+\left(\varphi_{Z_Y}^{\mathbb{P}}(\Gamma_Y)-\varphi_{Z_Y}^{\mathbb{P}}(1+\Gamma_Y)+\varphi_{Z_Y}^{\mathbb{P}}(1)-1\right)\lambda_{Y,u^-}.
\end{aligned}$$

Proof. Starting from Equation (1),

$$\begin{aligned}
& \mathrm{E}_t^{\mathbb{P}}[\exp(Y_T)]\\
= & \exp(Y_T)\,\mathrm{E}_t^{\mathbb{P}}\left[\exp\left(\int_t^T \alpha_{u^-}^{\mathbb{P}}du+\int_t^T\sqrt{V_{u^-}}dW_{Y,u}+\int_t^T dJ_{Y,u}\right)\right]\\
= & \exp(Y_T)\,\mathrm{E}_t^{\mathbb{P}}\left[\exp\begin{pmatrix}\int_t^T \alpha_{u^-}^{\mathbb{P}}du+\frac{1}{2}\int_t^T V_{u^-}du+\left(\varphi_{Z_Y}^{\mathbb{P}}(1)-1\right)\int_t^T\lambda_{Y,u^-}du\\ +\int_t^T\sqrt{V_{u^-}}dW_{Y,u}-\frac{1}{2}\int_t^T V_{u^-}du\\ +\int_t^T dJ_{Y,u}-\left(\varphi_{Z_Y}^{\mathbb{P}}(1)-1\right)\int_t^T\lambda_{Y,u^-}du\end{pmatrix}\right]\\
= & \exp(Y_T)\\
& \times\mathrm{E}_t^{\mathbb{P}}\left[\mathrm{E}_t^{\mathbb{P}}\left[\exp\begin{pmatrix}\int_t^T \alpha_{u^-}^{\mathbb{P}}du+\frac{1}{2}\int_t^T V_{u^-}du+\left(\varphi_{Z_Y}^{\mathbb{P}}(1)-1\right)\int_t^T\lambda_{Y,u^-}du\\ +\int_t^T\sqrt{V_{u^-}}dW_{Y,u}-\frac{1}{2}\int_t^T V_{u^-}du\\ +\int_t^T dJ_{Y,u}-\left(\varphi_{Z_Y}^{\mathbb{P}}(1)-1\right)\int_t^T\lambda_{Y,u^-}du\end{pmatrix}\middle|\int_t^T\lambda_{Y,u^-}du\right]\right]\\
= & \exp(Y_T)\,\mathrm{E}_t^{\mathbb{P}}\left[\exp\left(\int_t^T\left(\alpha_{u^-}^{\mathbb{P}}+\frac{1}{2}V_{u^-}du+\left(\varphi_{Z_Y}^{\mathbb{P}}(1)-1\right)\lambda_{Y,u^-}\right)du\right)\right]
\end{aligned}$$

$$= \exp\left(Y_T\right) \mathrm{E}_t^{\mathbb{P}}\left[\exp\left(\int_t^T m_{u^-}^{\mathbb{P}} du\right)\right]$$

Therefore,

$$\begin{aligned}
& m_{u^-}^{\mathbb{P}} = \alpha_{u^-}^{\mathbb{P}} + \frac{1}{2}V_{u^-}du + \left(\varphi_{Z_Y}^{\mathbb{P}}\left(1\right) - 1\right)\lambda_{Y,u^-} \\
= \; & r - q - \frac{1}{2}V_{u^-} + \sqrt{V_{u^-}}\Lambda_{Y,u^-} + \left(\xi_Y^{\mathbb{P}} - \zeta_Y^{\mathbb{P}}\right)\lambda_{Y,u^-} + \left(\xi_V^{\mathbb{P}} - \zeta_V^{\mathbb{P}}\right)\lambda_{V,u^-} \\
& + \frac{1}{2}V_{u^-}du + \left(\varphi_{Z_Y}^{\mathbb{P}}\left(1\right) - 1\right)\lambda_{Y,u^-} \\
= \; & r - q + \sqrt{V_{u^-}}\Lambda_{Y,u^-} + \left(\xi_Y^{\mathbb{P}} - \zeta_Y^{\mathbb{P}} + \varphi_{Z_Y}^{\mathbb{P}}\left(1\right) - 1\right)\lambda_{Y,u^-} + \left(\xi_V^{\mathbb{P}} - \zeta_V^{\mathbb{P}}\right)\lambda_{V,u^-} \\
= \; & r - q + \sqrt{V_{u^-}}\Lambda_{Y,u^-} \\
& + \left(\varphi_{Z_Y}^{\mathbb{P}}\left(1\right) - \varphi_{Z_Y}^{\mathbb{P}}\left(1+\Gamma_Y\right) + \varphi_{Z_Y}^{\mathbb{P}}\left(1\right) - 1\right)\lambda_{Y,u^-} + \left(\varphi_{Z_V}^{\mathbb{P}}\left(1\right) - \varphi_{Z_V}^{\mathbb{P}}\left(\Gamma_V\right)\right)\lambda_{V,u^-}.
\end{aligned}$$

□

B Option pricing

B.1 Moment generating function of the log-equity price variation

Lemma 11 *The risk-neutral moment generating function of Y_T satisfies*

$$\varphi_{Y_T|Y_t,V_t}^{\mathbb{Q}}\left(u, Y_t, V_t\right) = \mathrm{E}^{\mathbb{Q}}\left[\exp\left(uY_T\right)|Y_t, V_t\right] = \exp\left(\mathcal{A}\left(u,t,T\right) + uY_t + \mathcal{C}\left(u,t,T\right)V_t\right).$$

where $\mathcal{C}\left(u,t,T\right)$ and $\mathcal{A}(u;t,T)$ are provided at Equations (24) and (25) respectively.

Proof. The proof is based on Filipovic and Mayerhofer (2009) and Duffie et al. (2000).

According to Duffie et al. (2000), $\mathcal{A}(u;t,T)$, $\mathcal{B}(u;t,T)$ and $\mathcal{C}(u;t,T)$ satisfy the complex-valued ordinary differential equations (ODEs)

$$\begin{aligned}
\mathcal{A}'(u;t,T) &= r - \begin{bmatrix} r - q - \lambda_{Y,0}^{\mathbb{Q}}\left(\varphi_{Z_Y}^{\mathbb{Q}}\left(1\right) - 1\right) \\ \kappa^{\mathbb{Q}}\theta^{\mathbb{Q}} \end{bmatrix}^{\top} \begin{bmatrix} \mathcal{B}(u;t,T) \\ \mathcal{C}(u;t,T) \end{bmatrix} - \lambda_{Y,0}^{\mathbb{Q}}\left(\varphi_{Z_Y}^{\mathbb{Q}}\left(\mathcal{B}(u;t,T)\right) - 1\right) \\
&\quad - \lambda_{V,0}^{\mathbb{Q}}\left(\varphi_{Z_V}^{\mathbb{Q}}\left(\mathcal{C}(u;t,T)\right) - 1\right), \\
\mathcal{B}'(u;t,T) &= 0, \\
\mathcal{C}'(u;t,T) &= \begin{bmatrix} \frac{1}{2} + \lambda_{Y,1}^{\mathbb{Q}}\left(\varphi_{Z_Y}^{\mathbb{Q}}\left(1\right) - 1\right) \\ \kappa^{\mathbb{Q}} \end{bmatrix}^{\top} \begin{bmatrix} \mathcal{B}(u;t,T) \\ \mathcal{C}(u;t,T) \end{bmatrix} - \frac{1}{2}\begin{bmatrix} \mathcal{B}(u;t,T) \\ \mathcal{C}(u;t,T) \end{bmatrix}^{\top} \begin{bmatrix} 1 & \sigma\rho \\ \sigma\rho & \sigma^2 \end{bmatrix} \begin{bmatrix} \beta(u;t,T) \\ \mathcal{C}(u;t,T) \end{bmatrix} \\
&\quad - \lambda_{Y,1}^{\mathbb{Q}}\left(\varphi_{Z_Y}^{\mathbb{Q}}\left(u\right) - 1\right),
\end{aligned} \tag{36}$$

with initial conditions $\mathcal{A}(u;T,T) = 0$, $\mathcal{B}(u;T,T) = u$ and $\mathcal{C}(u;T,T) = 0$. The second ODE is obvious: since $\mathcal{B}(u;T,T) = u$ and $\mathcal{B}'(u;t,T) = 0$, it means that $\mathcal{B}(u;t,T) = u$. Then, from this equation, we can try to find the solution to the third ODE (i.e. $\mathcal{C}(u;t,T)$). As in Filipovic and Mayerhofer (2009), the solution to this ODE is given by Equation (24). Finally, the expression for $\mathcal{A}(u;t,T)$ provided at Equation (25) is obtained from a simple integration since there are no $\mathcal{A}$ in the right hand side of Equation (36). □

B.2 Quadratic variation of option prices

The option price is a function of time, returns and variance: $O_t = O_t(Y_t, V_t)$. Assume that O is twice continuously differentiable. Itō's formula implies that

$$\begin{aligned}
&O_t(Y_t,V_t) - O_0(Y_0,V_0)\\
&= \int_0^t \frac{\partial O_u}{\partial u}(Y_{u^-},V_{u^-})\,du + \int_0^t \frac{\partial O_u}{\partial y}(Y_{u^-},V_{u^-})\,dY_u + \int_0^t \frac{\partial O_u}{\partial v}(Y_{u^-},V)\,dV_u\\
&+ \frac{1}{2}\int_0^t \frac{\partial^2 O_u}{\partial y^2}(Y_{u^-},V_{u^-})\,d[Y,Y]_u^c + \frac{1}{2}\int_0^t \frac{\partial^2 O_u}{\partial v^2}(Y_{u^-},V_{u^-})\,d[V,V]_u^c + \int_0^t \frac{\partial^2 O_u}{\partial v\partial y}(Y_{u^-},V_{u^-})\,d[Y,V]_u^c\\
&+ \sum_{0<u\le t}\{O_u(Y_u,V_u) - O_u(Y_{u^-},V_{u^-})\} - \sum_{0<u\le t}\left\{\frac{\partial O_u}{\partial y}(Y_{u^-},V_{u^-})(Y_u - Y_{u^-})\right\}\\
&- \sum_{0<u\le t}\left\{\frac{\partial O_u}{\partial v}(Y_{u^-},V_{u^-})(V_u - V_{u^-})\right\}.
\end{aligned}$$

Replacing Equation (1) in the latter leads to

$$\begin{aligned}
&O_t(Y_t,V_t) - O_0(Y_0,V_0)\\
= &\int_0^t \frac{\partial O_u}{\partial u}(Y_{u^-},V_{u^-})\,du + \int_0^t \frac{\partial O_u}{\partial y}(Y_{u^-},V_{u^-})\,\alpha_{u^-}du + \int_0^t \frac{\partial O_u}{\partial y}(Y_{u^-},V_{u^-})\,\rho\sqrt{V_{u^-}}dW_{V,u}\\
&+ \int_0^t \frac{\partial O_u}{\partial y}(Y_{u^-},V_{u^-})\sqrt{1-\rho^2}\sqrt{V_{u^-}}dW_{\perp,u} + \int_0^t \frac{\partial O_u}{\partial y}(Y_{u^-},V_{u^-})\,dJ_{Y,u}\\
&+ \int_0^t \frac{\partial O_u}{\partial v}(Y_{u^-},V_{u^-})\,\kappa(\theta - V_{u^-})\,du + \int_0^t \frac{\partial O_u}{\partial v}(Y_{u^-},V_{u^-})\,\sigma\sqrt{V_{u^-}}dW_{V,u} + \int_0^t \frac{\partial O_u}{\partial v}(Y_{u^-},V_{u^-})\,dJ_{V,u}\\
&+\frac{1}{2}\int_0^t \frac{\partial^2 O_u}{\partial y^2}(Y_{u^-},V_{u^-})\,V_{u^-}du + \frac{1}{2}\int_0^t \frac{\partial^2 O_u}{\partial v^2}(Y_{u^-},V_{u^-})\,\sigma^2 V_{u^-}du + \int_0^t \frac{\partial^2 O_u}{\partial v\partial y}(Y_{u^-},V_{u^-})\,\sigma\rho V_{u^-}du\\
&+ \sum_{0<u\le t}\{O_u(Y_u,V_u) - O_u(Y_{u^-},V_{u^-})\} - \int_0^t \frac{\partial O_u}{\partial y}(Y_{u^-},V_{u^-})\,dJ_{Y,u} - \int_0^t \frac{\partial O_u}{\partial v}(Y_{u^-},V_{u^-})\,dJ_{V,u}.
\end{aligned}$$

Then,

$$\begin{aligned}
&O_t(Y_t,V_t) - O_0(Y_0,V_0)\\
= &\int_0^t \left\{\begin{array}{l} \frac{\partial O_u}{\partial u}(Y_{u^-},V_{u^-}) + \alpha_{u^-}\frac{\partial O_u}{\partial y}(Y_{u^-},V_{u^-}) + \frac{\partial O_u}{\partial v}(Y_{u^-},V_{u^-})\,\kappa(\theta - V_{u^-})\\ + \left(\frac{1}{2}\frac{\partial^2 O_u}{\partial y^2}(Y_{u^-},V_{u^-}) + \frac{1}{2}\frac{\partial^2 O_u}{\partial v^2}(Y_{u^-},V_{u^-})\,\sigma^2 + \frac{\partial^2 O_u}{\partial v\partial y}(Y_{u^-},V_{u^-})\,\sigma\rho\right)V_{u^-} \end{array}\right\} du\\
&+ \int_0^t \left(\rho\frac{\partial O_u}{\partial y}(Y_{u^-},V_{u^-}) + \sigma\frac{\partial O_u}{\partial v}(Y_{u^-},V_{u^-})\right)\sqrt{V_{u^-}}dW_{V,u} + \int_0^t \frac{\partial O_u}{\partial y}(Y_{u^-},V_{u^-})\sqrt{1-\rho^2}\sqrt{V_{u^-}}dW_{\perp,u}\\
&+ \sum_{0<u\le t}\{O_u(Y_u,V_u) - O_u(Y_{u^-},V_{u^-})\}.
\end{aligned}$$

Finally, the quadratic variation is

$$\begin{aligned}
&[O,O]_t\\
= &\int_0^t \left(\rho\frac{\partial O_u}{\partial y}(Y_{u^-},V_{u^-}) + \sigma\frac{\partial O_u}{\partial v}(Y_{u^-},V_{u^-})\right)^2 V_{u^-}du + \int_0^t \left(\frac{\partial O_u}{\partial y}(Y_{u^-},V_{u^-})\right)^2 \left(1-\rho^2\right)V_{u^-}du\\
&+ \sum_{0<u\le t}\{O_u(Y_u,V_u) - O_u(Y_{u^-},V_{u^-})\}^2\\
= &\int_0^t \left(\left(\frac{\partial O_u}{\partial y}(Y_{u^-},V_{u^-})\right)^2 + 2\sigma\rho\frac{\partial O_u}{\partial y}(Y_{u^-},V_{u^-})\frac{\partial O_u}{\partial v}(Y_{u^-},V_{u^-}) + \sigma^2\left(\frac{\partial O_u}{\partial v}(Y_{u^-},V_{u^-})\right)^2\right)V_{u^-}du
\end{aligned}$$

$$+\sum_{0<u\leq t}\left\{O_u\left(Y_u,V_u\right)-O_u\left(Y_{u^-},V_{u^-}\right)\right\}^2.$$

B.2.1 Derivative calculation for ΔOQV

Starting from Equation (23),

$$\frac{\partial}{\partial y}C_t(y,v)=\exp\left(y-q(T-t)\right)\left(P_1(y,v)+\frac{\partial P_1}{\partial x}P_1(y,v)\right)-K\exp\left(-r(T-t)\right)\frac{\partial P_2}{\partial y}(y,v)$$

and

$$\frac{\partial}{\partial v}C_t(y,v)=\exp\left(y-q(T-t)\right)\frac{\partial P_1}{\partial v}P_1(y,v)-K\exp\left(-r(T-t)\right)\frac{\partial P_2}{\partial v}(y,v).$$

The derivatives $\frac{\partial}{\partial y}P_1(y,v,k;t,T)$ and $\frac{\partial}{\partial y}P_2(y,v,k;t,T)$ can be calculated by computing the derivative of the integrand.[49] For $x\in\{y,v\}$,

$$\begin{aligned}
\frac{\partial P_1}{\partial x}(y,v)&=\frac{\partial}{\partial x}\left[\frac{1}{2}+\frac{1}{\pi}\int_0^\infty \mathrm{Re}\left(\frac{1}{u\mathrm{i}}\exp\left(-\mathrm{i}uk-y\right)\varphi^{\mathbb{Q}}_{Y_T|Y_t,V_t}\left(u\mathrm{i}+1,y,v\right)\right)du\right]\\
=&\ \frac{1}{\pi}\int_0^\infty\frac{\partial}{\partial x}\mathrm{Re}\left(\frac{1}{u\mathrm{i}}\exp\left(-\mathrm{i}uk-y\right)\varphi^{\mathbb{Q}}_{Y_T|Y_t,V_t}\left(u\mathrm{i}+1,y,v\right)\right)du\\
=&\ \frac{1}{\pi}\int_0^\infty\frac{\partial}{\partial x}\mathrm{Re}\left(\frac{1}{u\mathrm{i}}\exp\left(-\mathrm{i}uk-y\right)\exp\left(\mathcal{A}\left(u\mathrm{i}+1,t,T\right)+\left(u\mathrm{i}+1\right)\,y+\mathcal{C}\left(u\mathrm{i}+1,t,T\right)v\right)\right)du
\end{aligned}$$

where the last expression comes from the specific shape of the moment generating function. Because $\exp\left(a+\mathrm{i}b\right)=\exp\left(a\right)\times\left(\cos b+\mathrm{i}\sin b\right)$, the last expression becomes

$$\begin{aligned}
&\frac{1}{\pi}\int_0^\infty\frac{\partial}{\partial x}\mathrm{Re}\left(\frac{1}{u\mathrm{i}}\exp\left(\begin{array}{c}\mathrm{Re}\left[\mathcal{A}\left(u\mathrm{i}+1,t,T\right)\right]+\mathrm{Re}\left[\mathcal{C}\left(u\mathrm{i}+1,t,T\right)\right]v\\+\mathrm{i}\mathrm{Im}\left[\mathcal{A}\left(u\mathrm{i}+1,t,T\right)\right]+\mathrm{i}\mathrm{Im}\left[\mathcal{C}\left(u\mathrm{i}+1,t,T\right)\right]v+\mathrm{i}u\left(y-k\right)\end{array}\right)\right)du\\
=&\ \frac{1}{\pi}\int_0^\infty\frac{\partial}{\partial x}\mathrm{Re}\left(\frac{1}{u\mathrm{i}}\left(\begin{array}{c}\exp\left(\mathrm{Re}\left[\mathcal{A}\left(u\mathrm{i}+1,t,T\right)\right]+\mathrm{Re}\left[\mathcal{C}\left(u\mathrm{i}+1,t,T\right)\right]v\right)\\\times\left[\begin{array}{c}\cos\left(\mathrm{Im}\left[\alpha\left(u\mathrm{i}+1,t,T\right)\right]+\mathrm{Im}\left[\mathcal{C}\left(u\mathrm{i}+1,t,T\right)\right]v+u\left(y-k\right)\right)\\+\mathrm{i}\sin\left(\mathrm{Im}\left[\alpha\left(u\mathrm{i}+1,t,T\right)\right]+\mathrm{Im}\left[\mathcal{C}\left(u\mathrm{i}+1,t,T\right)\right]v+u\left(y-k\right)\right)\end{array}\right]\end{array}\right)\right)du\\
=&\ \frac{1}{\pi}\int_0^\infty\frac{\partial}{\partial x}\mathrm{Re}\left(\frac{1}{u}\left(\begin{array}{c}\exp\left(\mathrm{Re}\left[\alpha\left(u\mathrm{i}+1,t,T\right)\right]+\mathrm{Re}\left[\mathcal{C}\left(u\mathrm{i}+1,t,T\right)\right]v\right)\\\times\left[\begin{array}{c}-\mathrm{i}\cos\left(\mathrm{Im}\left[\mathcal{A}\left(u\mathrm{i}+1,t,T\right)\right]+\mathrm{Im}\left[\mathcal{C}\left(u\mathrm{i}+1,t,T\right)\right]v+u\left(y-k\right)\right)\\+\sin\left(\mathrm{Im}\left[\mathcal{A}\left(u\mathrm{i}+1,t,T\right)\right]+\mathrm{Im}\left[\mathcal{C}\left(u\mathrm{i}+1,t,T\right)\right]v+u\left(y-k\right)\right)\end{array}\right]\end{array}\right)\right)du\\
=&\ \frac{1}{\pi}\int_0^\infty\frac{\partial}{\partial x}\left(\frac{1}{u}\left(\begin{array}{c}\exp\left(\mathrm{Re}\left[\mathcal{A}\left(u\mathrm{i}+1,t,T\right)\right]+\mathrm{Re}\left[\mathcal{C}\left(u\mathrm{i}+1,t,T\right)\right]v\right)\\\times\sin\left(\mathrm{Im}\left[\mathcal{A}\left(u\mathrm{i}+1,t,T\right)\right]+\mathrm{Im}\left[\mathcal{C}\left(u\mathrm{i}+1,t,T\right)\right]v+u\left(y-k\right)\right)\end{array}\right)\right)du.
\end{aligned}$$

If $x=y$, then

$$\frac{\partial P_1}{\partial y}(y,v)=\frac{1}{\pi}\int_0^\infty\left(\begin{array}{c}\exp\left(\mathrm{Re}\left[\alpha\left(u\mathrm{i}+1,t,T\right)\right]+\mathrm{Re}\left[\gamma\left(u\mathrm{i}+1,t,T\right)v\right]\right)\\\times\cos\left(\mathrm{Im}\left[\alpha\left(u\mathrm{i}+1,t,T\right)\right]+\mathrm{Im}\left[\gamma\left(u\mathrm{i}+1,t,T\right)v\right]+u\left(y-k\right)\right)\end{array}\right)du$$

For $x=v$,

$$\frac{\partial P_1}{\partial v}(y,v)=\frac{1}{\pi}\int_0^\infty\left(\begin{array}{c}\frac{1}{u}\left(\begin{array}{c}\mathrm{Re}\left[\mathcal{C}\left(u\mathrm{i}+1,t,T\right)\right]\exp\left(\mathrm{Re}\left[\mathcal{A}\left(u\mathrm{i}+1,t,T\right)\right]+\mathrm{Re}\left[\mathcal{C}\left(u\mathrm{i}+1,t,T\right)v\right]\right)\\\times\sin\left(\mathrm{Im}\left[\mathcal{A}\left(u\mathrm{i}+1,t,T\right)\right]+\mathrm{Im}\left[\mathcal{C}\left(u\mathrm{i}+1,t,T\right)v\right]+u\left(y-k\right)\right)\end{array}\right)\\+\frac{1}{u}\left(\begin{array}{c}\mathrm{Im}\left[\mathcal{C}\left(u\mathrm{i}+1,t,T\right)\right]\exp\left(\mathrm{Re}\left[\mathcal{A}\left(u\mathrm{i}+1,t,T\right)\right]+\mathrm{Re}\left[\mathcal{C}\left(u\mathrm{i}+1,t,T\right)v\right]\right)\\\times\cos\left(\mathrm{Im}\left[\mathcal{A}\left(u\mathrm{i}+1,t,T\right)\right]+\mathrm{Im}\left[\mathcal{C}\left(u\mathrm{i}+1,t,T\right)v\right]+u\left(y-k\right)\right)\end{array}\right)\end{array}\right)du.$$

[49]Note that Leibniz integral rule is used here. One should verify that the integrand is a Lebesgue-integrable function of x for each u, that for almost all x, the derivative of the integrand (w.r.t. x) exists for all x, and that there is an integrable function θ such that $\left|\frac{\partial}{\partial y}\mathrm{Re}\left(\frac{e^{-iuk-y}f(ui+1,v;t,T)}{iu}\right)\right|\leq\theta(u)$ for all x and almost every u.

C Simulation-based results: Additional results

C.1 Filtering tests

Figures 8 to 12 show an example of the filtered values based on different data sources. For this experiment, M is set to 5. In general, using the five different data sources yields accurate filtered values (with narrower confidence intervals). Instantaneous variance and log-equity jumps are more precisely filtered when using the option realized variance. When only log-equity values are used, the various filtered values are very imprecise. This observation is consistent with Table 2: the error measures are higher when we only consider the log-equity values in the filtering step.

C.2 Option data: How much is enough?

We use the simulation experiment of Section 4.1, but this time, fifteen implied volatilities are observed on each day. These European OTM options have a maturity of 30, 90 and 150 business days, and call-equivalent deltas of 0.20, 0.35, 0.50, 0.65 and 0.80 respectively. The filter is run using $M = 5$.

The idea behind this test is to only use part of the option data available and select a limited number of maturities or call-equivalent deltas. From this subsample, we apply the filter and compare filtered values to real simulated values and to filtered values computed using the whole dataset.

Table 15 shows RMSE for various filtered values. These error measures are computed with respect to true values and filtered means again.

Regarding the option maturity, it has a marginal impact on the results. However, according to Panel A, it seems that the use of two maturities is better than one. Therefore, adding more options helps the filtering of latent quantities, regardless of the maturity of the option. According to Panel B of Table 15, OTM put options filter the jump components more adequately.

D Descriptive statistics of realized variations

Table 16 exhibits descriptive statistics of realized variance, bipower variation and option realized variance.

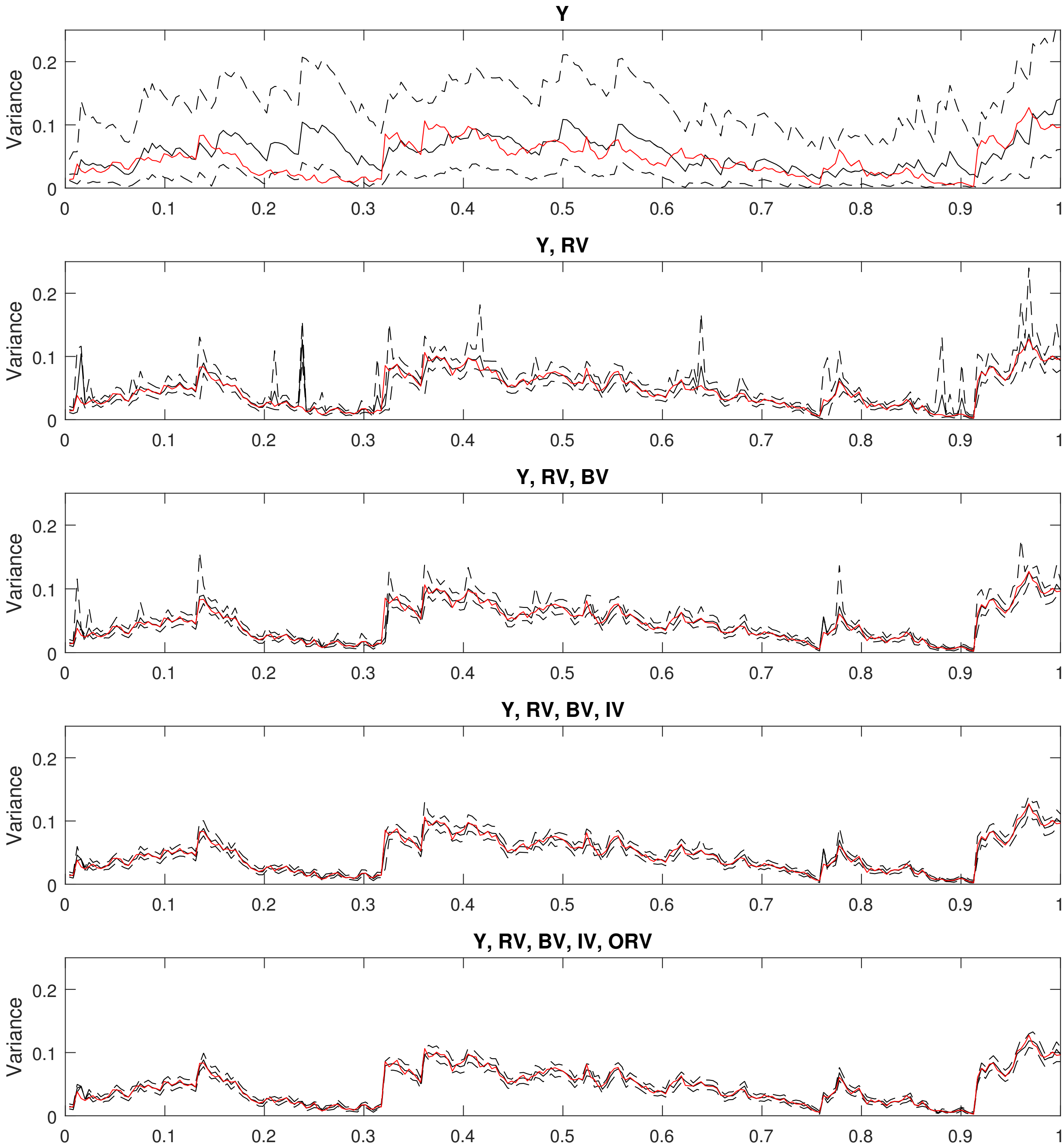

Figure 8: Filtered instantaneous variance using various data sources. Variance path's means obtained by the particle filters, true spot variance path, and 95% and confidence intervals computed using empirical quantiles (from particle filters) are shown in this figure using different data sources. The mean of the filtered density (obtained using particle filters) is taken as the filtered instantaneous variance. Y means daily log-equity value, RV means realized variance, BV means bipower variation, IV means implied volatility here, and ORV means option realized variance.

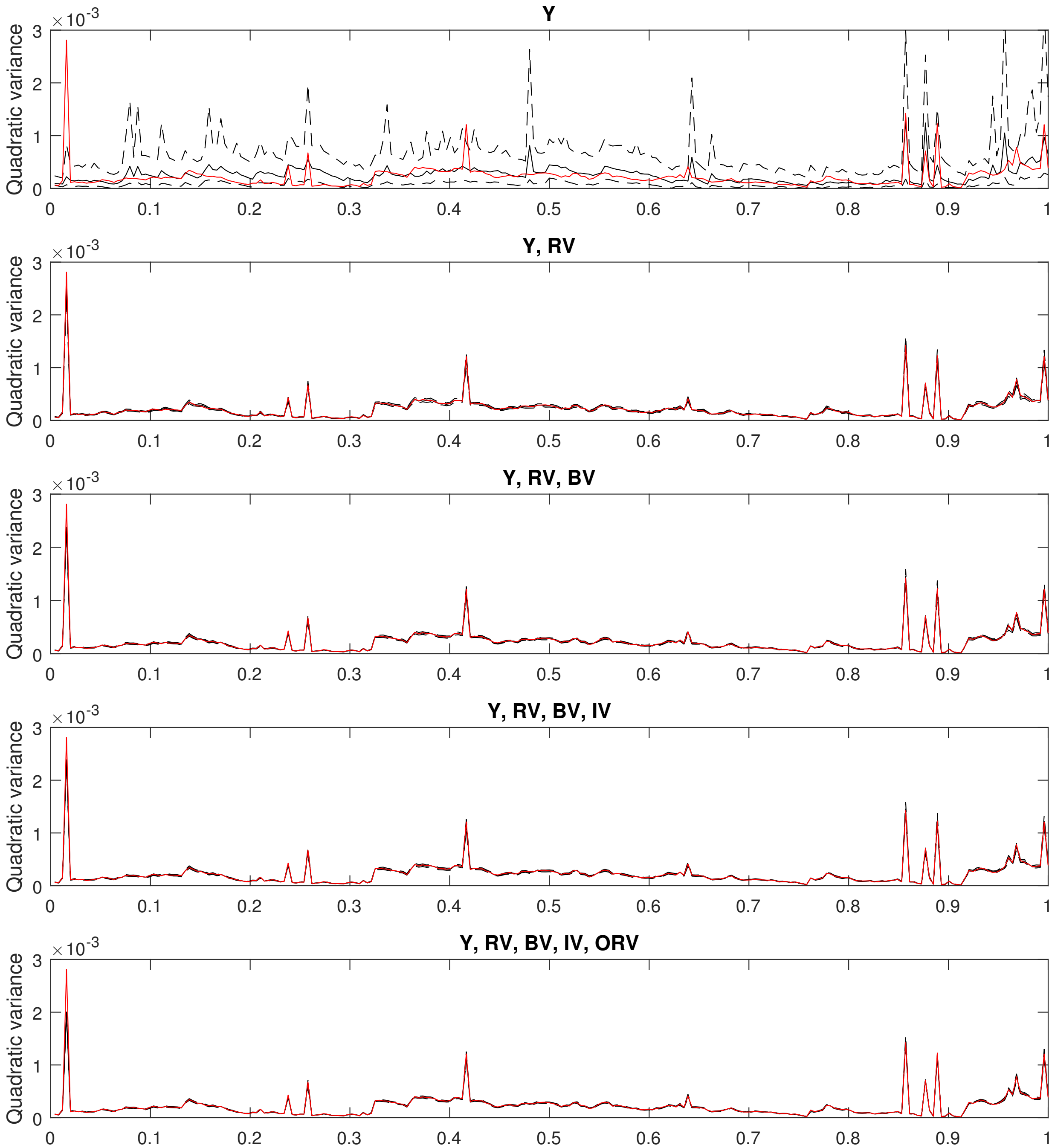

Figure 9: Filtered quadratic variation using various data sources. Quadratic variation path's means obtained by the particle filters, true quadratic variation path, and 95% and confidence intervals computed using empirical quantiles (from particle filters) are shown in this figure using different data sources. Y means daily log-equity value, RV means realized variance, BV means bipower variation, IV means implied volatility here, and ORV means option realized variance.

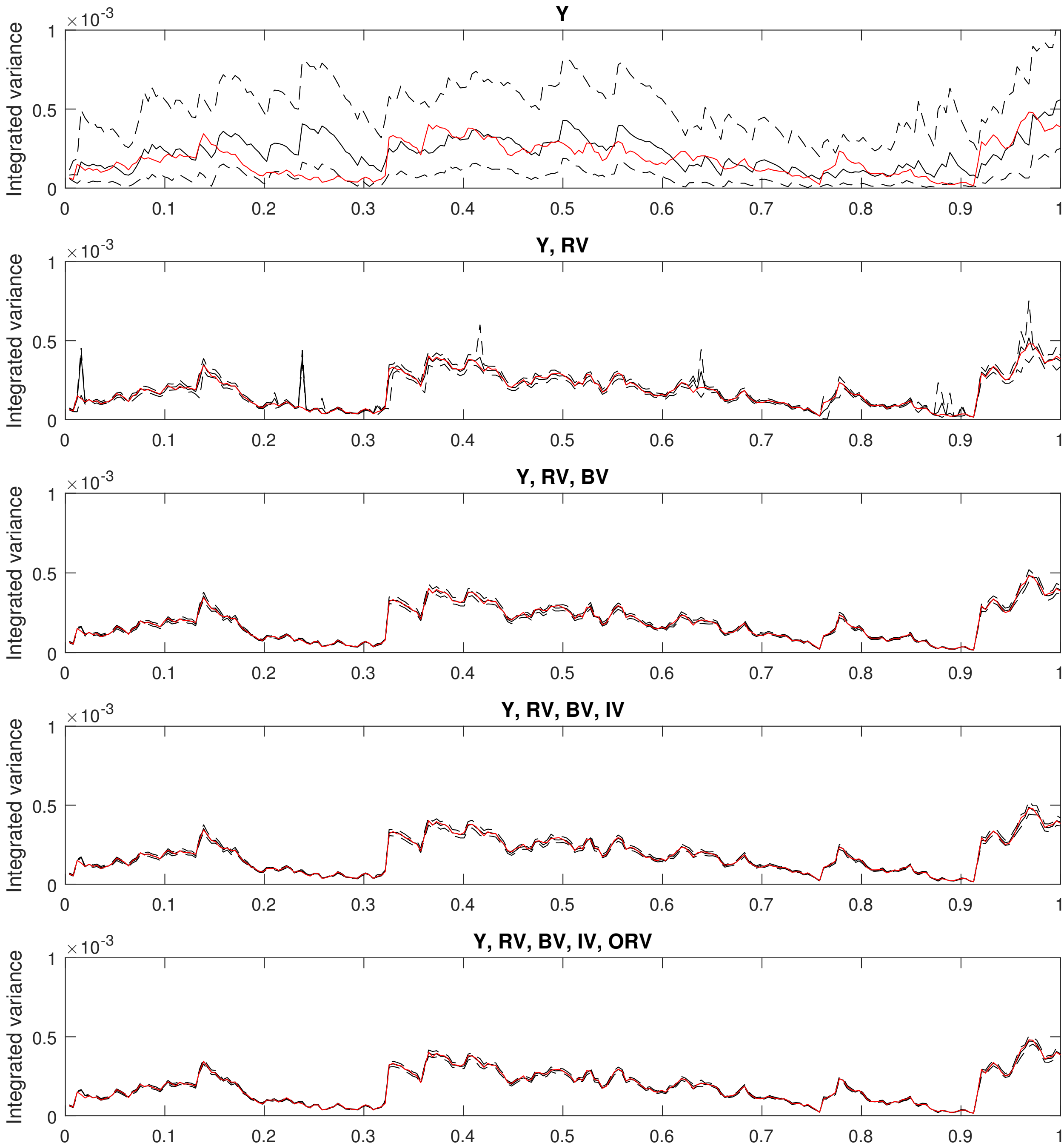

Figure 10: Filtered integrated variance using various data sources. Integrated variance path's means obtained by the particle filters, true integrated variance path, and 95% and confidence intervals computed using empirical quantiles (from particle filters) are shown in this figure using different data sources. Y means daily log-equity value, RV means realized variance, BV means bipower variation, IV means implied volatility here, and ORV means option realized variance.

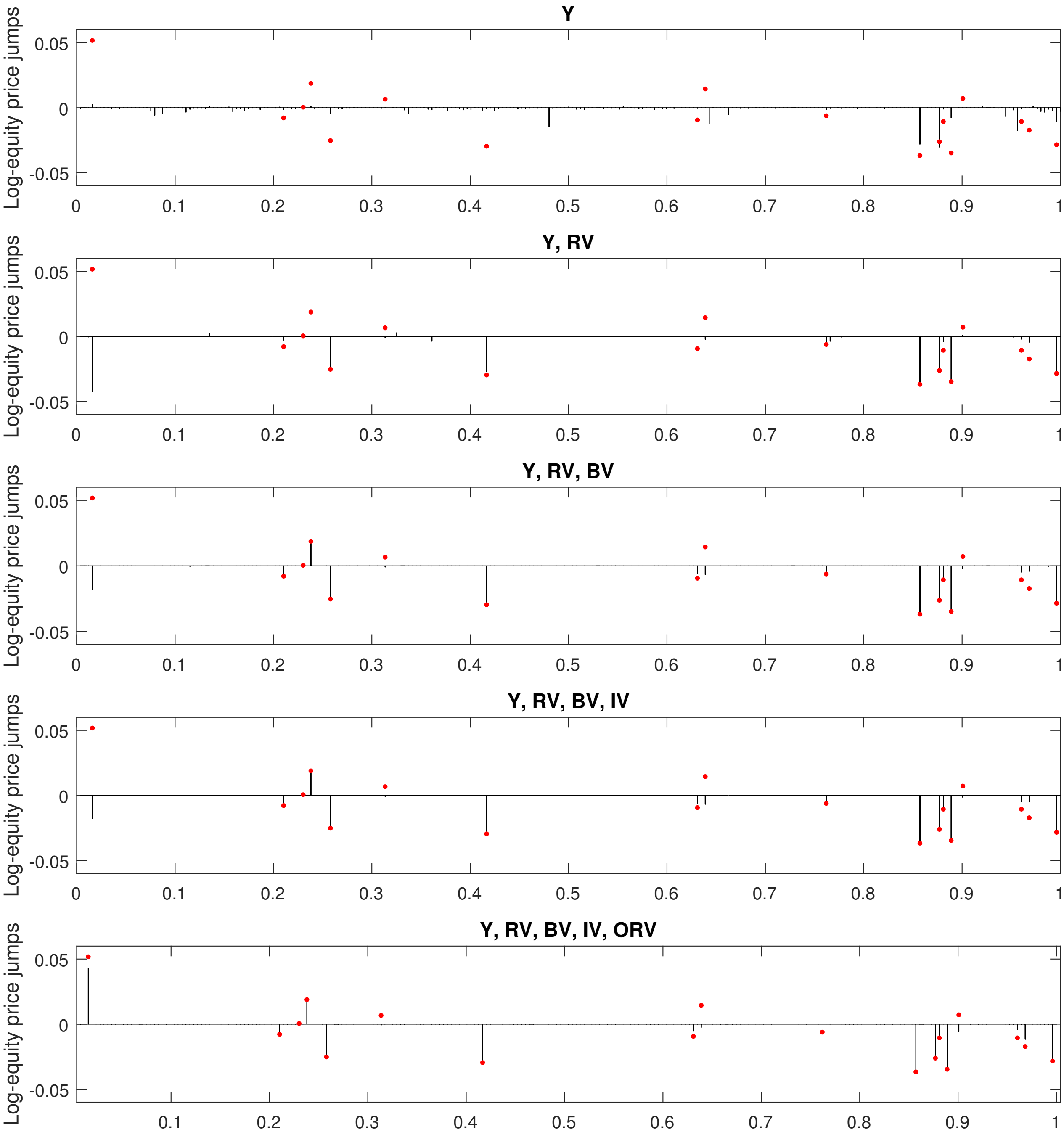

Figure 11: Filtered log-equity jumps using various data sources. Return jump path's means obtained by the particle filters and true return jump path are shown in this figure using different data sources. Y means daily log-equity value, RV means realized variance, BV means bipower variation, IV means implied volatility here, and ORV means option realized variance.

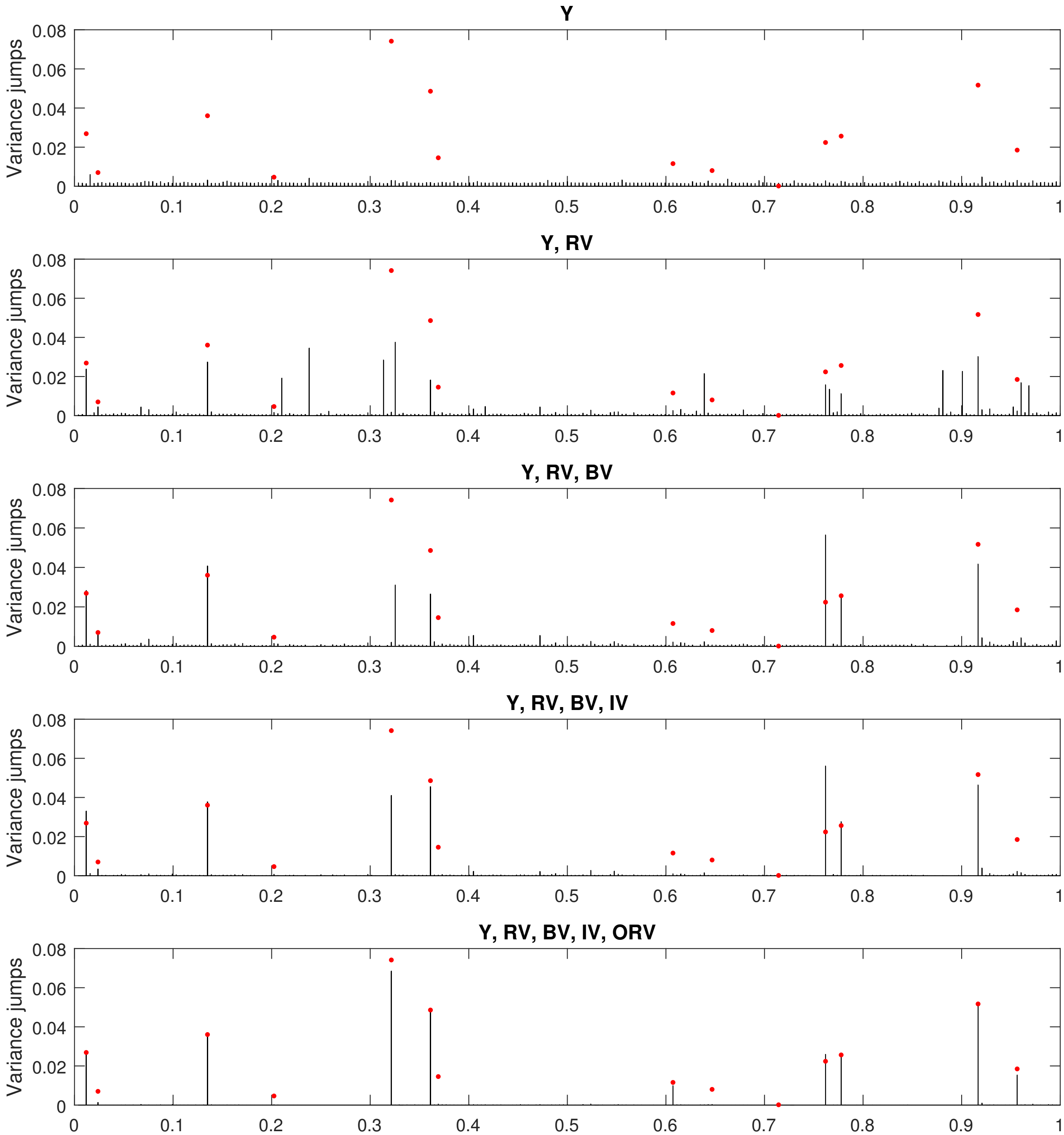

Figure 12: Filtered variance jumps using various data sources. Variance jump path's means obtained by the particle filters and true variance jump path are shown in this figure using different data sources. Y means daily returns, RV means realized variance, BV means bipower variation, IV means implied volatility here, and ORV means option realized variance.

Table 15: RMSE for various quantities across 100 simulated paths when using only a limited number of options.

Panel A: Maturities	RMSE (true)					RMSE (filtered)				
	V	ΔQV	ΔI	Z_Y	Z_V	V	ΔQV	ΔI	Z_Y	Z_V
DTM = 30	5.9196	0.0212	0.0116	1.8850	2.2890	3.9730	0.0238	0.0135	0.7718	1.0889
DTM = 90	6.3944	0.0202	0.0122	1.8452	1.8596	4.0821	0.0226	0.0140	0.7283	0.9411
DTM = 150	6.6394	0.0198	0.0126	1.9275	1.9132	4.1860	0.0229	0.0143	0.7591	0.8998
DTM = 30, 90	6.0780	0.0201	0.0116	1.8852	1.9806	3.8558	0.0226	0.0133	0.7273	0.8593
DTM = 30, 150	6.1739	0.0188	0.0118	1.8551	2.0669	3.8661	0.0232	0.0135	0.7240	0.8453
DTM = 120, 150	6.4748	0.0194	0.0122	1.8500	1.8894	3.9892	0.0224	0.0137	0.7676	0.7847

Panel B: Moneynesses	RMSE (true)					RMSE (filtered)				
	V	ΔQV	ΔI	Z_Y	Z_V	V	ΔQV	ΔI	Z_Y	Z_V
$\Delta^e = 0.20$	6.7777	0.0271	0.0147	1.8839	2.3313	4.6669	0.0290	0.0158	0.8560	1.2977
$\Delta^e = 0.35$	6.8674	0.0265	0.0149	1.9021	2.6694	4.7140	0.0286	0.0158	0.7991	1.7129
$\Delta^e = 0.50$	6.9247	0.0246	0.0150	1.9514	3.1289	4.8637	0.0272	0.0162	0.8819	2.1768
$\Delta^e = 0.65$	6.8310	0.0244	0.0149	1.8926	2.4371	4.9126	0.0298	0.0167	0.9845	1.5027
$\Delta^e = 0.80$	6.7287	0.0263	0.0145	1.9438	2.0052	4.7973	0.0307	0.0163	0.9010	1.2448
$\Delta^e = 0.20, 0.35$	6.6490	0.0250	0.0144	1.8983	2.3443	4.4762	0.0266	0.0154	0.8107	1.3127
$\Delta^e = 0.65, 0.80$	6.6995	0.0244	0.0146	1.8956	2.1555	4.7616	0.0292	0.0164	0.8497	1.2778

[1] Quantities were multiplied by 1,000.
[2] Filtered values are computed as the mean of resampled particles obtained via a SIR particle filter with $M = 5$ using Y, RV, BV, I and ORV and every maturities and moneynesses.
[3] A maximum of fifteen implied volatilities are observed on each day: these European OTM options have a maturity of 30, 90 and 150 business days, and call-equivalent deltas of 0.20, 0.35, 0.50, 0.65 and 0.80 respectively.
[4] In the table, DTM means day to maturity and $\Delta^e = 0.20$ represents call-equivalent delta.

Table 16: Descriptive statistics of realized variance, bipower variation and option realized variance.

	Mean	S.D.	Skewness	Kurtosis	10%	90%
$RV \times 1000$	27.523	75.247	13.846	320.527	3.990	53.757
$BV \times 1000$	25.783	72.283	13.371	294.644	3.591	49.767
ORV, DTM = 30, $\Delta^e = 0.20$	24.001	83.350	8.827	104.327	0.792	55.478
ORV, DTM = 30, $\Delta^e = 0.35$	33.794	87.637	8.314	92.257	2.832	68.863
ORV, DTM = 30, $\Delta^e = 0.50$	33.373	68.679	8.518	104.435	6.387	65.347
ORV, DTM = 30, $\Delta^e = 0.65$	29.858	67.238	9.305	130.376	4.279	59.223
ORV, DTM = 30, $\Delta^e = 0.80$	19.484	46.732	6.753	66.278	1.307	44.229
ORV, DTM = 90, $\Delta^e = 0.20$	17.434	78.232	9.779	119.597	0.695	22.679
ORV, DTM = 90, $\Delta^e = 0.35$	26.705	77.032	10.151	141.495	2.510	53.110
ORV, DTM = 90, $\Delta^e = 0.50$	34.453	74.512	8.202	97.525	5.806	66.649
ORV, DTM = 90, $\Delta^e = 0.65$	25.184	53.298	8.336	109.830	3.671	47.970
ORV, DTM = 90, $\Delta^e = 0.80$	15.027	55.173	16.408	363.312	1.272	30.695

[1] S.D. stands for standard deviation. 10% and 90% represent the 10% and 90% quantiles of empirical samples respectively.
[2] RV and BV are given on an annualized basis.

References

Aït-Sahalia, Y., and A. W. Lo. 1998. Nonparametric estimation of state-price densities implicit in financial asset prices. Journal of Finance 53:499–547.

Alizadeh, S., M. W. Brandt, and F. X. Diebold. 2002. Range-based estimation of stochastic volatility models. Journal of Finance 57:1047–1091.

Andersen, T. G., T. Bollerslev, F. X. Diebold, and H. Ebens. 2001. The distribution of realized stock return volatility. Journal of Financial Economics 61:43–76.

Andersen, T. G., O. Bondarenko, V. Todorov, and G. Tauchen. 2015a. The fine structure of equity-index option dynamics. Journal of Econometrics 187:532–546.

Andersen, T. G., N. Fusari, and V. Todorov. 2015b. The risk premia embedded in index options. Journal of Financial Economics 117:558–584.

Audrino, F., and M. R. Fengler. 2015. Are classical option pricing models consistent with observed option second-order moments? Evidence from high-frequency data. Journal of Banking & Finance 61:46–63.

Bakshi, G., C. Cao, and Z. Chen. 1997. Empirical performance of alternative option pricing models. Journal of Finance 52:2003–2049.

Bandi, F. M., and R. Reno. 2016. Price and volatility co-jumps. Journal of Financial Economics 119:107–146.

Bardgett, C., E. Gourier, and M. Leippold. 2015. Inferring volatility dynamics and risk premia from the S&P 500 and VIX markets. Working paper pp. 1–73.

Barndorff-Nielsen, O. E., and N. Shephard. 2002. Estimating quadratic variation using realized variance. Journal of Applied Econometrics 17:457–477.

Barndorff-Nielsen, O. E., and N. Shephard. 2004. Power and bipower variation with stochastic volatility and jumps. Journal of Financial Econometrics 2:1–37.

Bates, D. S. 1996. Jumps and stochastic volatility: Exchange rate processes implicit in deutsche mark options. Review of Financial Studies 9:69–107.

Bates, D. S. 2000. Post-'87 crash fears in the S&P 500 futures option market. Journal of Econometrics 94:181–238.

Bates, D. S. 2006. Maximum likelihood estimation of latent affine processes. Review of Financial Studies 19:909–965.

Black, F., and M. Scholes. 1973. The Pricing of Options and Corporate Liabilities. Journal of Political Economy 81:637–654.

Bollerslev, T. 1986. Generalized autoregressive conditional heteroskedasticity. Journal of Econometrics 31:307–327.

Broadie, M., M. Chernov, and M. Johannes. 2007. Model specification and risk premia: Evidence from futures options. Journal of Finance 62:1453–1490.

Broadie, M., and O. Kaya. 2006. Exact simulation of stochastic volatility and other affine jump diffusion processes. Operations Research 54:217–231.

Chernov, M., A. R. Gallant, E. Ghysels, and G. Tauchen. 2003. Alternative models for stock price dynamics. Journal of Econometrics 116:225–257.

Chernov, M., and E. Ghysels. 2000. A study towards a unified approach to the joint estimation of objective and risk neutral measures for the purpose of options valuation. Journal of Financial Economics 56:407–458.

Christoffersen, P., B. Feunou, K. Jacobs, and N. Meddahi. 2012a. The economic value of realized volatility: Using high-frequency returns for option valuation. Working paper .

Christoffersen, P., B. Feunou, and Y. Jeon. 2015. Option valuation with observable volatility and jump dynamics. Journal of Banking & Finance 61:S101–S120.

Christoffersen, P., K. Jacobs, and C. Ornthanalai. 2012b. Dynamic jump intensities and risk premiums: evidence from S&P500 returns and options. Journal of Financial Economics 106:447–472.

Cont, R., and T. Kokholm. 2013. A consistent pricing model for index options and volatility derivatives. Mathematical Finance 23:248–274.

Diebold, F. X., and R. S. Mariano. 1995. Comparing Predictive Accuracy. Journal of Business & Economic Statistics 13:253–263.

Duffie, D., J. Pan, and K. Singleton. 2000. Transform analysis and asset pricing for affine jump-diffusions. Econometrica 68:1343–1376.

Duffie, D., and K. Singleton. 1993. Simulated moments estimation of Markov models of asset prices. Econometrica 61:929–952.

Dumas, B., J. Fleming, and R. E. Whaley. 1998. Implied volatility functions: empirical tests. Journal of Finance 53:2059–2106.

Engle, R. F. 1982. Autoregressive Conditional Heteroscedasticity with Estimates of the Variance of United Kingdom Inflation. Econometrica 50:987–1007.

Eraker, B. 2001. MCMC analysis of diffusion models with application to finance. Journal of Business & Economic Statistics 19:177–191.

Eraker, B. 2004. Do stock prices and volatility jump? Reconciling evidence from spot and option prices. Journal of Finance 59:1367–1404.

Eraker, B., M. Johannes, and N. Polson. 2003. The impact of jumps in volatility and returns. Journal of Finance 58:1269–1300.

Filipovic, D., and E. Mayerhofer. 2009. Affine diffusion processes: Theory and applications. Advanced Financial Modelling 8:125.

Fulop, A., J. Li, and J. Yu. 2014. Self-Exciting Jumps, Learning, and Asset Pricing Implications. Review of Financial Studies

Gallant, A. R., and G. Tauchen. 2010. Simulated score methods and indirect inference for continuous-time models. Handbook of Financial Econometrics 1:427–477.

Gil-Pelaez, J. 1951. Note on the inversion theorem. Biometrika 38:481–482.

Gordon, N. J., D. J. Salmond, and A. F. Smith. 1993. Novel approach to nonlinear/non-Gaussian Bayesian state estimation. IEE Proceedings F (Radar and Signal Processing) 140:107–113.

Heston, S. 1993. A closed-form solution for options with stochastic volatility with applications to bond and currency options. Review of Financial Studies 6:327.

Hu, F., and J. V. Zidek. 2002. The weighted likelihood. Canadian Journal of Statistics 30:347–371.

Hürzeler, M., and H. R. Künsch. 2001. Approximating and maximising the likelihood for a general state-space model. In Sequential Monte Carlo Methods in Practice, pp. 159–175. Springer.

Jackwerth, J. C., and M. Rubinstein. 1996. Recovering probability distributions from option prices. The Journal of Finance 51:1611–1631.

Johannes, M. S., N. G. Polson, and J. R. Stroud. 2009. Optimal filtering of jump diffusions: Extracting latent states from asset prices. Review of Financial Studies 22:2759–2799.

Jones, C. S. 1998. Bayesian estimation of continuous-time finance models. Working paper pp. 1–52.

Malik, S., and M. K. Pitt. 2011. Particle filters for continuous likelihood evaluation and maximisation. Journal of Econometrics 165:190–209.

Merton, R. C. 1980. On estimating the expected return on the market: An exploratory investigation. Journal of financial economics 8:323–361.

Newey, W., and K. West. 1987. A simple, positive semi-definite, heteroskedasticity and autocorrelation consistent covariance matrix. Econometrica 55:703–708.

Ornthanalai, C. 2014. Levy jump risk: Evidence from options and returns. Journal of Financial Economics 112:69–90.

Pan, J. 2002. The jump-risk premia implicit in options: Evidence from an integrated time-series study. Journal of Financial Economics 63:3–50.

Protter, P. 2004. Stochastic integration and differential equations. Springer.

Renault, E. 1997. Econometric models of option pricing errors. Econometric Society Monographs 28:223–278.

Santa-Clara, P., and S. Yan. 2010. Crashes, volatility, and the equity premium: Lessons from S&P 500 options. The Review of Economics and Statistics 92:435–451.

Stephan, J. A., and R. E. Whaley. 1990. Intraday price change and trading volume relations in the stock and stock option markets. Journal of Finance 45:191–220.

Todorov, V., and G. Tauchen. 2011. Volatility jumps. Journal of Business & Economic Statistics 29:356–371.

Tse, S. T., and J. W. Wan. 2013. Low-bias simulation scheme for the Heston model by Inverse Gaussian approximation. Quantitative Finance 13:919–937.

van Haastrecht, A., and A. Pelsser. 2010. Efficient, alsmost exact simulation of the Heston stochastic volatility model. International Journal of Theoretical and Applied Finance 13:1–43.

Zhang, L., P. A. Mykland, and Y. Aït-Sahalia. 2005. A tale of two time scales. Journal of the American Statistical Association 100.